Volume II

Midwest Regional Carbon Sequestration Partnership (MRCSP) Phase III (Development Phase)

Integrated Monitoring Volume: A Summary of Monitoring Studies Conducted in Niagaran Carbonate Pinnacle Reefs During Enhanced Oil Recovery with CO_2

Prepared by:

Battelle
505 King Avenue
Columbus, Ohio 43201

Principle Investigator: Dr. Neeraj Gupta

Authors: Mark Kelley, Matt Place, Amber Conner, Sanjay Mawalkar, Srikanta Mishra, Joel Sminchak, and Neeraj Gupta

Submitted to:

The U.S. Department of Energy, National Energy Technology Laboratory
Program Manager: Andrea McNemar

DOE Project #DE-FC26-05NT42589

September 2020

NOTICE

This report was prepared by Battelle as an account of work sponsored by an agency of the United States Government and other project sponsors, including Core Energy, LLC and The Ohio Development Services Agency. Neither the United States Government, nor any agency thereof, nor any of their employees, nor Battelle and other cosponsors, makes any warranty, express or implied, or assumes any liability or responsibility for the accuracy, completeness, or usefulness of any information, apparatus, product, or process disclosed, or represents that its use would not infringe privately owned rights. Reference herein to any specific commercial product, process, or service by trade name, trademark, manufacturer, or otherwise does not necessarily constitute or imply its endorsement, recommendations, or favoring by the United States Government or any agency thereof. The views and the opinions of authors expressed herein do not necessarily state or reflect those of the United States Government or any agency thereof.

Battelle does not engage in research for advertising, sales promotion, or endorsement of our clients' interests including raising investment capital or recommending investments decisions, or other publicity purposes, or for any use in litigation.

Battelle endeavors at all times to produce work of the highest quality, consistent with our contract commitments. However, because of the research and/or experimental nature of this work the client undertakes the sole responsibility for the consequence of any use or misuse of, or inability to use, any information, apparatus, process or result obtained from Battelle, and Battelle, its employees, officers, or Trustees have no legal liability for the accuracy, adequacy, or efficacy thereof.

ACKNOWLEDGEMENTS

Sponsorships - This report is part of a series of reports prepared under the Midwestern Regional Carbon Sequestration Partnership (MRCSP) Phase III (Development Phase). These reports summarize and detail the findings of the work conducted under the Phase III project. The primary funding for the MRCSP program is from the US Department of Energy's National Energy Technology Laboratory (NETL) under DOE project number DE-FC26-05NT42589 with Ms. Andrea McNemar as the DOE project manager. The past DOE project managers for MRCSP include Dawn Deel, Lynn Brickett and Traci Rodosta. Many others in the DOE leadership supported, encouraged, and enabled the MRCSP work including but not limited to Kanwal Mahajan, John Litynski, Darin Damiani, and Sean Plasynski.

The Michigan Basin large-scale test received significant in-kind cost share from Core Energy, LLC, who also provided essential access to the field test site and related data. This contribution by Core Energy CEO Robert Mannes, VP Operations Rick Pardini, and Allan Modroo, VP Exploration, and the entire Core Energy staff is gratefully acknowledged. MRCSP work in Ohio has been supported by the Ohio Coal Development Office in the Ohio Development Services Agency under various grants (CDO D-10-7, CDO-D-13-22, CDO-D-D-13-24, and CDO-D-15-08) with Mr. Greg Payne as the OCDO project manager. Finally, several industry sponsors and numerous technical team members from State Geological Surveys, universities, field service providers have supported MRCSP through cash and in-kind contributions over the years as listed in the individual reports.

Program Leadership – During the MRCSP Phase III project period, several Battelle staff and external collaborators contributed to the successful completion of the program through their efforts in field work, geological data analysis and interpretation, and/or reporting. The primary project managers over the MRCSP performance period have included Rebecca Wessinger, Neeraj Gupta, Jared Walker, Rod Osborne, Darrell Paul, and David Ball. Additional project management support has been provided by Andrew Burchwell, Christa Duffy, Caitlin McNeil, and Jacqueline Gerst over the years.

Principal Investigator: Neeraj Gupta (614-424-3820/ gupta@battelle.org)

Report Authors and Principal Technical Contributors – Mark Kelley, Matt Place, Amber Conner, Sanjay Mawalkar, Srikanta Mishra, Joel Sminchak, and Neeraj Gupta

MRCSP Phase III Technical Contributors – In addition to those listed above, numerous experts from Battelle and supporting organizations contributed to MRCSP work. Selected Battelle contributors include Jackie Gerst, Ashwin Pasumarti, Carol Brantley, Samin Raziperchikolaee, Will Garnes, Priya Ravi Ganesh, Joel Main, Manoj Kumar Valluri, Valerie Smith, Lydia Cumming, Andrew Burchwell, Laura Keister, John Miller, Jared Hawkins, Isis Fukai, Mackenzie Scharenberg, Benjamin Grove, Heather McCarren, James Holley, Zach Cotter, Mark Moody, Glenn Larsen, Jacob Markiewicz, Amber Conner, Caitlin Holley, and Rod Osborne.

Select supporting technical contributors include Björn Paulsson, Ruiqing He (Paulsson, Inc.) Volker Oye, Ismael Vera Rodriguez (NORSAR), Julie Sheets, Sue Welch, David Cole (Ohio State University), Marie-Josée Banwell, Giacomo Falorni, Vicky Hsiao (TRE Canada), Conrad Kolb (Schlumberger), Liviu Grindei, Mary Humphries (VSProwess), Thomas Coleman (Silixa), David Brock, Bill Shroyer (Sage Rider), Alain Bonneville (PNNL), Andrew Black (Tellus Gravity), Richard Van Dok (Sterling Seismic & Reservoir Services), Tom Bratton, Janice Gregory Sloan (APEX Petroleum Engineering), Jehad Abou-Saleh, Yonghwee Kim (Baker Hughes).

EXECUTIVE SUMMARY

Between February 2013 and September 2016, the MRCSP Phase III large-scale test injected over 1 million metric tons of CO_2 into a group of Silurian-age (Niagaran) pinnacle reef reservoirs in Otsego County Michigan that are operated by Core Energy, LLC. There are over 800 pinnacle reefs in northern Michigan, and collectively, these geologic features have sufficient capacity to store several hundred million metric tons of CO_2. Moreover, most of the reefs are oil-bearing and went through primary production in the 1970s and 1980s; therefore, by injecting CO_2 into the reefs, there is a real opportunity to realize additional (enhanced) oil recovery (EOR) and to permanently store CO_2 after EOR. Core Energy currently operates several reefs for EOR using CO_2.

A key objective of the MRCSP Phase III project is to evaluate the effectiveness of various technologies for monitoring CO_2 that has been injected into deep geologic formations (i.e., the Niagaran reefs). Monitoring may be required at CO_2 storage sites for a variety of reasons, including to meet UIC Class II (EOR sites) or Class VI (storage only sites) permit requirements or EPA greenhouse gas reporting rule requirements or to qualify for tax credits under the 45Q tax credit rule. The results of this monitoring study should prove useful to operators considering using carbonate pinnacle reefs of Northern Michigan for CO_2 storage.

The MRCSP Phase III project included a comprehensive monitoring program in parallel with injecting over one million tonnes of CO_2 into ten Niagaran pinnacle reefs operated by Core Energy. Figure ES-1 and Table ES-1 identify the monitoring technologies conducted at each of ten pinnacle reefs. The monitoring program included the following:

- At all ten reefs, a basic monitoring suite consisting of CO_2 mass-balance accounting (i.e., injection rate, cumulative CO_2 injected, production rate, cumulative CO_2 produced) and reservoir pressure.

- At the Dover 33 reef, six additional monitoring techniques, including Vertical Seismic Profile (VSP) monitoring; geochemistry monitoring; borehole gravity (BHG) monitoring; pulsed neutron capture (PNC) logging; satellite monitoring (INSAR – Satellite); and micro-seismicity monitoring.

- At the Bagley reef and the Charlton 19 reef, two additional monitoring techniques, including geochemistry monitoring and PNC logging.

- At the Chester 16 reef, five additional monitoring techniques, including Distributed Acoustic Sensing (DAS) Vertical Seismic Profile (VSP) monitoring, cross-well seismic monitoring, Distributed Temperature Sensing (DTS), geochemistry monitoring, and Pulsed Neuron Capture logging (PNC) logging.

A separate report has been prepared for each of the 11 monitoring technologies listed in Table ES-1 These reports, which provide a detailed discussion of the data acquisition and interpretation methodology and results. These 11 monitoring reports are collated into a single document entitled ***Integrated Monitoring Volume for CO_2 Storage with Enhanced Oil Recovery in Northern Michigan***. Table ES-2 lists the reports included in the Integrated Monitoring Volume. The reader interested in developing a general understanding of the MRCSP Phase III monitoring program should find the information in this report to be satisfactory;

however, the reader interested in gaining a detailed understanding of one or more monitoring technologies is directed to the individual monitoring reports.

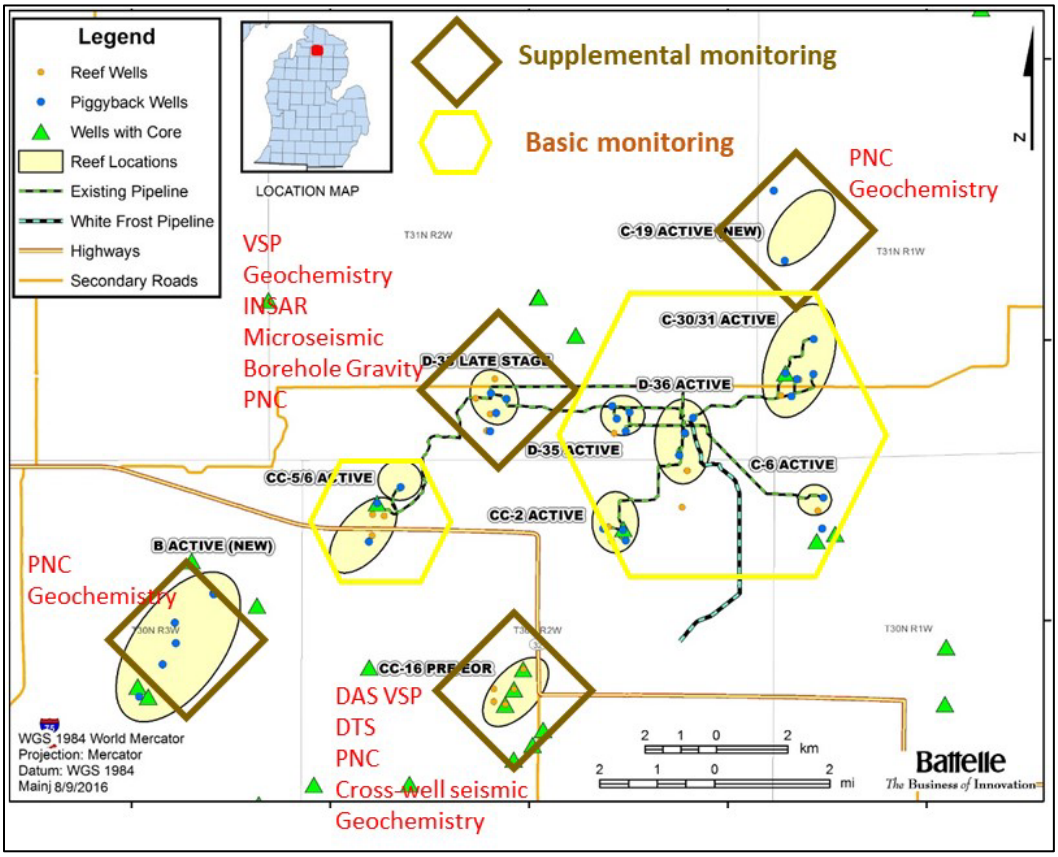

Figure ES-1. Monitoring methods employed at various reefs during the MRCSP Phase III Program.

Table ES-1. Monitoring Methods and Objectives as Implemented by Reef.

	Monitoring Objective				Monitoring by Reef				
Monitoring Technology	**CO_2 injection/ production; net amount stored**	**Leak Detection/ well integrity**	**CO_2 plume tracking/ interaction**	**physical response to injection; induced seismicity, uplift;**	**Dover 33**	**Charlton 19**	**Chester 16**	**Bagley**	**Other reefs**
Mass Balance Accounting	X				X	X	X	X	X
Reservoir Pressure				X	X	X	X	X	X
Temperature (DTS)		X	X				X		
PNC Logging		X	X		X	X	X	X	
Borehole Gravity			X		X				
Geochemistry			X		X	X	X	X	
VSP – Geophone[a]		X	X		X				
VSP – DAS[a]		X	X				X		
Cross-well Seismic			X				X		
Microseismicity				X	X				
InSAR (Satellite radar)				X	X				

a. Two varieties of VSP were implemented, including conventional VSP using geophones conveyed on a tubing string (Dover 33) and DAS VSP using fiber optic cable permanently mounted to the outside of the deep casing string (Chester 16).

Table ES-2. Reports Included in the Integrated Monitoring Volume for CO_2 Storage with Enhanced Oil Recovery in Northern Michigan

Volume	Report Title	Authors/Citation
II.A	Mass Balance Accounting or CO_2 Storage with Enhanced Oil Recovery in Northern Michigan	Mawalkar, S., Burchwell, A., Keister, L., Pasumarti, A., and Gupta, N. 2020. MRCSP topical report prepared for DOE-NETL project DE-FC26-05NT42589, Battelle Memorial Institute, Columbus, OH
II.B	Time-Lapse Vertical Seismic Profiling (VSP) for CO_2 Storage in a Depleted Oil Field in Northern Michigan	Kelley, M., Haagsma, A., and Gupta, N. 2020. MRCSP topical report prepared for DOE-NETL project DE-FC26-05NT42589, Battelle Memorial Institute, Columbus, OH
II.C	Distributed Acoustic Sensing (DAS) Seismic Monitoring of CO_2 Injected for Enhanced Oil Recovery in Northern Michigan	Kelley, M., Grindei, L., Humphries, M., Coleman, T., Modroo, A., and Gupta, N. 2020. MRCSP topical report prepared for DOE-NETL project DE-FC26-05NT42589, Battelle Memorial Institute, Columbus, OH
II.D	Cross-Well Seismic Monitoring of CO_2 Injected for Enhanced Oil Recovery in Northern Michigan	Kelley, M., Kolb, C., and Gupta, N. 2020. MRCSP topical report prepared for DOE-NETL project DE-FC26-05NT42589, Battelle Memorial Institute, Columbus, OH
II.E	InSAR Monitoring to Evaluate Surface Changes with CO_2 Storage in a Depleted Oil Field in Northern Michigan	Place, M., Banwell, MJ., Falorni, G., and Gupta, N. 2020. MRCSP topical report prepared for DOE-NETL project DE-FC26-05NT42589, Battelle Memorial Institute, Columbus, OH
II.F	Pulsed Neutron Capture for monitoring CO_2 Storage with Enhanced Oil Recovery in Northern Michigan	Conner, A., Place, M., Chace, D., and Gupta, N 2020. MRCSP topical report prepared for DOE-NETL project DE-FC26-05NT42589, Battelle Memorial Institute, Columbus, OH
II.G	Assessment of Borehole Gravity (Density) Monitoring for CO_2 Injection in a Depleted Oil Field in Northern Michigan	Place, M., Bonneville, A., Black, A., and Gupta, N. 2020. MRCSP topical report prepared for DOE-NETL project DE-FC26-05NT42589, Battelle Memorial Institute, Columbus, OH
II.H	Distributed Temperature Sensing (DTS) to Monitor CO_2 Migration in an Enhanced Oil Recovery Field in Northern Michigan	Mawalkar, S., Burchwell, A., and Gupta, N. 2020. MRCSP topical report prepared for DOE-NETL project DE-FC26-05NT42589, Battelle Memorial Institute, Columbus, OH
II.I	Geochemical Changes in Response to CO_2 Injection in a CO_2-EOR Complex in Northern Michigan	Place, M., Hawkins, J., Grove, B., Keister, L., Sheets, J., Welch, S., Cole, D., and Gupta, N. 2020. MRCSP topical report prepared for DOE-NETL project DE-FC26-05NT42589, Battelle Memorial Institute, Columbus, OH
II.J	Microseismic Monitoring Study to Assess the Potential for Induced Seismicity in a Depleted Oil Field in Northern Michigan	Kelley, M., Place, M., and Gupta, N. 2020. MRCSP topical report prepared for DOE-NETL project DE-FC26-05NT42589, Battelle Memorial Institute, Columbus, OH
II.K	Analysis of Transient Pressure and Rate Data in a Complex of Enhanced Oil Recovery Fields in Northern Michigan.	Mishra, S., Kelley, M., Raziperchikolaee, S., Ravi Ganesh, P., Valluri, M., Keister, L., Burchwell, A., Mawalkar, S., Place, M., and Gupta, N. 2020. MRCSP topical report prepared for DOE-NETL project DE-FC26-05NT42589, Battelle Memorial Institute, Columbus, OH

As a result of the extensive body of monitoring data developed, new information was acquired about the effectiveness of the carbonate pinnacle reefs for long-term CO_2 storage. The major lessons learned are listed below.

- The carbonate reef reservoirs act as closed reservoirs because they are surrounded/overlain by low permeability carbonates and evaporites which prevent CO_2 leakage out of the reservoir, making them ideal geologic features for permanent CO_2 storage.
- It is possible to recover almost all CO_2 injected into a reef during CO_2-EOR. In other words, the reefs do not irreversibly sequester significant amounts of CO_2 during the EOR process.
- CO_2 injection into the pinnacle reef reservoirs does not appear to cause ***significant*** land displacement (uplift, subsidence) in the area overlying the reefs.
- CO_2 injection into the pinnacle reef reservoirs does not appear to cause ***significant*** seismic activity that could activate fractures and/or faults that could lead to CO_2 leakage out of the reservoir, even when reservoir pressure is near discovery pressure.
- The carbonate reef reservoirs may contain intervals/zones of salt plugging which reduces porosity and limits CO_2 storage capacity.
- Lateral migration of CO_2 within the carbonate pinnacle reef reservoirs away from the injection well may occur preferentially in thin intervals .
- The carbonate pinnacle reef reservoirs may occur as single isolated “pods” (e.g., Dove 33) or in groups of two or more closely-spaced/overlapping pods (e.g., Charlton 19, Chester 16, Bagley).
- The overall low porosity of the carbonate pinnacle-reef reservoirs presents a significant challenge for using borehole seismic monitoring methods to detect and delineate the injected CO_2.
- Fracture pressures (the pressure at which the formation will fracture) in depleted formations/intervals can be extremely low owing to the lowering of pore pressure below hydrostatic
- Injection of CO_2 into the carbonate reef reservoirs increases the likelihood of precipitation of carbonate minerals (dolomite, calcite, huntite, and magnesite), owing to the extremely high concentrations of calcium, magnesium, sodium, potassium and chloride in the reef brines which causes them to be supersaturated with respect to these minerals. .

TABLE OF CONTENTS

Page

LIST OF TABLES

LIST OF FIGURES

ACRONYMS AND ABBREVIATIONS

AI	Acoustic Impedance
ACRs	Artificial Corner Reflectors
AOI	areas of interest
BHG	Borehole Gravity
BHP	bottom hole pressure
CO_2	Carbon Dioxide
CCS	Carbon capture and storage
CCUS	Carbon capture, utilization, and storage
CSK	COSMO-Skymed
DAS	Distributed Acoustic Sensing
DOE	Department of Energy
DS	distributed scatterers
DTS	Distributed Temperature Sensing
EOR	Enhanced Oil Recovery
ERS	European Remote Sensing
FWI	Full Waveform Inversion
GL	Ground Level
GPa	Gigapascals
GPF	Gas Processing Facility
HP	high pressure
INSAR	Interferometric synthetic aperture radar
LP	low pressure
MBA	Mass balance accounting
MD	Measured depths
MRCSP	Midwest Regional Carbon Sequestration Partnership
MT	metric tons
NETL	National Energy Technology Laboratory
PNC	Pulsed Neuron Capture logging
PS	permanent scatterers
Psi	Per Square Inch
RC	Reflection Coefficient
SEM	Scanning Electron Microscope
SNR	Signal-to-Noise Ratio
TDS	Totally dissolved solids

V_P	Compressional-wave Velocity
V_s	Shear-wave Velocity
VSP	Vertical Seismic Profile
WVSP	Walkaway VSP
XRD	X-Ray Diffraction

1.0 CO_2 MASS BALANCE ACCOUNTING

1.1 Objective and Description of the Technology

CO_2 Mass balance accounting (MBA) is the process of measuring the amount of CO_2 injected into a reef and the amount withdrawn through hydrocarbon production or deliberate CO_2 withdrawal, and system leaks. the difference is the net stored amount of CO_2 (also called associated storage amount). MBA was the method for documenting that the Phase III goal of injecting 1 million metric tons (MT) of CO_2 was achieved.

1.2 Methodology

The premise of MBA involves accurate measurement of the various inputs and outputs of CO_2 into/from individual reefs and the entire system of the 10 reefs during the Enhanced Oil Recovery (EOR) process, with the goal being to determine a reliable estimate of the amount of CO_2 stored in each of the reef reservoirs and collectively at any time. Methodology includes quantities measured and instrumentation for making the measurements. For the purposes of this report, most of the mass balance accounting data is for the period February 3, 2013 (the beginning of Battelle's Midwest Regional Carbon Sequestration Partnership (MRCSP) Phase III monitoring efforts) through September 30, 2019, a period of 6 years, 9 months.

1.2.1 Measurement Quantities

Below are the CO_2 input and output pathways that were monitored during the Phase III program.

- CO_2 (input) from new source – Core Energy receives new CO_2 from a natural gas processing facility located in Chester County, approximately 11 miles south of the Dover 36 Facility. After running through various stages of compression and dehydration, CO_2 is compressed to approximately 1,300 psi (supercritical phase) for transport to the Dover 36 Facility via a 6-inch carbon-steel pipe where it is blended with recycled CO_2 from the reefs and injected into various EOR reefs. During the MRCSP monitoring period (February 2013 to September 2019), approximately 1.62 million MT of new CO_2 was made available by the Chester 10 Facility (Table1-1). The MBA report (Mawalkar et al., 2020a) highlights the accounting of the ~1.6 million MT of (purchased) CO_2 injected in 10 EOR reefs operated by Core Energy. The total quantity of CO_2 injected during this time was ~3.4 million MT, as the produced/recycle gas is added to new CO_2 available from the Chester 10 Facility, in a closed-loop production cycle at the Dover 36 Facility.

Table 1-1. Quantities of new CO_2 used for EOR.

Prod Year	Pure CO_2 (MMCF)	Pure CO_2 (MT)
2013	3,464	182,321
2014	2,998	157,798
2015	3,139	165,222
2016	3,733	196,448
2017	5,900	310,550
2018	6,166	324,583
2019	5,447	286,673
Total	30,848	1,623,595

- CO_2 (output) from Produced Fluids – Produced fluids from the reefs are routed to separators at the Dover 36 processing facility, which is co-located at the Dover 36 reef. Production fluids (mixture of oil, gas, water) are routed through high-pressure (HP) separators and low-pressure (LP) separators. The bulk of the CO_2 gas in the product stream is captured at the HP separators. The remaining liquid

product stream (containing mostly oil and brine) from the HP separator is sent to an LP separator for stripping of any remaining entrained gas. The LP separators also separate the oil from water. The produced gas, which primarily consists of CO_2 (>95% by weight), is separated from the produced fluid and routed through a Coriolis mass flow meter at each of the HP separators. It then is sent to the recycle compressor. The system of Coriolis mass flow meters (attached to the HP separators) and vortex flow meters (attached to the LP separators) measures the total mass of recycle gas produced from each operational reef. Additionally, one Coriolis mass flow meter measures the total mass of recycle gas captured at the LP separators, while another meter measures the total quantity of produced gas from all operational EOR reefs.

- CO_2 (input) from produced fluids (recycled CO_2) –The produced gas separated in the HP separator is directly sent to the main recycle compressor, while the gas separated from the LP separator is first sent to a booster compressor before it is compressed at the recycle compressor. The recycle compressor (having multiple stages of dehydration and compression) compresses the gas to approximately 1,400 psi for reinjection into the EOR reefs. A network of pipes and valves at the Dover 36 Facility allows the recycled gas to be co-mingled with new CO_2 coming from the Chester 10 Facility.
- CO_2 from Brine - Brine is separated by the LP separators. The collected brine is sent to a brine disposal well located onsite at the Dover 36 Facility. The LP separators record the quantity of water produced from each reef. The brine is assumed to be free of CO_2.
- $CO_2$2 dissolved in Sale Oil (output) – recovered oil is gathered in collection tanks before flowing through a Lease Automatic Custody Transfer meter for offsite sales. A small amount of CO_2 remains entrained in the oil after the CO_2 separation process, which bleeds off as the oil moves through the LP meters into a temporary storage/gathering tank.
- Vented CO_2 (output) – While rare, operational outages periodically occur, which forces produced gas to be vented to the atmosphere. Core Energy has orifice-type flow meters installed at its wet and dry vent locations to measure the mass of recycle gas that is vented. During the more than six years of MRCSP monitoring, a total of 1202 MT of gas was vented, representing less than 0.06% of the produced volume of gas.

1.2.2 Instrumentation

Coriolis mass flow meters are central to mass balance calculations. Coriolis flow meters are extremely accurate, with liquid mass flow accuracy of 0.10% and gas mass flow accuracy between 0.35% and 0.5%. These meters measure the bulk of the mass of CO_2 being injected to injection wells and the mass of gas produced at the HP separators where most of the recycle gas is captured. The Coriolis flow meters also provide the density and temperature of CO_2 being injected to various injection wells. These parameters are useful for doing a well-test analysis of CO_2 injection at various reefs. The production metering and computer systems were last updated at the Dover 36 Facility in October 2016, when new Coriolis flow meters were installed at five HP separators and at the aggregate recycle line (from the main recycle compressor). The LP separators have vortex type flow meters that measure CO_2 on a volume basis. The volume of gas is then converted to mass basis by using 19,000 cubic feet (ft^3) per MT of CO_2 as a standard conversion factor.

1.3 Key Results

The MBA report describes CO_2-EOR operations and the mass balance calculations of CO_2 for the monitoring period February 2013 through September 2019 and for the period starting in 1996 when CO_2 EOR first began through Sept 2019. During this period, MRCSP has successfully monitored injection of over 1.6 million MT of new CO_2 in the 10-reef EOR complex. The MBA report also shows that the total associated CO_2 storage in the EOR complex since injection began in 1996, is ~2.7 million MT.

1.3.1 Individual Reefs

For each reef, results of the MBA (through Sept 2019) are shown on a plot of CO_2 cumulative injection and production vs. date. Figure 1-1 is an example for the Dover 33 reef. Note that for this reef, CO_2 injection began prior to the Phase III program in 2013. CO_2 MBA calculations were performed for the period starting in 1996 when CO_2 was first injected through September 2019, and for the period corresponding to the Phase III program. The results are as follows:

- For the period starting with the commencement of EOR in 1996 through September 2019, a total of 1,604,775 MT of CO_2 was injected into the Dover 33 reef while 1,293,876 MT of recycle CO2 gas were produced. The net CO2 stored during this time is therefore 310,899 MT.
- For the MRCSP monitoring period, 325,272 MT of CO_2 were injected and 219,360 MT of CO_2 were produced. A net 105,912 MT of CO_2 were stored in the reef during the MRCSP monitoring period.

1.3.2 All Reefs Combined

Figure 1-1 combines all relevant injection and production values over the life of enhanced recovery within the MRCSP 10- reef complex. The orange line details the key metric in these operations, namely the net CO_2 that remains stored within the reefs at the end of every calendar year. Through the life of enhanced production operations with the 10 reefs, approximately 2.7 million MT of CO_2 remain stored within the reef complex as of September 30, 2019.

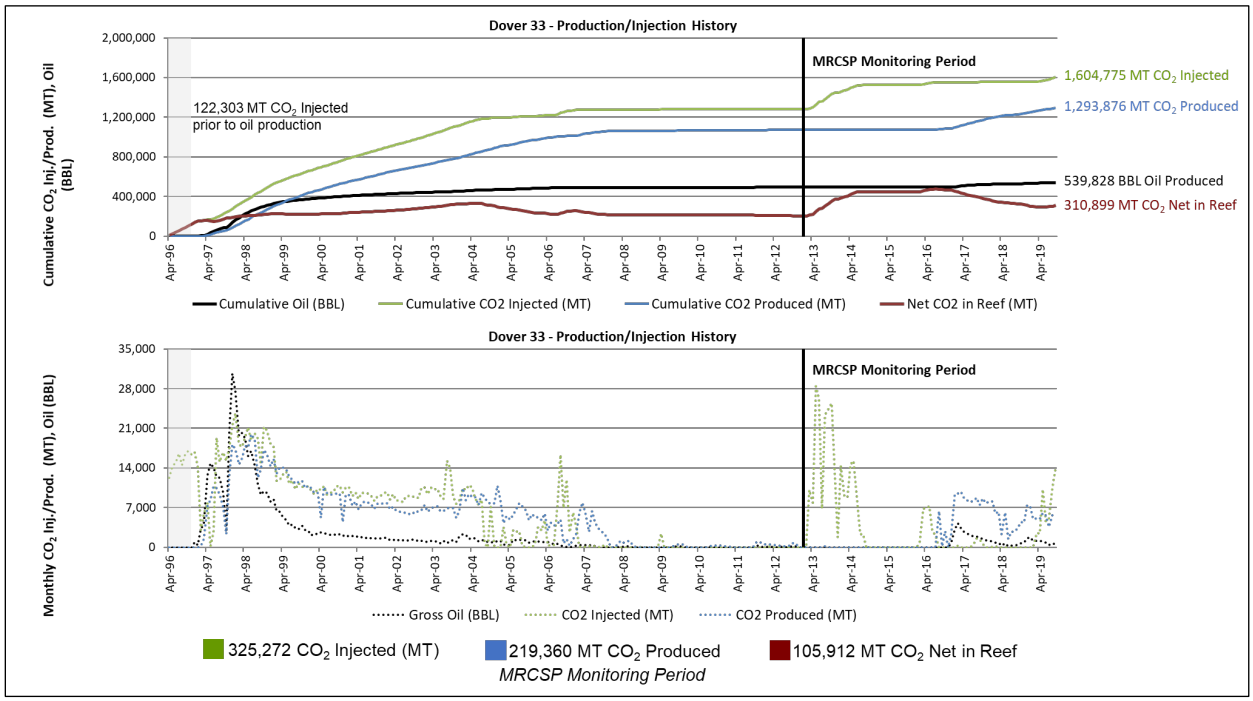

Figure 1-1. CO_2 Injection and Production History at Dover 33 since 1996.

Figure 1-2 shows the distribution of the net amount of CO_2 stored (approximately 2.7 million MT) in the 10-reef EOR complex since EOR began in 1996, and over 1.5 million net MT of CO_2 stored in last 6+ years of the MRCSP monitoring period. The main objective of MRCSP monitoring net 1 million MT CO_2 stored target was achieved in March 2018.

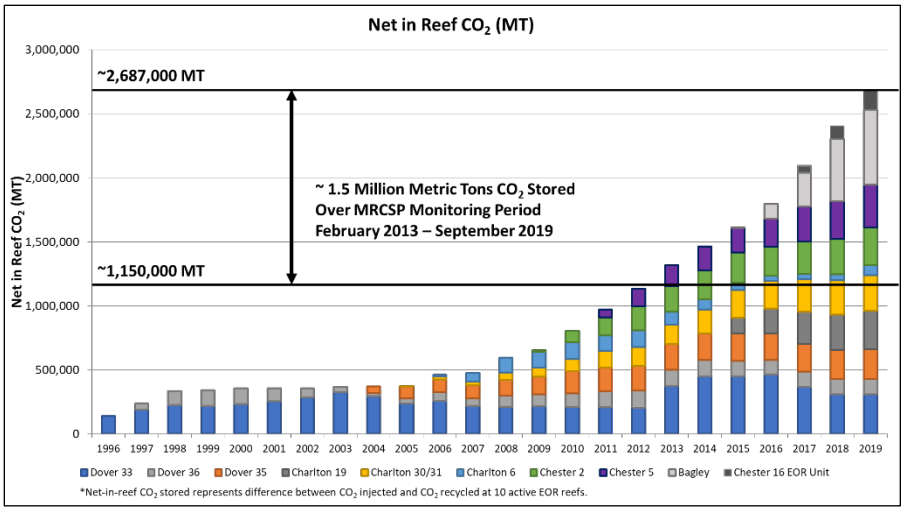

Figure. 1-2. Net in-reef CO_2 over the life of secondary recovery within the MRCSP reef complex.

1.4 Summary

The primary objective of the MRCSP program is to store at least 1 million MT of CO_2. This storage objective also implies that the CO_2 is stored safely, securely, and permanently. In order to qualify the success of the storage from the perspective of long-term sustainability, the accurate accounting of all fluids that enter and exit the storage zone are of critical importance. The MRCSP program performed long-term storage tests at Dover 33 reef and successfully monitored new CO_2 floods at two reefs. Combined, the MRCSP monitored EOR operation at 10 reefs accounting for CO_2 injection/production and net CO_2 stored.

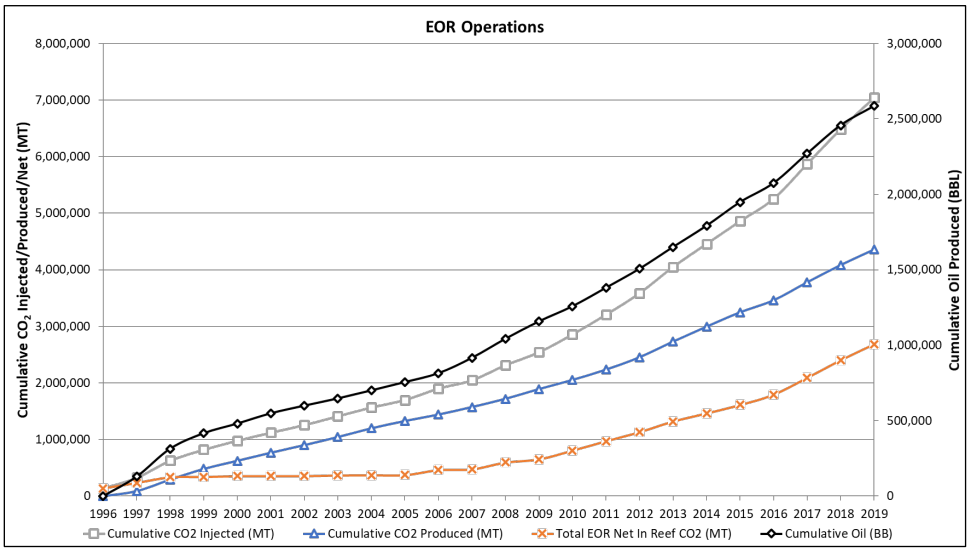

Figure 1-3. Cumulative CO_2 Injected and Oil and CO_2 Produced for the MRCSP Reef Complex.

2.0 TIME-LAPSE VERTICAL SEISMIC PROFILING (VSP)

2.1 Objective and Description of the Technology

Unlike conventional seismic surveys in which the energy source (e.g., vibroseis truck, dynamite) and receivers (geophones, accelerometers) are placed on land surface, in a Vertical Seismic Profile (VSP), receivers are positioned in a borehole or a cased well (usually on a wireline or a tubing string) rather than on land surface; the receivers record downgoing and reflected (upgoing) seismic energy originating from a seismic source at the surface (DiSiena et al., 1984) (Figure 2-1). Although 3D seismic imaging has been the primary tool used for geophysical reservoir monitoring to date, VSP has characteristics that make this technique particularly suitable for time-lapse surveying. In particular, the use of downhole receivers provides some advantages:

- Increased frequency content improves vertical and lateral resolution, making it possible to examine the reservoir in greater detail, both statically and dynamically.
- Improved signal-to-noise ratio (SNR) makes it possible to measure and quantify time-lapse changes in the reservoir with a high degree of confidence.

A time-lapse VSP study consisting of a baseline (pre- CO_2 injection) and a repeat survey (after injection of 271,000 tonnes of CO_2) was conducted at the Dover 33 reef to evaluate the effectiveness of time-lapse VSP for detecting and delineating a plume of CO_2 injected into the Brown Niagaran and A-1 Carbonate formations within the Dover 33 reef between March 2013 and September 2016.

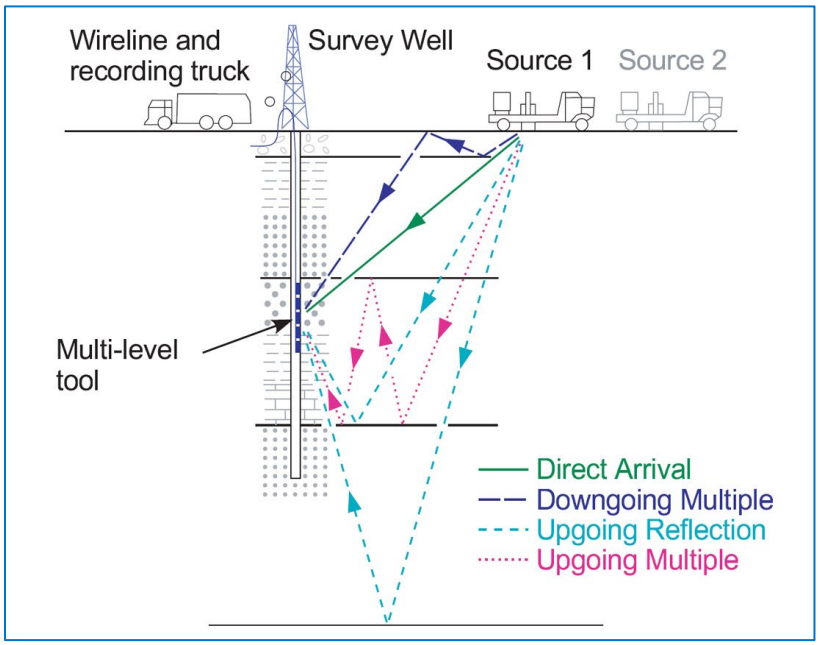

Figure 2-1. Schematic diagram of a VSP survey indicating a survey well, seismic source, receiver, wireline and recording trucks (from DiSiena et al., 1984).

2.2 Methodology Time-Lapse VSP

A common technique for imaging injected CO_2 involves calculating the difference between acoustic impedance amplitude recorded by two surveys. If nothing other than CO_2 injection has changed between the two surveys and the acquisition parameters are the same, amplitude difference has been shown to be a good indicator of the distribution of CO2.

There are many types of VSPs, but the type employed during this study is known as a walkaway VSP (WVSP). WVSPs feature a source that is moved to progressively farther offset locations and receivers held in a fixed location in the borehole. In this study, both vibroseis trucks and small dynamite charges emplaced in shallow borings were employed for sources that were arranged along five lines extending in different directions from the well that hosted an 80-level geophone array. Each of the five produced a 2D section originating at the well and extending away from the well along the transect. Multiple 2D VSP transects provides a pseudo-3D picture of the subsurface. The baseline VSP survey was acquired March 11-13, 2013 and the repeat survey was acquired September 16-18, 2016. SIGMA3 processed both surveys. Acquisition parameters are shown in Table 2-1. Figure 2-2 shows the layout of the baseline survey (the repeat survey was identical).

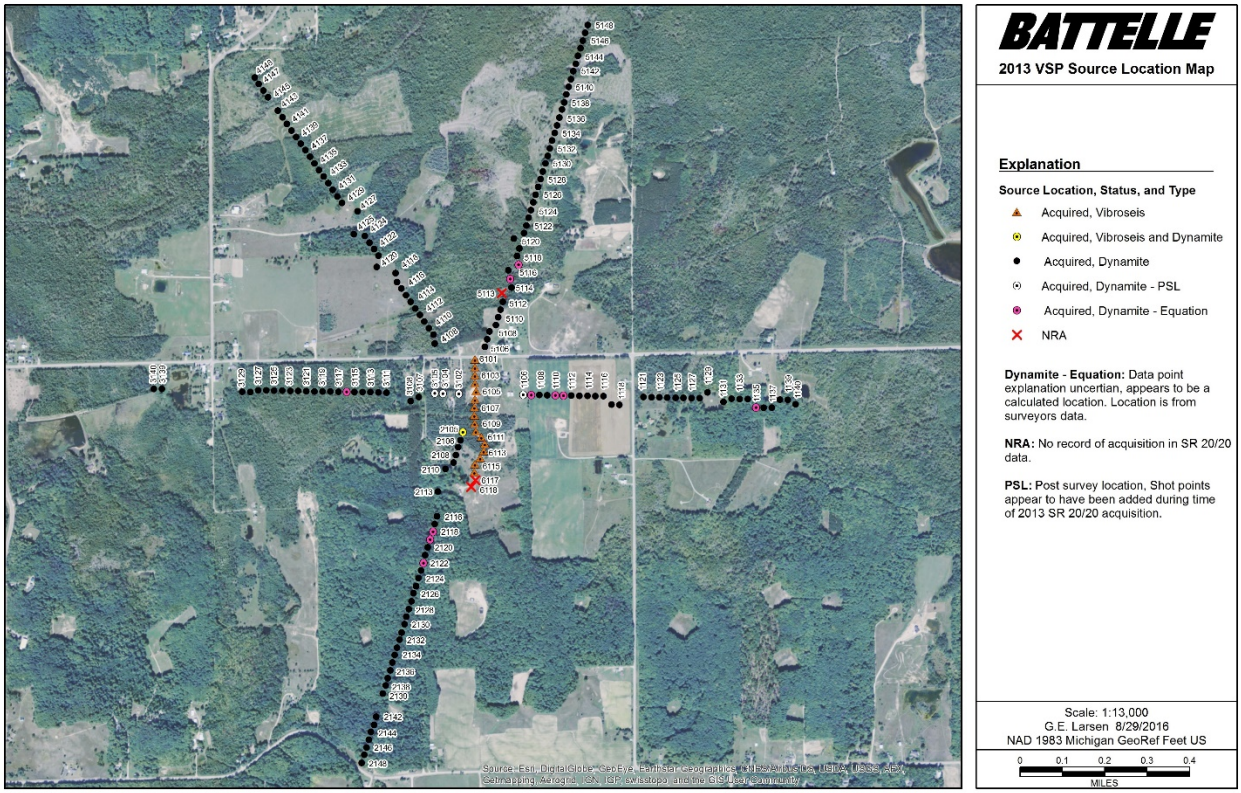

Figure 2-2. Source location map for 2013 baseline VSP survey.

Table 2-1. Data acquisition parameters for the baseline and repeat VSP surveys.

Source Parameter	Baseline Survey March 11-13, 2013	Repeat Survey September 16-18, 2016
Sweep Parameters	6-110 Hz, 18s sweep, 5s listen, 0.5/0.3 tapers linear	6-110 Hz, 18s sweep, 5s listen, 0.5/0.3 tapers linear
Dynamite Parameters	2,000 grams at 20 ft	90-2,000 grams at 10-20 ft[a]
Source Spacing	~100 ft	~100 ft
Receiver Array Contractor	SR2020.	SIGMA[3]
Receiver Array	80 levels (SR2020 Proprietary tool)	80 levels (Oyo GeoSpace DS-150)
Receiver Depth	1,294.7-5,240.4 ft; 50-ft spacing	1,294.8-5,181.4 ft; 49.2-ft spacing

a. Some variability due to proximity to pipelines and structures

The fundamental property measured by seismic technologies is reflectivity. Sound energy travels through different media (rocks) at different velocities and is reflected at interfaces where the media velocity and/or density changes. The amplitude and polarity of the reflections is proportional to the acoustic impedance change across an interface. A seismic trace records the events (the arrival of energy at a receiver). AI is the product of velocity and density; reflection (R) coefficient is defined as follows:

$$R = \frac{AI_1 - AI_2}{AI_1 + AI_2} = \frac{\rho_1 v_1 - \rho_2 v_2}{\rho_1 v_1 + \rho_2 v_2} \quad \text{(equation 1-1)}$$

If the magnitude of the AI change is sufficiently large, the effect may be visually observed by comparing an image of the VSP monitor survey obtained after CO_2 injection to an image of a baseline VSP image obtained before CO_2 injection. Differences between the two surveys can be evaluated more systematically by subtracting the monitor volume from the baseline volume.

2.3 Results

2.3.1 Time-Lapse VSP

Amplitude difference was calculated for P-wave (i.e., P-P) and P-S wave data, and results are shown as images in Figure 2-3 and Figure 2-4, respectively. In both cases, there are no major areas with significant amplitude difference.

2.3.2 Travel-Time Analysis

Because the results of the Time-Lapse VSP impedance differencing were inconclusive, an analysis that involved calculating P-wave and S-wave travel time differences between the 2013 and 2016 VSPs was conducted to look for a change that could be caused by the CO_2 plume. The results of this analysis were also inconclusive.

2.3.3 Supplemental Analyses

Three ancillary analyses were performed to attempt to explain why it was not possible to detect the CO_2 using impedance amplitude differencing or travel-time differencing. These included:

- an analysis of Signal to Noise Ratio
- a fluid substitution modeling analysis; and
- a series of laboratory experiment evaluated the effects of fluid substitution and pressure changes on acoustic velocities.

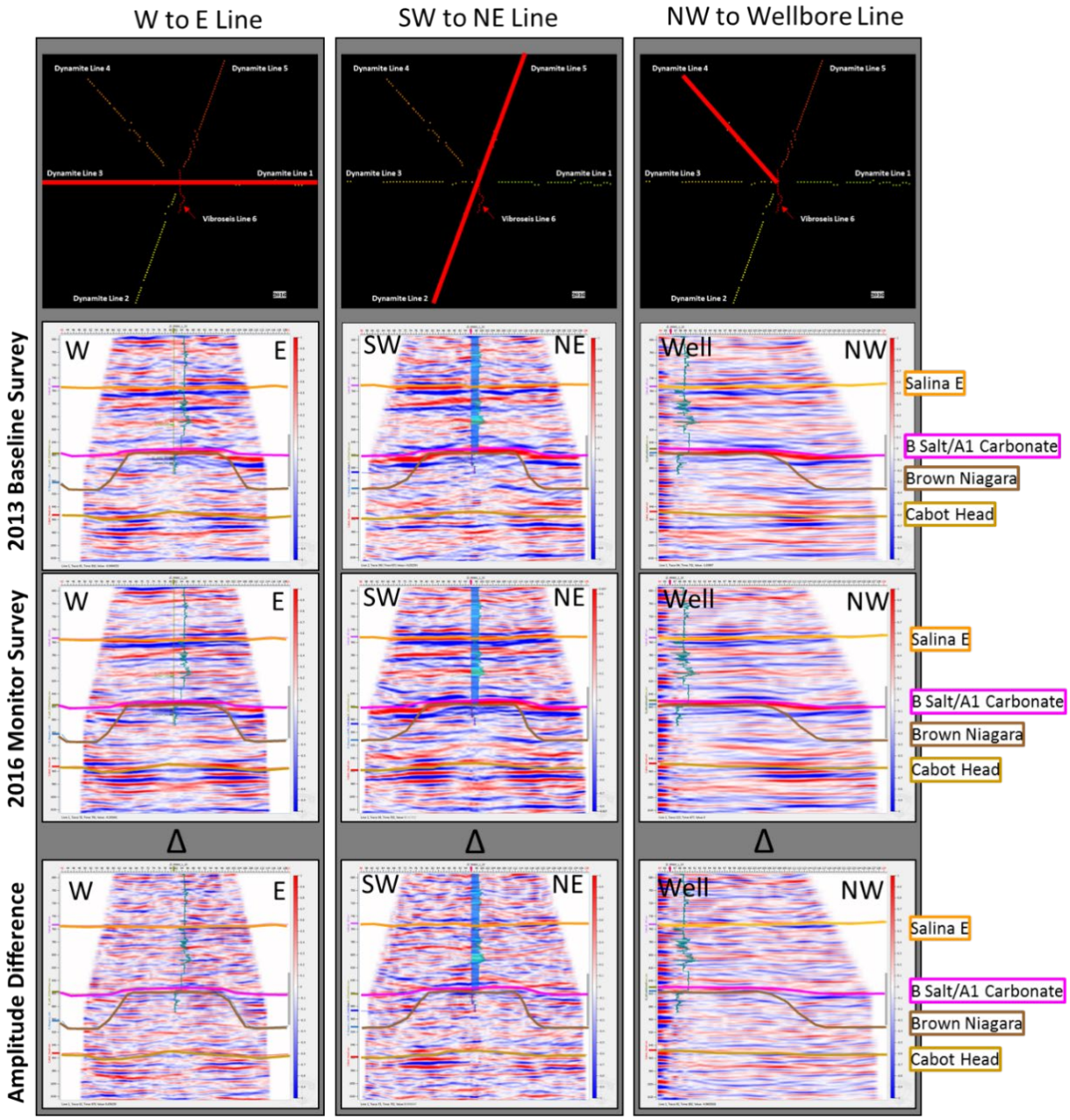

Figure 2-3. P-wave image data from the Dover 33. Top survey panel: 2013 baseline survey. Middle survey panel: 2016 monitor survey. Bottom panel: The difference (Δ) between the two.

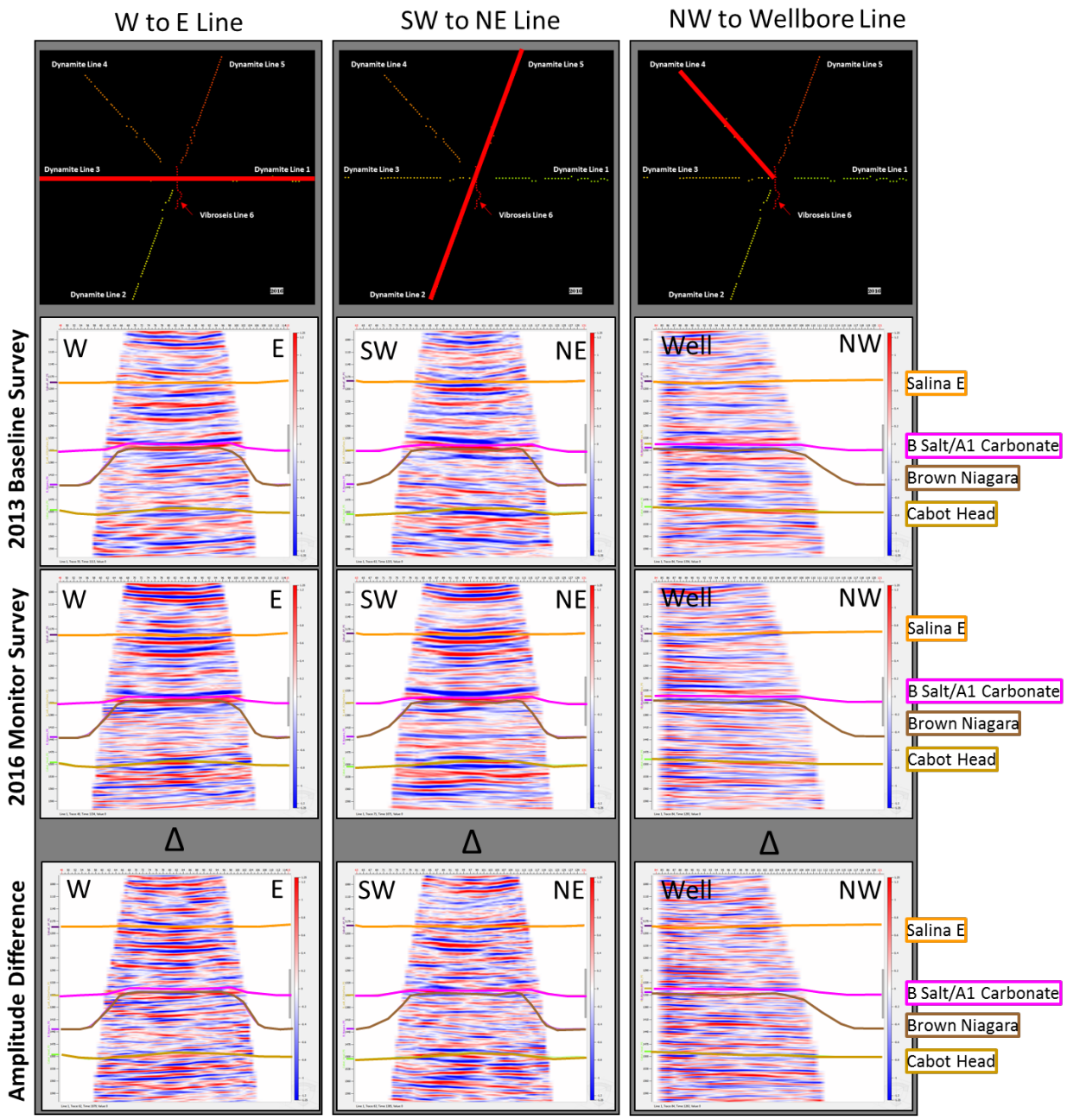

Figure 2-4. PS-wave image data from the Dover 33. Top survey panel: 2013 baseline survey. Middle survey panel: 2016 monitor survey. Bottom panel: The difference (Δ) between the two.

2.4 Discussion

The results of the impedance amplitude differencing analysis were inconclusive in showing the location of the injected CO_2. Similarly, an analysis of travel-time differences (for both P-wave and S-waves) between the baseline and repeat surveys indicated that there is not a significant difference between the two surveys. Possible reasons for this outcome are discussed below

- The 2013 VSP had a lower SNR compared to the SNR of the 2016 survey. This indicates that the quality of the 2013 VSP survey was lower than the 2016 data; therefore, the reliability of the data was somewhat compromised. While attempts were made to equalize the frequency content of both surveys and filter out noise due to differing weather and shot conditions, the difference in SNR was large enough to adversely affect the amplitude difference images and picked travel times.
- The fluid substitution effect on compressional velocity was estimated to be a decrease of 0.7% between the two VSP surveys (for a rock with 10% porosity). The estimated change in shear velocity over the same period is also a decrease of 0.7% . These results indicate that the effect of CO_2 injection into the Dover 33 reef on acoustic velocities will be very small. The predicted small changes may be below the level of detectability of seismic technologies.
- Results of laboratory testing of core samples from a newly drilled well (Lawnichak & Myszkier 9-33) in the Dover 33 reef indicate acoustic velocity sensitivity is approximately equal to air-water saturation (air was used as a proxy for water-CO_2), effective pressure, and brine- CO_2 saturations. In fact, velocities were most sensitive to change in stress (pressure), which could be responsible for masking changes due to CO_2 concentration.

One other factor that made it difficult to discern the subsurface distribution of the injected CO_2 in the Dover 33 reef is the presence of CO_2 in the reservoir pore space at the time the baseline VSP survey was obtained (February 2013). The exact amount /concentration of residual CO_2 (left over from the initial CO2-enhanced oil recovery efforts from 1996 to 2007 is not known, however, it is a fact that this would reduce the fluid substitution effect of CO_2 injection and make it more difficult to detect the CO_2 plume.

Time-lapse VSP monitoring for CO_2 storage projects has been deployed globally in clastic and carbonate reservoirs, both onshore and offshore. However, the method is most effective in rocks that are highly compressible (low dry bulk modulus [high compressibility]) and where there is a high contrast in the compressibility of fluids being substituted (i.e., saltwater with a fluid modulus of 2.25 gigapascals [GPa] (326,335 pounds per square inch [psi]) compared to live oil (oil containing dissolved gas) with a fluid modulus of 1.0 GPa (145,038 psi) or gas phase of CO_2) (Lumley et al., 1997; Lumley, 2010). Additionally, it is critical to have sufficient porosity and permeability to allow pathways for migration and subsequent storage space for the secondary fluids to be imaged (Lumley, 2010). If these variables are suboptimal, the seismic signal (impedance) caused by changes in pore fluids is far less likely to be detectable above the background noise of the dataset. In the real world, these boundary conditions for the ideal rock translate into a high-porosity sandstone.

3.0 TIME-LAPSE DISTRIBUTED ACOUSTIC SENSING (DAS) VERTICAL SEISMIC PROFILING (VSP)

3.1 Objective and Description of the Technology

Time-lapse DAS VSP was implemented at the Chester 16 reef to attempt to detect approximately 85,000 tonnes of CO_2 injected into the A-1 Carbonate and Brown Niagaran Formations.

In conventional VSPs, geophones are placed in the borehole or well for the receivers. In a Distributed Acoustic Sensing (DAS) VSP, a fiber optic cable replaces the geophones. Conventional geophones are point sensors, whereas with DAS, the optical fiber is the sensing element. A series of pulses are sent into the fiber and the naturally occurring backscattered light is recorded against time. A DAS system also includes a coherent optical time domain interferometer (instrument), commonly referred to as a lightbox or interrogator unit, at the surface connected to the fiber optical cable installed in the well. Seismic signals cause vibration, which in turn cause microscopic elongation or compression of the fiber (micro-strain). The amount of strain is measured by recording/interpreting Rayleigh backscatter light from an optical laser pulse sent through the fiber and reflected to the transmitting end. In doing this, the distributed sensor measures at all points along the fiber. DAS seismic acquisition has some significant advantages over acquisition with geophones.

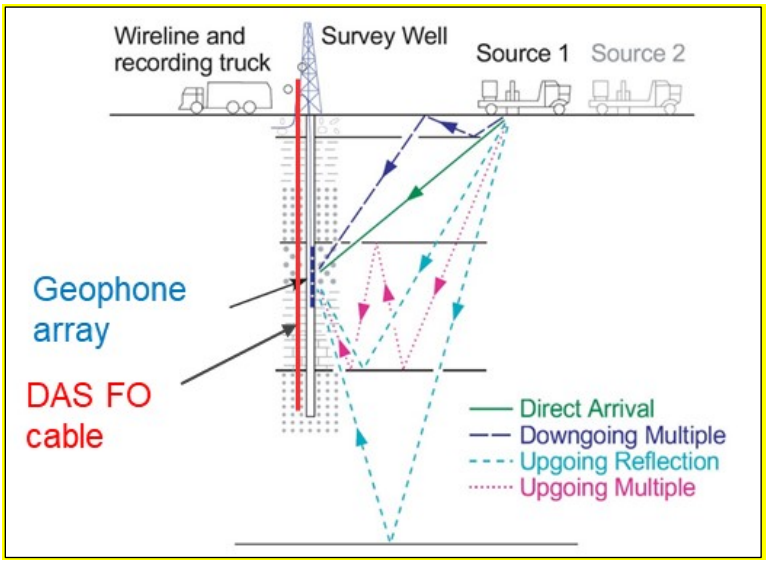

Figure 3-1. Schematic diagram of a conventional and DAS VSP survey indicating a survey well, seismic source, receiver, wireline, and recording trucks (modified from DiSiena et al., 1984).

3.2 Methodology

A baseline survey was conducted in February 2017 prior to injecting CO_2 and a repeat survey was conducted in August 2018. During the interim period between the baseline and repeat surveys, CO_2 was injected into the Chester 16 reef via the 6-16 injection well without production (withdrawal) of fluids from the reef. A grid of 181 source positions consisting of 44 vibrator positions, plus 137 dynamite shot locations, was used to give approximately continuous spatial coverage of the injection zone (A-1 Carbonate and upper Brown Niagaran) in the area between the two wells. Figure 3-2 shows the source layout and the image area at the top of the reef (5700 ft sub GL) assuming that only receivers below a depth of 2000 ft would provide useable data because the fiber optic cable above this depth was not cemented.

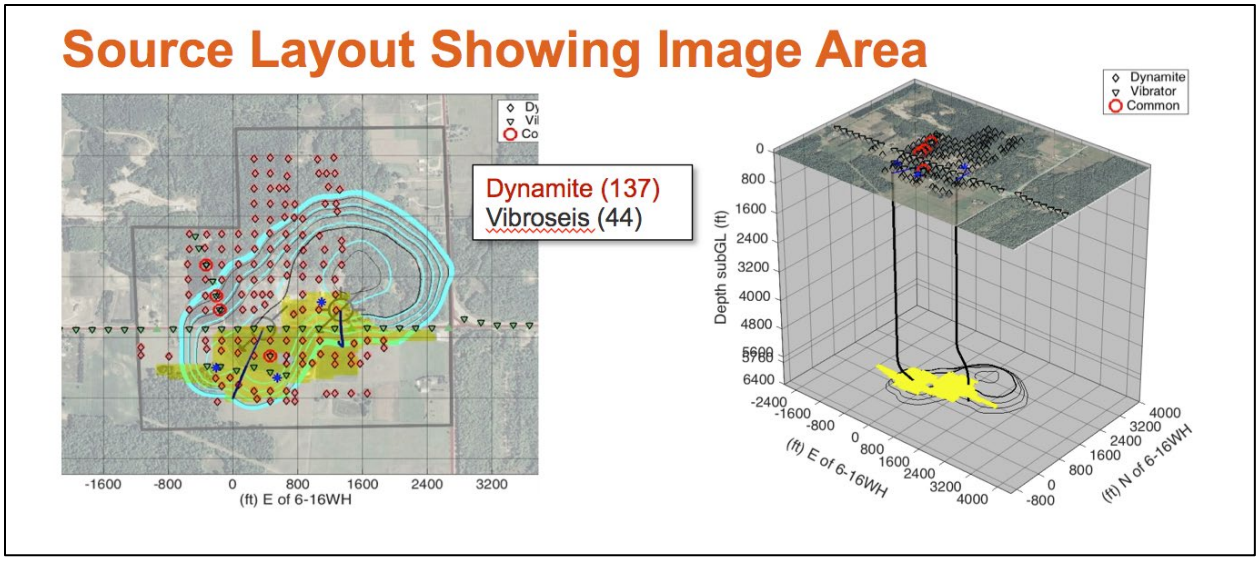

Figure 3-2. Plan view and perspective view showing the well trajectories, the reef topography interpreted from well logs and 3D surface seismic data, and the shotpoints that were chosen based on pre-job ray tracing.

Vibroseis acquisition parameters are shown in Table 3-1. Dynamite source points were mostly a 1 kg load in a 20-ft deep boring except for shot holes near houses which used a reduced load of 0.5 kg and areas with shallow groundwater which used four 5-ft borings with 0.5 kg load each.

Table 3-1. Vibroseis Acquisition Parameters.

Parameter	Baseline Survey	Repeat Survey
Number of sweeps	5 (full force) 10 (reduced force)	10 (full force) 15 (reduced force)
Number vibroseis trucks	3	3
Type	Linear	Linear
Frequency	10-150 Hz	10-150 Hz
Start / end tapers	0.5 s	0.5 s
Length	30 s	30 s
Listen time	4 s	4 s

The processing approach implemented in this study focused on monitoring the change in the amplitude of the reflection coefficient (R) between the baseline and repeat surveys due to the introduction of CO_2. Reflection coefficient is defined as follows:

$$R = \frac{AI_1 - AI_2}{AI_1 + AI_2} = \frac{\rho_1 v_1 - \rho_2 v_2}{\rho_1 v_1 + \rho_2 v_2}$$

Where AI is acoustic impedance, which is the product of bulk density of the rock-fluid system and acoustic velocity of the rock. Introduction of CO_2 into a porous layer can cause changes in density and velocity of the rock-fluid system, resulting in a change in AI within the layer or interval receiving the CO_2. This can result in a change in the reflection coefficient at the interface between the CO_2-containing layer and the overlying or underlying layer that has not received CO_2. If the magnitude of the AI contrast between adjacent intervals is sufficiently large, the effect may be visually detectable by calculating/plotting the difference in R between the two surveys.

A simple 1D vertical profile spreadsheet model was used to calculate expected change in R due to CO_2 injection to compare to actual monitoring results. The model is based on acoustic and density logs for the 6-16 well recorded after the well was drilled, but before commencing CO_2 injection. The model has seven geologic layers with homogeneous velocity and density. Seven different model scenarios were created to evaluate the effect of different magnitude changes in V and ρ on R. Only zones that received CO_2 directly via injection (A-1 Carbonate, upper portion of Brown Niagaran) and the A-2 Carbonate were adjusted. The results of the comparison indicate that the actual monitoring results compare well with the synthetic time-lapse results.

3.3 Key Results

Results of the DAS VSP study are 2-D time-lapse images that show the difference in R between the repeat survey and the baseline survey. These images combine data from multiple source locations. Ideally, the figures would have included data from all sources (i.e., vibroseis and dynamite) to provide the greatest spatial coverage of the reservoir. However, due to the low SNR of the dynamite data compared to the vibroseis data, the two source types were not combined and only vibroseis data were used in the migration process (i.e., to make the images). Consequently, the spatial coverage of the images is significantly smaller than the area that would have been realized if dynamite data were included. The well casings were not cemented completely to ground surface; consequently, only the cemented portion of the fiber optic DAS cable had sufficient acoustic coupling and provided useable data. This also reduced the image area compared to the originally planned image area.

Figure 3-3 shows a baseline and repeat reflection coefficient (RC) vertical cross section image through each well, along with a (repeat survey minus baseline survey) “difference image” for each pair of time-lapse images. The limited coverage of each image is because the images were produced from only vibroseis data. The images cover an area close to the 6-16 injection well and the 8-16 monitor well. The imaged area near the injection well is particularly small. The difference image for the area near the 6-16 well shows difference features within the injection interval (A-1 Carbonate Crest and upper Brown Niagaran); however, difference features with similar magnitude also appear above and below the injection interval. Therefore, these results are encouraging but not unequivocal. The difference image for the 8-16 monitoring well does not show difference features associated with the injection interval.

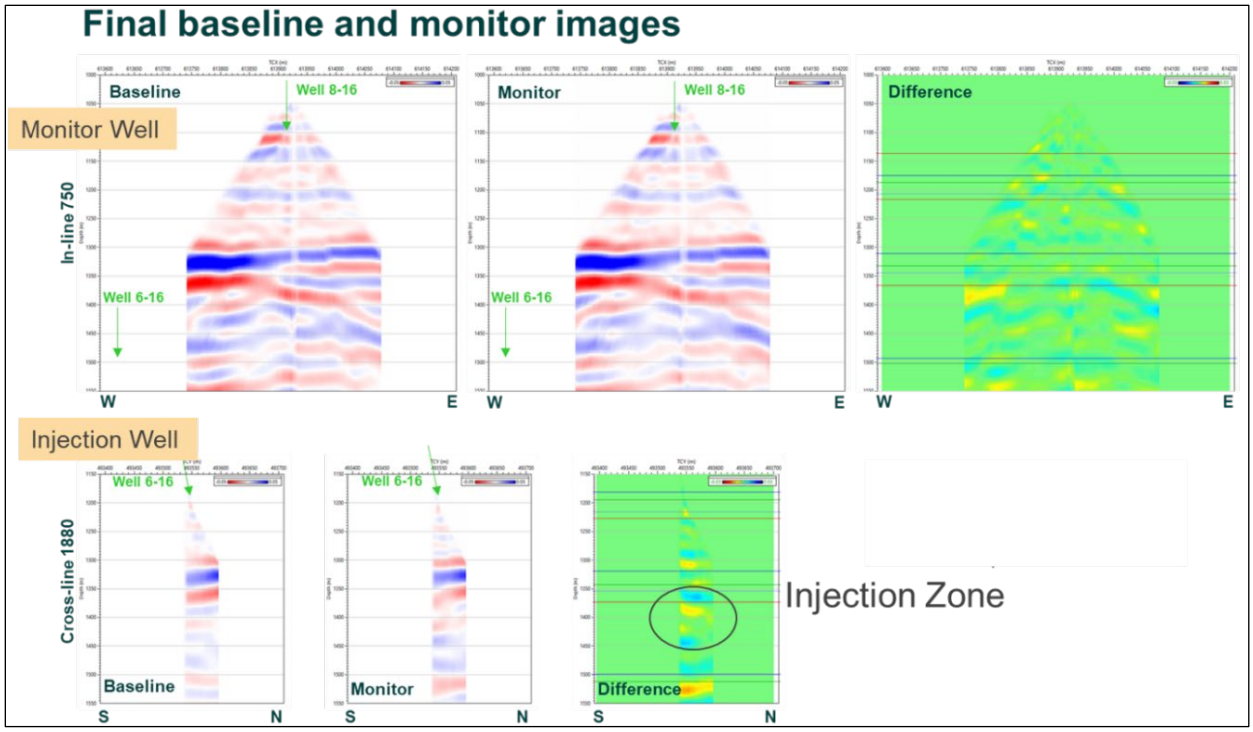

Figure 3-3. Final baseline and repeat migrated images for well 8-16 and well 6-16.

The difference images for the area near the 6-16 (injection) well show difference features within the injection interval (A-1 Carbonate Crest and upper Brown Niagaran) as expected; however, difference features with similar magnitude also appear above and below the injection interval, including areas where CO_2 is unlikely to exist. Therefore, these results are encouraging but not unequivocal. The difference image for the 8-16 monitoring well does not show a pattern (clustering) of difference features that suggests CO_2.

3.4 Discussion

This DAS VSP study was partially successful for detecting CO_2 injected into the Chester 16 pinnacle reef. The DAS monitoring results indicate a measurable change (decrease) in seismic reflection coefficient in the A-1 Carbonate and Brown Niagaran Formation (i.e., the two injection intervals, in the area near the 6-16 injection well). However, difference features were also indicated in strata above and below the injection zone. The DAS data also produced reflection coefficient (RC) difference features in the vicinity of the 8-16 monitoring well, both within the injection zone and outside the injection zone, casting doubt on the results.

For DAS VSP technology to clearly detect the injected CO_2, the injected fluid must cause a change in AI (velocity and/or density) large enough to cause a change in RC that can be visibly detected. Laboratory tests and fluid substitution modeling both suggest the seismic response to CO_2 injection will be small (~5% change in acoustic velocity Vp). Such a small change in AI will have a minor effect on R. This is a physics-based limitation and therefore cannot be avoided.

Other acquisition factors likely limited the effectiveness of the DAS VSP technology. These include the following.

- Dynamite signals were weak compared to vibroseis so the two data types could not be combined. Doing so raised the lower limit of detection (i.e., reduced the overall SNR). Therefore, the time-lapse (difference) analysis was done using only the higher quality vibroseis data. This reduced the image area to the immediate area surrounding the 6-16 and 8-16 wells rather than the area between the two wells as originally planned. It also created the possibility that area(s) with CO_2 were missed.
- The well casings were not cemented completely to ground surface; consequently, only the cemented portion of the fiber optic DAS cable had sufficient acoustic coupling and provided useable data. This also reduced the image area compared to the originally planned image area.
- The vibroseis data from the repeat survey had significantly lower (better) SNR than the baseline vibroseis data. This is most likely because more sweeps were performed at each vibroseis source location in the repeat survey compared to the baseline survey. Vibroseis acquisition parameters were modified for the repeat survey. When repeated, the number of sweeps was increased from five to 10 (full force locations) and from 10 to 15 (reduced force locations).
- In this study, the injection tubing string in the 6-16 injection well vibrated during the acquisition of the VSP (due to dynamite or vibroseis energy waves impacting the tubing string), which adversely affected the acquired DAS data. In future DAS VSP surveys, it may be worthwhile to remove the injection tubing string, if present, prior to acquiring the data.
- A larger mass of injected CO_2 might have been easier to detect. The repeat DAS VSP survey was conducted after injecting only 85,000 tonnes of CO_2, which was earlier than originally planned. Originally, the repeat survey was planned after the fill-up phase, which occurred after injection 5.3 BCF of CO_2 (approximately 280,000 tonnes). It was necessary to conduct the repeat survey earlier than planned because Core Energy was considering converting the 8-16 monitoring well to a horizontal injection well, which would have precluded further DAS monitoring in this well.

These acquisition factors can be avoided in future DAS VSP studies if preventive measures are taken.

4.0 CROSS-WELL SEISMIC MONITORING

A cross-well seismic survey was acquired in the Chester 16 reef from September 9 to 14, 2018 to attempt to locate 85,000 tonnes of CO_2that were injected into the A-1 Carbonate and Brown Niagaran Formations between February 2013 and September 2018. Conducting multiple cross-well seismic surveys over time (i.e., time-lapse cross-well seismic), which includes conducting a pre- CO_2 injection (baseline) survey, has been used elsewhere to monitor CO_2 injected into the subsurface. In this study, a baseline cross-well survey was not obtained; nevertheless, it was possible to generate an image that is a plausible, albeit not without anomalies, representation of the CO_2 plume. This conclusion is supported by other monitoring and modeling results from the Chester 16 reef that provide an independent indication about the likely position of the injected CO_2.

4.1 Objective and Description of the Technology

A cross-well seismic survey was acquired in the Chester 16 reef from September 9 to 14, 2018 to attempt to attempt to detect and delineate 85,000 tonnes of CO_2 that were injected into the A-1 Carbonate and Brown Niagaran Formations between February 2013 and September 2018.

Cross-well seismic profiling is a form of borehole geophysics that is conducted between a pair of wells with the source (tool) and receiver (array) each placed inside one the wells, as illustrated in Figure 4-1. In cross-well seismic imaging, a seismic source is placed in a wellbore and receivers in a nearby wellbore to provide high resolution images and estimates of reservoir properties between the wells (Figure 4-1). The receiver array is held fixed in one well while the source tool is moved upwards in the other well in small increments, whereby at each position the source tool is “activated.” A typical survey will involve numerous source points spanning the target interval. After one complete source run, the receiver array is repositioned (moved up by some specified distance that is less than the distance between geophones) and the source run is repeated. The advantages of cross-well imaging over surface seismic include the dramatic increase in available resolution in reflection imaging and the ability to directly measure a 2-D velocity field using tomography.

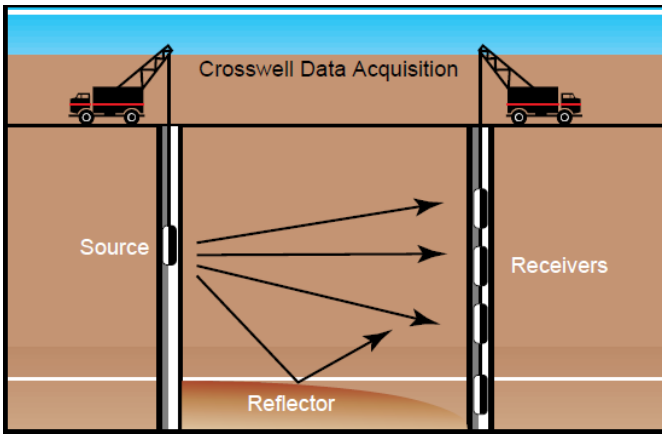

Figure 4-1. Cross-well data are collected by placing a seismic source in one well and a receiver string in a nearby well. Energy that propagates directly between wells without being scattered (i.e., direct arrivals) serves as the basis for constructing velocity images (tomograms). Energy that is reflected is used to construct reflection images (source: Harris and Langan (2001)).

The distance between the source and receivers (i.e., the well spacing) is considerably less than the propagation distances associated with surface seismic methods. This allows the use of much higher source frequencies than what is used with surface seismic methods, resulting in a significant increase in spatial resolution. Cross-well surveys can employ a frequency band between 20Hz and 2000 Hz, depending on the type of source used, the distance between wells, and the attenuation characteristics of the zone under investigation. The resolution of cross-well reflection imaging in carbonate reservoirs has been demonstrated to be 10 times or greater than that of surface seismic data, with vertical resolution of 5 to 10 feet.

Cross-well seismic tomography is the process of generating p-wave and s-wave velocity maps (tomograms) for the interwell region. The velocity field is usually represented by a color-coded map referred to as a tomogram, in which a color is assigned to the seismic velocity at each point. Because CO_2 causes a change in velocity, time-lapse cross-well tomography can reveal areas where velocity has changed due to CO_2. The method can reportedly identify a minimum velocity change of 1-2% provided the velocity anomaly is large enough to affect several raypaths and be identifiable in direct-arrival picks. In the case of the chester 16 crosss-well seismic survey, the cross-well tomography method was not successful due to complications caused by the deviated wells and the complex reef geometry. Therefore, an alternate workflow using Full Waveform Inversion (FWI) was used.

4.2 Methodology

Pre-job modeling was performed to design the cross-well survey prior to acquiring the data. The target interval for imaging CO_2 is a 400-ft thick interval from 5800 to 6200 ft MD, which spans all the A-1 Carbonate and the upper 230 ft (6-16 well) to 284 ft (8-16 well) of the Brown Niagaran. This interval also encompasses four of the five perforated intervals in the 6-16 injection well (Figure 4-2).

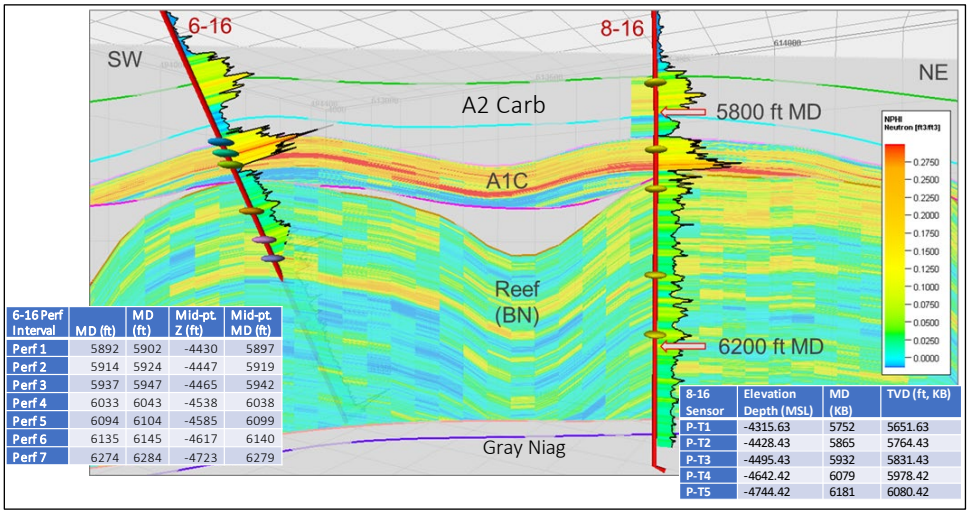

6-16 Perf Interval	MD (ft)	MD (ft)	Mid-pt Z (ft)	Mid-pt MD (ft)
Perf 1	5892	5902	-4430	5897
Perf 2	5914	5924	-4447	5919
Perf 3	5937	5947	-4465	5942
Perf 4	6033	6043	-4538	6038
Perf 5	6094	6104	-4585	6099
Perf 6	6135	6145	-4617	6140
Perf 7	6274	6284	-4723	6279

8-16 Sensor	Elevation Depth (MSL)	MD (KB)	TVD (ft, KB)
P-T1	-4315.63	5752	5651.63
P-T2	-4428.43	5865	5764.43
P-T3	-4495.43	5932	5831.43
P-T4	-4642.42	6079	5978.42
P-T5	-4744.42	6181	6080.42

Figure 4-2. Porosity cross-section showing depth of the 7 perforated intervals in the 6-16 well relative to the 400-ft thick target imaging interval from 5800 to 6200 ft.

The data was acquired by conducting five passes (fans) with the source tool in the 6-16 well, each time revisiting the same source depth points, across a 1,930-ft long interval extending from 4560 ft MD to 6490 ft MD in the 6-16 well. This interval spans 685 feet of the F-Salt and extends through 520 feet (out of 543 feet) of the Brown Niagaran. The source tool was activated every 10 feet during each pass, resulting in approximately 140 source activations per pass. The receiver array contained 35 geophones spaced 50 ft apart and spanned a 1,700 ft long interval that extends from 205 feet below the top of the F-

Salt through 385 feet of Brown Niagaran (out of 416 feet). For each consecutive source run, the receiver array was moved up 10 feet in the 8-16 well. Therefore, the effective receiver spacing, after combining all five fans, was 10 feet rather than the geophone spacing of 50 feet. This is illustrated in Figure 4-3.

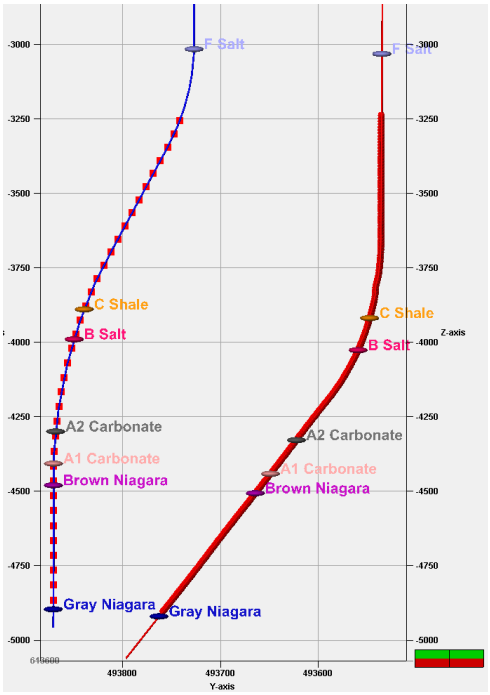

Figure 4-3. Fan 1 Receiver positions (left) and source activation points (right).

Data were processed using the FWI method. The FWI process requires an initial (velocity) model. In a typical time-lapse study, the initial velocity model would be created from the baseline (pre- CO_2 injection) cross-well seismic survey. However, in this study, a baseline cross-well seismic survey was not conducted. Therefore, an initial velocity model was created using pre-injection well (sonic) logs, realistic formation surfaces, and anisotropy estimates from the cross-well tomogram. This initial velocity model represents the pre- CO_2 injection baseline velocity field. Then, a post- CO_2 injection velocity distribution is calculated using a wavelet extracted from the actual cross-well seismic data. The process is repeated using gradually higher frequency wavelet (in this study, the process was successfully done with 55 Hz and 75 Hz wavelets. Then, the pre/post injection models are differenced to arrive at the final image in the workflow, which shows change in velocity due to CO_2 injection.

4.3 Key Results

The images presented in Figure 4-4 and Figure 4-5 show the interpreted CO_2 distribution (i.e., plume) based on the cross-well waveform tomography results. Figure 4-4 shows the final post- CO_2 injection velocity distribution using a wavelet with a frequency of 55 Hz, subtracted from the starting model. Figure 4-5 is the FWI image produced using a 75 Hz wavelet.

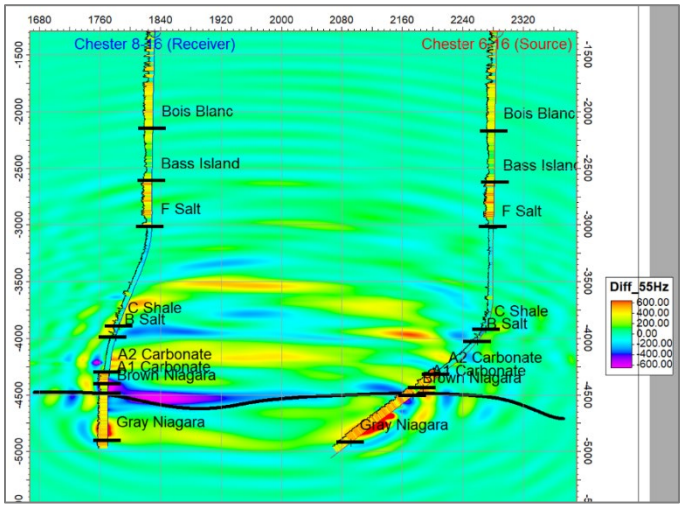

Figure 4-4. Compressional Velocity Difference Tomogram for 55 Hz Source Wavelet. Bold line is top of Brown Niagaran. Zone of major velocity change occurs in A-1 Carbonate.

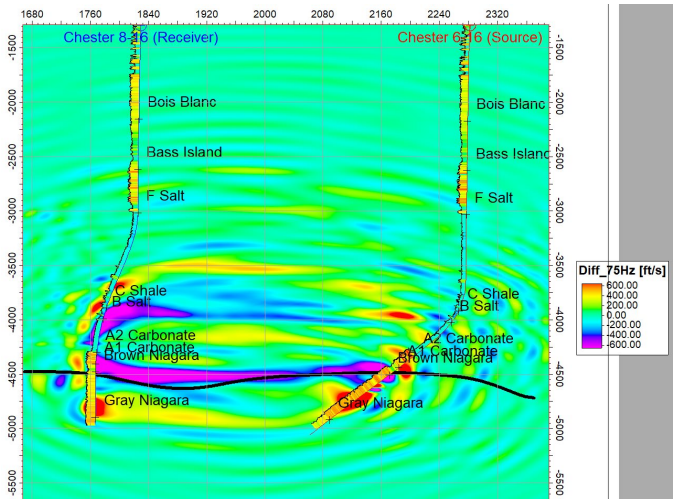

Figure 4-5. Compressional Velocity Difference Tomogram for 75 Hz Source Wavelet.

The most obvious feature in these figures is the collection of small discontinuous areas of apparent velocity change, with magnitude spanning from -400 (blue) to +600 ms (red), arranged in a swirl pattern around the two wells. These features are interpreted to be artifacts of the finite difference wavefield modeling. While the swirls appear to be anomalous, there is at least one zone that is plausibly due to the CO_2 plume, specifically the large purple-colored lens-shaped area just above the Brown Niagaran near the 8-16 monitoring well where velocity decreased by 600 ms. The location of this “cold spot” coincides with the A-1 Carbonate, which is one of two zones where CO_2 was injected at the 6-16 well. Also, this result is corroborated by other monitoring results (Distributed Temperature Sensing [DTS], PNC, pressure monitoring) for the Chester 16 reef. This also indicates the existence of the CO_2 plume in this same interval at the monitoring well location. The purple cold spot extends laterally in the A-1 Carbonate toward the injection where a blue cold spot (-400 ms) occurs. The two zones do not connect in Figure 4-4 but they do connect in Figure 4-5.

4.4 Discussion

Cross-well seismic was successfully implemented in this study to delineate CO_2, despite the fact that a pre-injection baseline survey was not performed. Nevertheless, it was still possible to generate an image that is a plausible representation of the CO_2 plume. This conclusion is supported by other monitoring and modeling results from the Chester 16 reef that provide an independent indication about the likely position of the injected CO_2. To the authors' knowledge, this is the first time this has been done. There no precedents for a successful cross-well seismic survey without a baseline survey, nor are there known examples of cross-well seismic examples in carbonate pinnacle reefs or using deviated wells.

5.0 INSAR

5.1 Objective and Description of the Technology

Battelle evaluated the potential use of Interferometric Synthetic Aperture Radar (InSAR) for monitoring the land surface deformation from the injection of CO_2 into the Dover 33 reef near Gaylord, Michigan. InSAR monitoring was applied to three separate time periods for the MRCSP project: Historical (1992-2000), Baseline (April 22, 2012 – October 23, 2012), and Long-Term Monitoring (April 22, 2012 – March 22, 2015). While the focus of the study was on the Dover 33 reef, the InSAR technology provided information for a 30 square-mile area that included the Dover 33 reef and several other reefs in the area that CO_2 injection was occurring. In addition, Artificial Corner Reflectors (ACRs) were installed and used at the MRCSP test site to improve the capability of the InSAR system in the study area that is often snow covered and has areas with dense vegetation and wooded lots.

Battelle conducted surface deformation monitoring and analysis for the Dover 33 reef to meet the following objectives:

- Contributing to the understanding of the CO_2 migration through the reservoir and how injection operations interact with the rest of the geologic column;
- Assessing technology performance and deploy adaptive methods, such as ACRs, to address snow coverage, vegetation, topography; and
- Building knowledge and experience in this potentially practical, cost-effective monitoring approach for future commercial-scale applications in similar settings.

InSAR is a satellite-based technology that provides high-precision information on the movement of ground surface in areas with high radar coherence (e.g., roads, buildings, bare soils). Depending on the setting, this technique may provide a useful tool for characterizing reservoirs by measuring surface deformations from activities such as brine water disposal; production of water, oil, and/or gas; and carbon capture, utilization, and storage (CCUS). The InSAR data package includes three main sets of data: (1) Geographic Information System (GIS) spatial data including displacement rates, cumulative displacements, and standard deviations); (2) time series graphs of measured points used to calculate displacement rates with linear regressions; and (3) database of shapefiles used to create the maps. The attractiveness of InSAR as a monitoring technology stems from:

- InSAR's ability to cover a large area remotely, this technology could be a cost-effective method to demonstrate storage security;
- Adding to the collective knowledge about the capabilities of this technology;
- Adding to the collective knowledge about the surface responses to CO_2 injection (in this case, the expected surface response was none).

InSAR technology has been used to monitor small-scale surface-level changes in response to the injection of CO_2 in the subsurface at other carbon sequestration test sites. The most prominent example is the In Salah project in Algeria, in which an injected mass of 3 million tons of carbon dioxide produced a measurable surface displacement of approximately 5 millimeters (mm)/year (yr).

This research was conducted for MRCSP because remote sensing technologies for monitoring land surface deformation can be a cost-effective method to demonstrate long-term geologic storage security. Where it can be applied, InSAR may become one of the essential methods for monitoring commercial-scale CO_2 injection efforts by providing large-scale snapshots of the surface response to elevated pressure over time, including inaccessible areas. This large-scale test provides a unique opportunity to

gain knowledge and experience in applying InSAR for CCUS monitoring, necessary to build capacity for future commercial-scale deployment.

5.2 Methodology

Deformation monitoring and analysis was performed for the late stage (Dover 33) reef. ACRs were used to monitor local deformation in areas with low radar coherence (e.g., areas with dense vegetation coverage) and to mitigate for snow coverage. InSAR methods work best in environments with low topographic relief, sparse or low-lying vegetation, and minimal changes to the land cover over time. The technical approach of the study included the following major activities:

1) Historical deformation study;
2) Baseline monitoring; and
3) Long-term deformation monitoring and analysis in response to CO_2 injection (with ACR installation prior to the restart of injection).

HISTORIC DEFORMATION STUDY

The purpose of the historical deformation study was to determine if large-scale ground movements could be detected over an 80 square kilometer (30 square mile) area of interest (AOI) that encompasses the Dover 33 reef and other reefs involved in CO_2-EOR, as well as a nearby natural gas storage field. TRE Canada completed the historical study using 60 images collected by the European Space Agency's European Remote Sensing (ERS) satellite between 1992 to 2000. The ERS mission was launched in 1992 and InSAR data was collected until 2000, providing a comprehensive, multiyear record of satellite data. TRE procured and processed the 60 SAR images with its proprietary SqueeSAR algorithm over a period of 6 weeks, with 51 of the 60 satellite images being usable for the analysis.

The data processing led to a density of 33 measurement points per square mile, which is in the lower range of expected values. This relatively low density was likely caused by the challenging ground conditions, the low quality of the data set, including gaps in imagery, and the low resolution of older satellite imagery. However, the conditions were suitable for the use of advanced processing algorithms such as SqueeSAR to monitor local deformations in areas with high radar coherence (e.g., roads, buildings, bare soils) that provided sources of stable permanent scatterers (PS) and distributed scatterers (DS).

BASELINE DEFORMATION STUDY

The baseline analysis was conducted on the first six months of radar imagery acquired from the COSMO-Skymed (CSK) constellation of satellites from April 22, 2012 through October 23, 2012. A total of 22 satellite images were obtained (a minimum of 15 images is required to reach a statistical robustness of results). The nature of the terrain, with low wooded slopes, farmed fields, and open areas, provided a reasonable density of natural reflectors. The SqueeSAR processing algorithm provided a density of 545 measurement points per square mile. Buildings and other man-made structures, as well as natural features such as exposed ground, are likely sources of stable PS and DS targets.

LONG-TERM DEFORMATION STUDY

While the focus of the study was the Dover 33 reef, the AOI covered a broader area in order to compare data over the Dover 33 reef with regional trends and with other reefs. The radar imagery available for the analysis consisted of 76 images acquired between April 22, 2012 and March 22, 2015. All images were acquired by CSK from a descending orbit.

Continuous CO_2 injection into the Dover 33 reef under the Midwest Regional Carbon Sequestration Program (MRCSP) began in March 2013 and was halted in August 2014 after reaching a bottom hole pressure (BHP) of approximately 3,300 pounds per square inch (psi) in the Lawnichak-Myszkier (L-M) 1-33 injection well. Ground surface movement trends across the entire AOI (including the Dover 33 reef) were measured both before and during CO_2 injection, using natural radar targets and 26 ACRs. Satellite imagery was processed in two steps for the current analysis. One processing effort comprised the full stack of images (full data set) from the start of satellite image acquisitions until the end of March 2015, while the second processing effort was performed on all images acquired after the start of CO_2 injection (co-injection data set).

The AOI was updated from 80 to 81 square kilometers (31 to 32 square miles) to include an additional reef (Charlton 19) located in the northeastern portion of the previous AOI. Battelle contemplated adding this new reef to the detailed monitoring program; however, timing of the new reef flood did not fit the program, so the monitoring analysis was ultimately limited to the Dover 33 reef.

5.3 Results

HISTORIC DEFORMATION STUDY

Data from the Historic Deformation Study indicate that most points throughout the AOI displayed little or no displacement over the period of analysis. No significantly strong ground deformation trends were visible (cumulative deformation was within 10 mm) at the majority of targets and an average surface deformation rate of -1.2 ± 0.5 mm/yr was identified for the AOI. The cause of this deformation is unknown but believed to be natural and the result of weather-related events, such as frost heaving and thawing. The line-of-sight (LOS) displacement rates for Dover 33 indicate no apparent differences in deformation between the on- and off-reef points. A low standard deviation of 0.5 mm/yr is due to the large number of images used in the data processing. Displacement values are calculated from a linear regression of the ground movement measured over the entire period covered by the satellite images.

The historical analysis indicated there was a mild seasonal component present over part of this area (typified by the appearance of cyclical deformation patterns). Therefore, it was expected that similar patterns would develop in the Baseline and Long-Term Deformation Studies. TRE indicated it would be possible to normalize the data for seasonal effects, and any statistically significant movement related to operations could then be isolated. The historical deformation analysis increased confidence in the ability of the technology to assess land surface deformation in this forested and agricultural area.

BASELINE DEFORMATION STUDY

The results indicate the 80 square kilometer AOI is predominantly stable with over 90% of the measurement points showing minimal deformation (displacement less than 5 mm) and an average surface deformation rate of -1.1 mm/yr relative to the reference point, which is outside the AOI. However, there are areas that display mild subsidence. The lower precision compared to the historical analysis is due to the small number of images. A zone of subsidence was observed in the area immediately north of the South Chester 15 gas storage field, but field observations revealed this zone was clear cut of trees just before or during the baseline monitoring period. The baseline monitoring around the Dover 33 reef indicates nearly all of the measurement points remained relatively stable with a cumulative displacement of ±5 mm over the monitoring period. The average data indicates there was a small amount of subsidence (-2 mm) over the baseline monitoring period, which is within the standard deviation of the data (±3.7 mm). In addition, there does not appear to be a difference in cumulative displacement between measurement points located over the reef compared to measurement points located off the reef. Finally,

there does not appear to be a spatial trend to the data (i.e., greater displacement toward the center of the reef and decreasing away from this location). It appears that measurement points with greater displacement are surrounded by points with little to no displacement.

LONG-TERM DEFORMATION STUDY

Cumulative displacement amounts across the AOI during the Long-Term Monitoring period (full data set) were between -60.5 to 50.7 mm, and slight uplift was observed, with an average uplift of 1.2 mm. These relatively large displacement values appeared at individual points and were very localized movements. However, a few areas of subsidence were detected (mostly outside the reef structures).

For the full data set, an average surface deformation rate of 0.04 ±0.4 mm/yr was identified within the nine reefs, compared to -0.2 ±0.4 mm/yr for the entire AOI (Figure 5-1). Maximum values ranged from -20.0 to +16.7 mm/yr over the reefs and from -21.4 to +16.7 mm/yr over the entire AOI.

For the co-injection data period, an average surface deformation rate of 1.0 ±0.9 mm/yr was identified within the nine reefs with a range of -16.6 mm/yr to +5.0 mm/yr. In the remainder of the AOI, an average surface deformation rate of 0.3 ±0.9 mm/yr was obtained, with rates ranging from -16.6 mm/yr to +15.8 mm/yr. Average displacement values are calculated from a linear regression of the ground movement measured relative to the reference point over each measurement period.

Surface deformation near the Dover 33 reef was measured using natural radar reflectors and ACRs installed in 2013, leading to 111 measurement points around the reef. Each point on the map corresponds to a PS or DS and is color-coded according to its annual rate of movement. Ground deformation rates from natural radar targets over the Dover 33 reef in the full data set showed little movement, with average rates of -0.3 mm/yr (Figure 5-1). A cumulative displacement of 0.7 mm was measured by the natural reflectors over the full data set and 1.2 mm during the CO_2 injection phase.

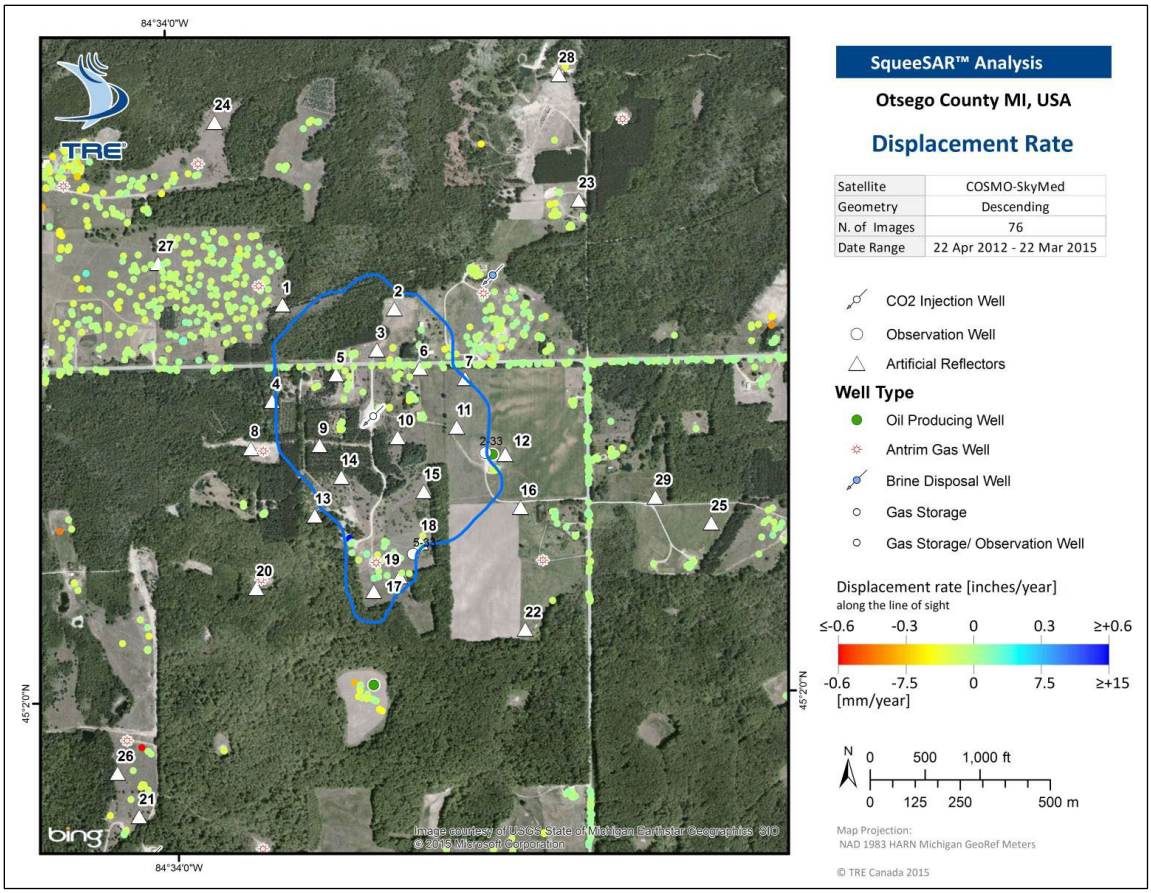

Figure 5-1. Displacement results from the full data set over the Dover 33 reef.

A total of 44 images were collected and processed for the ACR analysis between May 03, 2013 and March 22, 2015. Displacement rates over Dover 33 were between -0.1 mm/yr and +3.9 mm/yr. An average deformation rate of 1.1 mm/yr was obtained from the ACRs over Dover 33, while the average for all ACRs outside the reef was 0.01 mm/yr (Figure 5-2). The results indicate the reflectors within and outside of Dover 33 are mainly stable.

Displacement rates of all ACRs are minimal, ranging from -1.5 mm/yr to +3.9 mm/yr, with an average of +0.4 mm/yr. The five ACRs closest to the injection well were ACR 3, 5, 6, 10, and 14, and have displacement rates ranging from +0.2 to +2.4 mm/yr. Some of the fluctuations in the ACRs across the area are believed to be weather-related and due to snowfall in winter. These trends are visible in the time series analyses of the ACR data (ACR 14, 15, 20, 26), but no ground deformation trend related to CO_2 injection operations is observed in the ACR results. A +3 mm uplift is observed in the ACRs between November 2014 to February 2015, but this uplift is also noted across the entire AOI and is likely unrelated to injection activities and probably caused by a natural event, such as frost heaving.

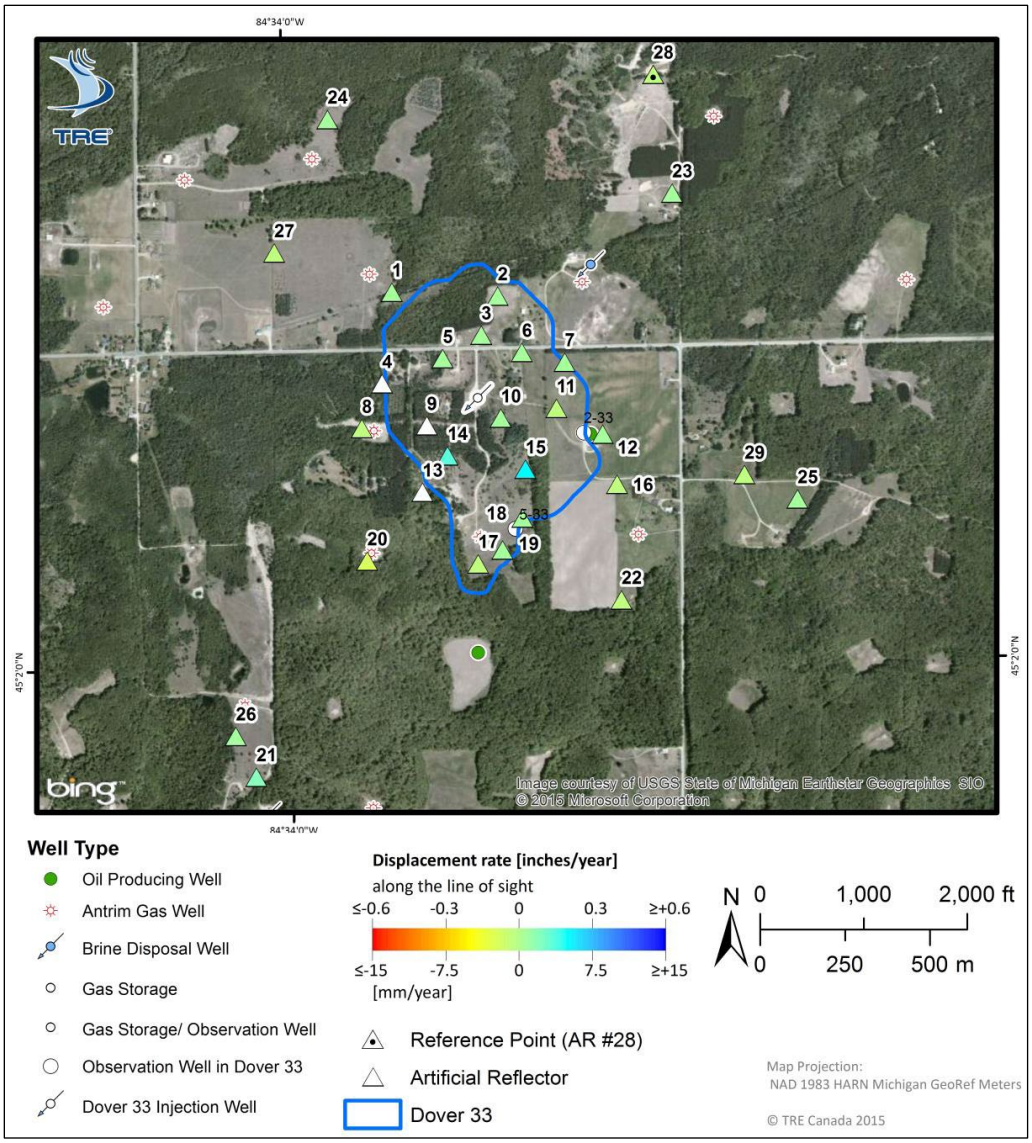

Figure 5-2. Average Displacement results from the full data set over the Dover 33 reef.

A comparison between the surface deformation and the reservoir pressure was performed to determine if there was a correlation between deformation and pressure. The reservoir pressure increased from approximately 800 psi to over 3,300 psi with the injection of 244,000 tons of CO_2, but the ground deformation measured with the ACRs and natural reflectors remained within ±5 mm and no discernable correlation between surface deformation and reservoir pressure was determined.

5.4 Discussion

InSAR was used to monitor ground surface deformation over the Dover 33 reef during carbon capture and storage (CCS) operations in three stages. An initial historical analysis covering the timeframe of 1992 to 1999 using the ERS satellite provided an overview of natural ground deformation over the 83 km2 AOI. A second analysis provided a baseline monitoring over a period of six months (April 2012 to October 2012) prior to the start of CO_2 injection into the Dover 33 reef. While this analysis focused on the Dover 33 reef, ground deformation data were collected from the entire AOI. Further processing provided ground deformation measurements during the Dover 33 CO_2 injection with 16-day satellite revisit data from April

2012 to March 2015. A total of 29 ACRs were installed in 2013 to supplement the distribution of natural measurement points within and around the Dover 33 reef.

The results of the current monitoring analysis indicate there was no discernible ground surface response to CO_2 injection into the Dover 33 reef, either from natural radar targets or artificial reflectors. Deformation trends remain similar to those observed in the baseline results. This was confirmed both in the spatial domain (Dover 33 vs AOI) and the temporal domain (co-injection vs full processing data sets). Finally, no correlations were observed in the comparison of ground deformation against the reservoir pressure and injected CO_2 volume. The small degree of deformation observed during the monitoring is generally localized to single monitoring locations and believed to be the result of natural events, such as freeze/thaw cycles or near surface aquifer drawdown/recharge.

The ACRs exhibited average displacement values of 1.1 mm/yr over the Dover 33 reef and 0.01 mm/yr outside the reef. However, no clear ground deformation in response to the CO_2 injection was observed when comparing the deformation data to the CO_2 injection and reservoir pressure data. Further, the geomechanical study predicted that no surface deformation would be anticipated as the result of the mass of CO_2 injected into the Dover 33 reef. The signature of the ground movement observed at the In Salah project in Algeria was contrasted with the lack of uplift observed at the Dover 33 reef. The comparison highlights the completely different behavior of ground surface response between the two sites.

6.0 PULSED NEUTRON CAPTURE TECHNOLOGY

6.1 Objective and Description of the Technology

Pulsed neutron capture (PNC) logging is used to identify the presence of reservoir fluids in cased-holed wells and to aid in monitoring the migration of injected CO_2. The goal of this study was to monitor CO_2 migration, storage integrity, and to test the viability and effectiveness of the PNC technology on reefs in various stages of CO_2-EOR activities in low porosity-permeability fields.

The PNC tool emits a neutron burst and then measures the neutron reaction, absorption or scattering, of target elements. The rate of reaction, in time, is measured between detectors on the tool to generate a log of the response. Each measurement is associated with a fluid type, such as hydrocarbons and water. Formation brines and hydrocarbons all have a measurement value which can be used to determine fluid saturations at various depths surrounding the borehole. These measurements are used to determine fluid saturations and lithologies in near wellbore conditions.

The fields studied by MRCSP were in various stages of production life-cycles: highly depleted fields that have already undergone significant CO_2-EOR in the past and were used solely for CO_2 storage (no production) and those currently undergoing CO_2-EOR. Reefs for PNC monitoring within the MRCSP study were selected to incorporate reefs in various stages of life cycles, lithologies and porosities to present a comprehensive analysis of PNC effectiveness for saturation analysis. Figure 6-1 shows the reefs where PNC monitoring was conducted.

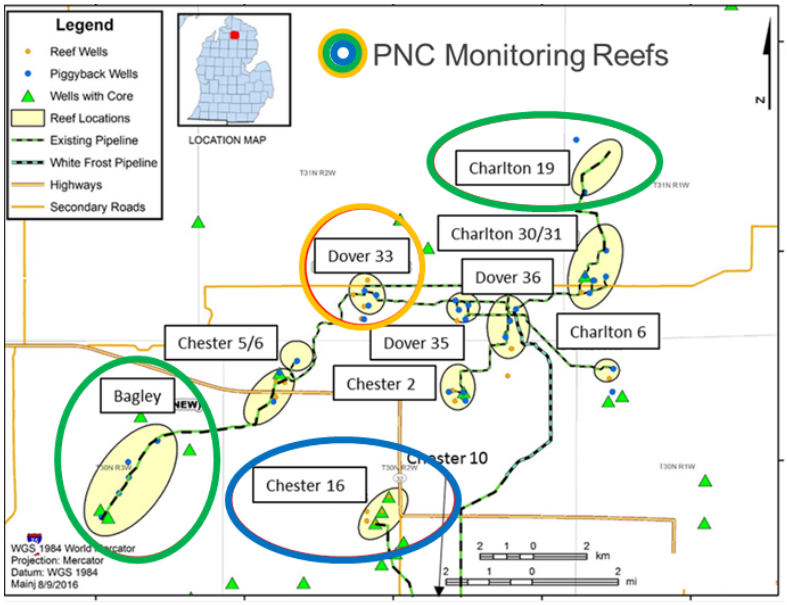

Figure 6-1. Map of PNC monitored reefs. Yellow circle is the depleted CO_2-EOR reef, Dover 33. Green circles indicate active CO_2-EOR reefs, Charlton 19 and Bagley. The blue circle indicates the new CO_2-EOR reef, Chester 16.

6.2 Methodology

Within the MRCSP monitoring program, for PNC logging and modeling analyses, workflows were generated for consistency. They included: 1) well configuration, 2) field logging and data acquisition of wireline logs to determine well conditions, and 3) analysis of finalized saturation profiles.

- Well Configuration, during the extended logging program, different completion scenarios were encountered and studied, resulting in an understanding of the completion design best suited for monitoring within the constraints of field operation. A preferred tubing configuration was constructed to ensure consistency in logging procedures between baseline and repeat logging events. Logging was conducted through tubing and with a packer if there were the presence of perforations in the well. The packer was set above the perforations with the tubing extended through the logged interval with enough pipe to ensure the tool string is secure within the tubing during the logging run.
- Acquisition of wireline logs were conducted to determine if changes in porosity occurred over the monitoring program. Changes in porosity influence the PNC logging measurements. Increases in porosity allow fluids to bombard the pores and decreases in porosity will indicate the lack of fluid in pore spaces.
- Analysis of finalized saturation profiles: time-lapse monitoring was utilized to determine CO_2 migration in each study reef. Changes in saturations were determined by analyzing the time-lapse PNC data (baseline/initial and repeat data) and calculating the percent change for each well. Additionally, injection wells or proximity monitoring wells were selected for each reef to monitor migration from near injection points to selected monitored producing wells. Cross-sections, crossplots, and beanplots were used to further assess saturation changes in each well.

6.3 REEF ANALYSIS

The Dover 33, Charlton 19, Bagley, and Chester 16 reefs afforded an opportunity to monitor CO_2 in several wells and varying conditions. There were several important findings during these tasks and challenges, which are summarized below:

DOVER 33 REEF

The Dover 33 Reef was a well-established CO_2-EOR field prior to PNC logging. Injection was performed in 1-33 and CO_2 monitoring was conducted in the 2-33, 5-33, and 9-33 wells from 2012 to 2017. Fluid saturation measurements indicated increases in gas and oil saturations for 5-33.

Fluid saturation measurements in 2-33 was problematic due the horizontal well configuration, which was on the oil-water contact. There were notable indications of water saturation decline over time due to injection of CO_2 and reef pressure. The 9-33 well PNC logging measurements, a newly drilled well in the reef, indicated the reservoir intervals were predominately oil saturated, which was part of EOR efforts.

BAGLEY REEF

The Bagley field indicated little to no response between the J-M 1-11 well and the Glasser well despite pressure changes of approximately 800 psi. There was little to no major saturation increases in the Glasser well. The J-M 1-11 had significant salt plugging in the A1 Carb which hindered fluid saturation changes along the prime potential reservoir interval. Figure 6-2 shows an example of the PNC measurements in the well. High sigma values indicated high salinity (salt) which inhibits saturation changes.

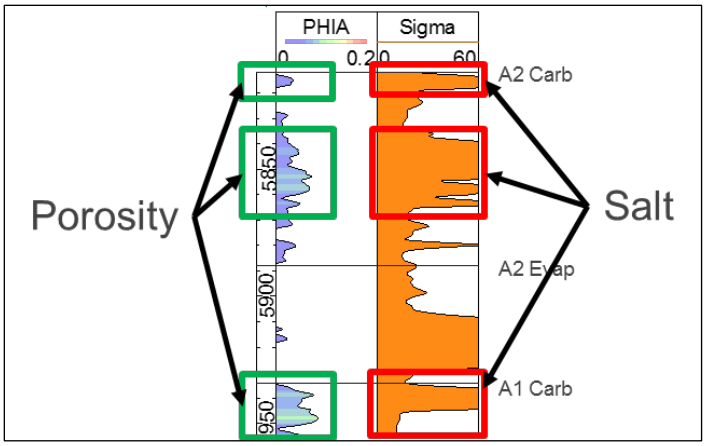

Figure 6-2. Wireline derived porosity calculated from neutron porosity and bulk density data (Column 1), overestimates porosity in salt intervals (salt indicated by high sigma values in Column 2).

EL MAC HILLS REEF

The El Mac Hills Reef was a well-established CO_2-EOR field prior to PNC logging. Saturation monitoring was challenging in the El Mac Hills reef and did not present as a model candidate for analyzing CO_2 migration for the following reasons:

- Cement bond variation in the 1-19D indicated erroneous saturation change measurements due to less than 75% bond quality within the well. Attenuation of the 1-19D model did not yield reliable results due to large amounts of data manipulation of the Monte Carlo formula.
- Repeat logging events were not possible in several of the wells due to production and injection activities (1-18A and 2-18).

CHESTER 16 REEF

The Chester 16 was a newly developed EOR flood with two new wells and provided a prime opportunity to monitor CO_2 migration. This allowed collection of baseline data and repeat data after the CO_2 flood was. Saturation changes were monitored after several injection events. The Chester 8-16 well was not perforated, and no production occurred in the well. Raw data was analyzed for the A-1 Carbonate, and Brown Niagara formations, 3. Additionally, a wireline temperature log was conducted in February of 2018 to determine where CO_2 break-through occurred in the formation. PNC data, baseline, repeat, and the temperature data were analyzed to determine the zone of CO_2 break-through and to assist with calibrating monitoring technology in the Chester 6-16 injection well. PNC saturation measurements provided supplemental data to verify depths of distributed temperature sensor (DTS) analysis data in the Chester 16 Reef. Wireline temperature measurements and changes to temperature, due to CO_2, correlated with changes in sigma measurements from time-lapse PNC monitoring. However, final saturation estimates for Chester 8-16 indicated a predominantly oil saturated interval with intermittent gas saturation which suggests that unprocessed sigma data provided better assessment of basic fluid condition changes in the well.

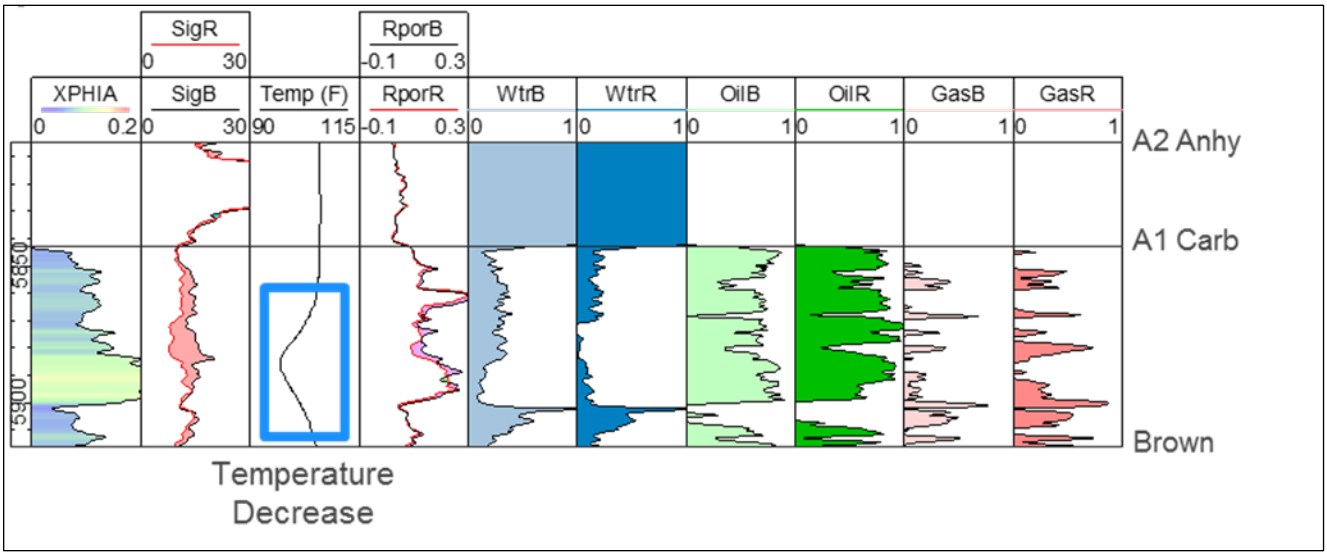

Figure 6-3. Chester 8-16 temperature decrease across depths at 5,861 MD feet to 5,910 MD feet.

- Acidizing of the Chester 6-16 well potentially changed the porosity and saturation profile.
- Chester 8-16 presented the best monitoring conditions due to lack of well perforations or equipment in the well (i.e., packers). No changes to the tubing, fluids, or production was observed in this well.
- Temperature logs combined with base-unprocessed PNC field data presented the best assessment of CO_2 break-through in the well.

6.4 DISCUSSION

The Dover 33, Charlton 19, Bagley, and Chester 16 reefs afforded an opportunity to monitor CO_2 in several wells and varying conditions. The Chester 8-16 provided the best-case scenario for evaluating the tool's ability to identify CO_2 breakthrough. This is as anticipated, because it was a new well, without prior CO_2 injection, and without any perforations. However, it was through the raw unprocessed field data that best practices were established. Key challenges and findings are as follows:

- Well configuration should be consistent between time-lapse logging events.
  - In the event of high pressures and well control needs, all fluids and configuration changes should be well documented and considered if estimating saturations.
- Raw unprocessed field data presents the best and most simplistic monitoring of CO_2 breakthrough from the injection well to monitoring wells.
- The limited tool resolution to differentiate between CO_2 and CH_4 can potentially be negated if a significant tracer is placed in the CO_2 or brine injection fluids.
  - Saturations assessments are estimated and not qualitative due to near wellbore evaluation depths of the tool.
  - Additionally, low porosity reservoirs are problematic due to zero resolution between gas and oil sigma response.
  - Reservoirs should have porosities of at least 6% to establish meaningful saturation data.
  - Storage integrity monitoring was problematic due to high salt content in the A2 Carbonate and A2 Evaporite secondary caprock formations. Chlorine in the salts bombard the PNC and cause sigma values outside the measurable constraints of the tool. The measurements can cause erroneous gas and oil saturation measurements in the formations which are not true integrity indicators in a caprock formation. These intervals will be estimated as 100% water saturation.

7.0 BOREHOLE GRAVITY STUDY

7.1 Objective and Description of the Technology

Objectives for the MRCSP program include assessing new technologies for tracking CO_2, brine, and oil movements underground; and monitoring options in a closed reservoir with oil, residual oil zone, and water zones. Battelle evaluated the borehole gravity (BHG) technology to specifically investigate the ability of the technique to monitor the flow and storage zones of the injected CO_2 during the injection and production stages. Battelle performed three BHG surveys in 2013, 2016, and 2018 in the Dover 33 reef when the reservoir was at different phases of CO_2-EOR process and at different pressures. The three BHG surveys were performed to monitor the changes in gravity/density as a result of the injection and withdraw of CO_2 into and from the reef. The gravity/density changes were then modeled to determine the flow and storage zones of the injected CO_2 in the reef.

Prior to 2013 the Dover 33 reef was nearly depleted of oil and gas due to long-term EOR activity occurring between 1996 and 2012 and the reservoir was a relatively low pressure. Between 2013 and 2016, Core Energy (Battelle) injected 264,586 metric tons of CO_2 into the reef and between July 2016 and July 2018, 136,271 tons of CO_2 were produced from this reef, leaving 128,315 tons of CO_2 remaining in the reef. There was also a relatively small amount of oil produced in that time. The 2018 reservoir pressure was approximately midway between the 2013 and 2016 reservoir pressures.

Measuring gravity is a potentially useful method for monitoring of changing fluid distributions within a reservoir. The method is a passive measurement of the existing gravity field and it bridges the radius of investigation gap between the near-borehole examination by well logging tools and the larger volumes examined by many of the seismic methods. In a time-lapse mode, the method is responsive only to temporal density distribution changes, such as those associated with CO_2 injection and production.

However, the accuracy requirements for the time-lapse gravity surveys are extremely important because the signals are on the order of tens of microGals. To be relevant, the gravity tool must measure differences in gravity over time to within a few microGals. Because the normal vertical gravity gradient within a well is approximately 29 microGal/foot, the tool must be placed at the same measurement locations during each of the time lapse surveys (ideally to within 0.1 foot).

BHG measurements are collected over discrete intervals in the borehole by stopping the BHG meter at preselected observation depths, often referred to as stations. The vertical gradient of gravity (z), $\Delta g/\Delta z$, is determined for the interval of interest by measuring the gravity difference, Δg, and the vertical distance between two consecutive stations, Δz. The gravity difference for each interval is then used to calculate the average density between two BHG stations (Figure 7-1). The assumption made to calculate apparent density ρ_a is based on an earth model composed of infinitely extended horizontal slabs.

A major distinction exists between single-event gravity surveys, where the goal is to recover absolute earth densities and density distributions, and time-lapse gravity surveys, where density changes over time are measured. The largest sources of spatial gravity variations are the free-air effect, latitude effect, and regional and local geology, including terrain, lithology, and structural variations. These time-static sources of gravity variation are cancelled by time-differencing survey data from different times. The remaining time-lapse, or 4D, signal is representative of temporal changes in formation densities (such as those due to CO_2 or other fluid injections or redistributions).

The radius of investigation into the formation, ρ_a is an averaged value over a volume about five times the vertical spacing between two adjacent stations. The volume that can be investigated by a borehole gravimeter provides a unique advantage of the technology compared to volumes sampled by traditional

logging tools that typically are limited to the volume within centimeters of the borehole, or within the borehole itself from core data analysis. This also means that borehole gravity densities are not affected by the casing and borehole rugosity. Because of the large investigation volume at the Michigan field site, the formation density measured within a Niagaran reef structure is often lower than the open hole gamma density log due to the presence of lower density halite flanking the reefs.

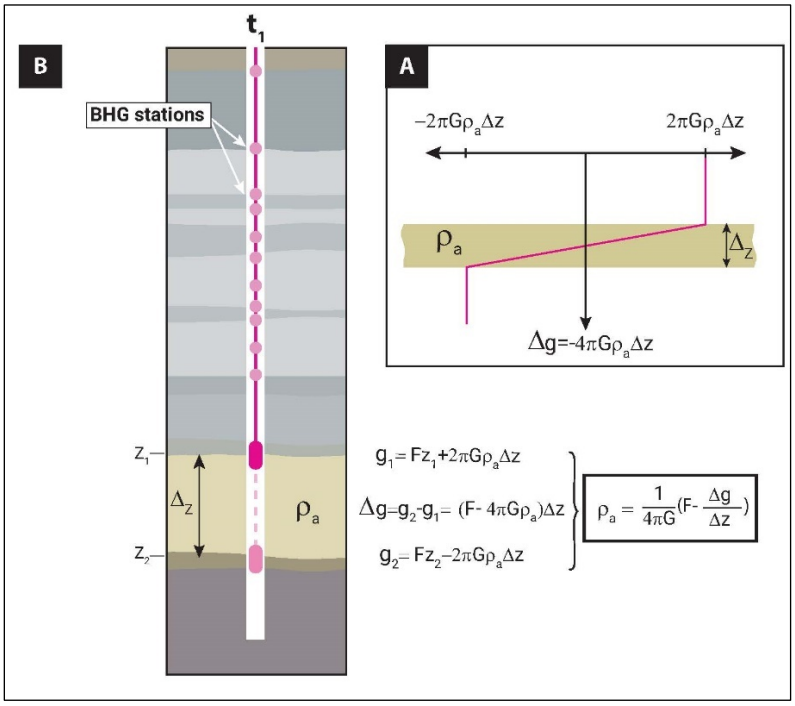

Figure 7-1. Cross section of the gravitational model for an infinitely extended horizontal slab (a) and its application in a borehole for the determination of the density (b) at a specific time (t1).

7.2 Methodology

Three BHG surveys were performed at the Dover 33 reef (in the Lawnichak-Myszkier 1-33 well) when the reef was at different stages in the EOR process. During the 2013 baseline BHG survey, the reservoir pressure was approximately 800 psi with residual gaseous CO_2 remaining in the reef from the initial CO_2 EOR activities (1995-2012). At the time of the 2016 survey, the reservoir pressure was approximately 3,500 psi with a CO_2 density of 880 kg/m3 (7.3 lb/gal) resulting from the injection of CO_2 into the reef. In July 2018, the reservoir pressure was approximately 1,200 psi and a CO_2 density of 290 kg/m3 (2.3 lb/gal) during the final gravity survey. Figure 7-2 summarizes the changes in fluid mass between the BHG surveys and provides an indication of changes expected between the three gravity surveys. Between the 2013 and 2016 surveys, 264,586 metric tons of CO_2 were injected into the reef while 6 metric tons of oil and 16 metric tons of brine were removed from the reef, resulting in a net change of 264,564 metric tons. The reef went into a production phase between the 2016 and 2018 surveys and 136,271, 4,243, and 2,542 metric tons of CO_2, oil, and brine, respectively were removed from the reef, reducing the overall bulk density in the reef.

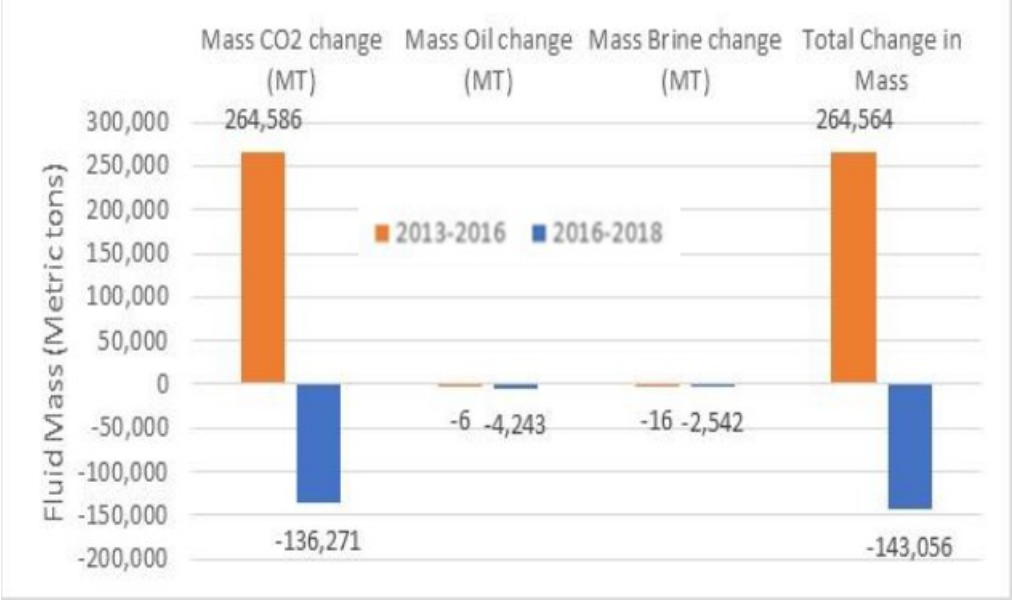

Figure 7-2. Changes in reservoir fluid mass between 2013-2016 (orange) and 2016-2018 (blue).

The surveys performed in 2013, 2016, and 2018 all included the same station depths and number of logging passes or sweeps per zone. The surveys were divided into three zones plus three near-surface stations for a total of approximately 40 stations, depending on the survey. An extra logging pass (sweep) through deep reef zone (Zone 1) was performed during the 2018 survey as QC data processing after the first four sweeps indicated a unique drift pattern was negatively impacting data accuracy. While performing this fifth pass, it was found that the tidal corrections used during Passes 1 through 4 had been calculated for the default file settings location of a Colorado test well. The tidal corrections were corrected in post processing and no additional readings were made related to this issue.

Table 7-1. Zones, station spacings, depths, and numbers of sweeps during the BHG surveys.

Zone	Station Spacing	Depth (MD)	Number of Sweeps
Zone 1	20 to 40 ft	5,176-5,540 ft	4/5
Zone 2	120 to 280 ft	3,253-5,176 ft	3
Zone 3	190 to 380 ft	660-3253 ft	3
Near Surface Zone	3 Stations	10, 34, and 240 ft	1

Following the field effort to collect the gravity data, the data were corrected for small errors in the station depth using the gamma ray and casing collar locator data to reference each of the surveys to the other surveys. The data were then processed using a Matlab-based program to: combine the data from the multiple sweeps over each zone; filter the data for noisy points; apply corrections for sensor tilt, temperature, gravitational tide, etc; compute least squares drift and gravity residuals; and compute conventional and inversion interval densities and error estimates.

The gravity data from the three BHG surveys were also modeled to determine where the CO_2 went in the reef after the injection, what is left after the withdrawal, and where it is located. To make this forward modeling possible, a time-lapse density model based on the reservoir model is required. In the absence of density values and of multiphase flow modelling corresponding to the periods of injection and production, the porosity and permeability distribution in the reef was used as a way of constraining the density distribution. This approach is to progressively fill the empty porous space of the 3D reef model starting from the injection point until a maximum distance from the well is reached while the permeability

stays greater or equal to a defined threshold, (for example only connected cells with permeability >6 mD and within a maximum radius of 200 meters from the well were considered). By varying these parameters in each range, a series of time-lapse density grids ("CO_2 plume") were obtained that could then be used to generate the gravity anomaly to be compared to the observed time-lapse values.

7.3 Results

The time-lapse gravity signals, i.e., the gravity signal differences between the 2013, 2016, and 2018 surveys are only related to changes in subsurface density distribution. In this project, the changes that were investigated are those due to the injection of CO_2 into the reservoir.

Above the reservoir the BHG density values between the three surveys are relatively comparable and all show zones with low density geologic formations (i.e., the Detroit River Salt between 2,300 and 2,700 feet, the Salina F Salt between 3,900 and 4,700 feet, and the Salina B Salt between 4,900 and 5,200 feet). Also, relatively dense geologic formations are found between 3,400 and 3,900 ft (Bass Island Dolomite). The comparable and consistent density trends in the upper portion of the well would be expected because no CO_2 injection or intrusion occurred in this area and limited perturbance to the geology likely occurred across these intervals during the monitoring period.

Near the reef (Figure 7-3), the differences in density (caused by the injection of CO_2) become apparent. Within the reef, the density typically increases up to 0.04 g/cm^3 between the 2013 and 2016 surveys from the injection of CO_2 and then decreases nearly 0.04 g/cm^3 between the 2016 and 2018 surveys as CO_2 and oil are produced from the reef. Often, the 2018 density lies between the densities calculated from the 2013 and 2016 survey data, which is the expected result given the intermediate mass of CO_2 in the reef at the time of the 2018 survey.

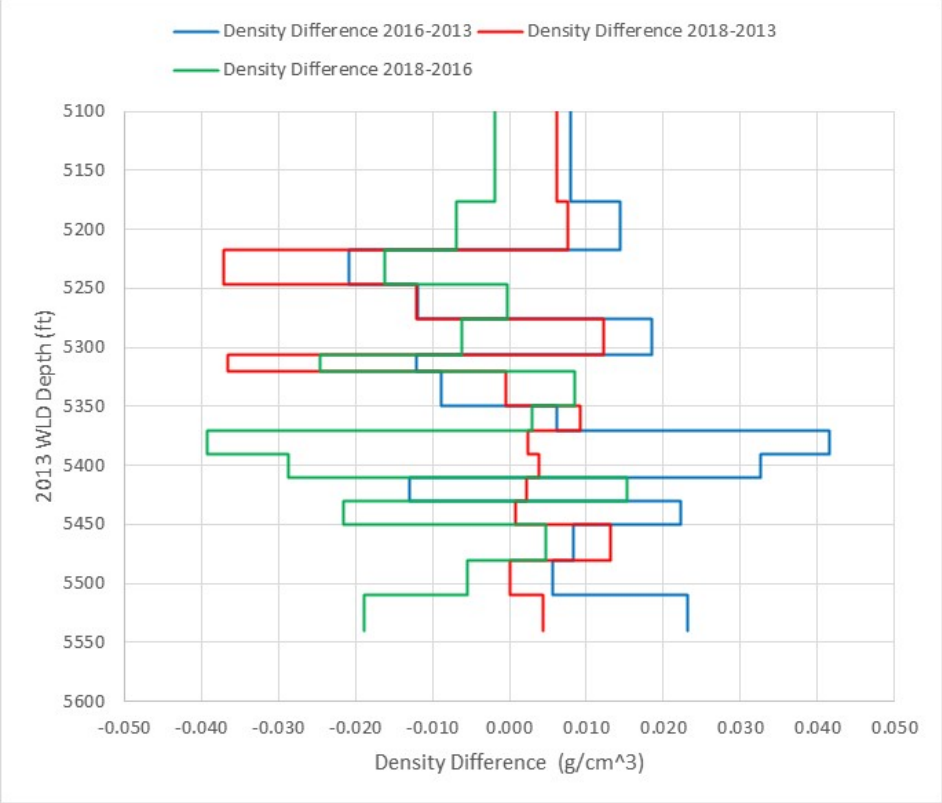

Figure 7-3. 4D Borehole Gravity Density Differences (Zoomed to Zone 1 only).

The best fits for the modeling of the injection period (between 2013 and 2016) are obtained without imposing a minimum permeability. The model with a plume radius of 300 m appears to provide the optimal fit for the anomaly at the top of the reef or just above it. Figure 7-4 presents the corresponding time-lapse density distribution in the reef and it is important to note that most of the CO_2 is concentrated in the lower part of the reef.

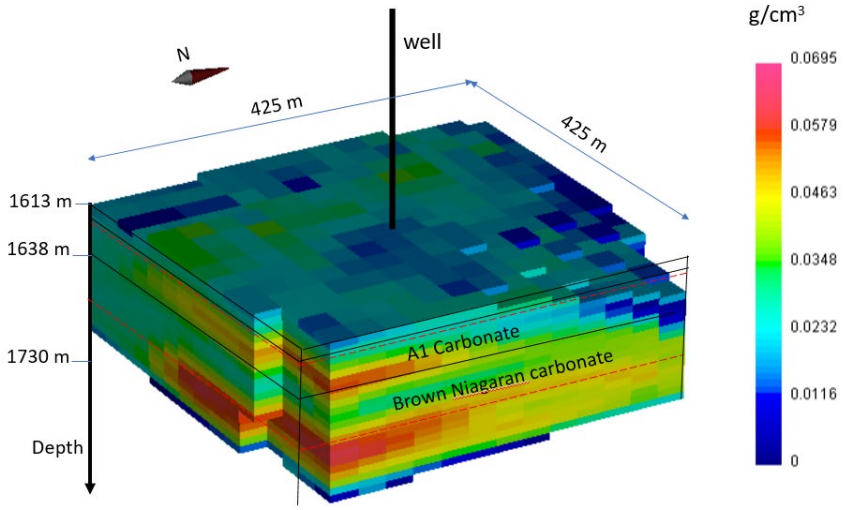

Figure 7-4. 2013-2016 injection period: three-dimensional perspective diagram of the modelled time-lapse density that represents the CO_2 plume in the reef for the best fitting solution K=0- R=300. The vertical black line represents the L-M 1-33 well. The horizontal black lines are the limits between the main geological units and the depth interval between the two horizontal red dashed lines is the perforated interval of the injection well.

For the production phase (2016-2018), the best fits are obtained without imposing a minimum permeability and the plume with a radius of 300 m provides the optimal fit for the anomaly at the top of the reef or just above it, as observed for the injection period. Also, as modeled in the injection period, the maximum decrease of CO_2 density during the production period is concentrated in the lower part of the reef where the porosity is maximum.

7.4 Discussion

The borehole gravity data collected during the 2013, 2016, and 2018 surveys represent the state-of-the-art in terms of data acquisition and pre-processing. The depth control in particular was meticulously conducted. Their quality and the low level of uncertainty make them useful for delineating the CO_2 plume position over time deployment and the oil sweeping extent and mechanisms in the Dover 33 reef. The following preliminary conclusions can be drawn:

- The time-lapse Bouguer gravity plots clearly show the effects of the changing mass of CO_2 within the reservoir, consistent with increasing mass from 2013 to 2016 and a decreasing mass from 2016 to 2018.
- The positive anomaly after the injection period in 2016 is likely due to the filling of the reef reservoir by CO_2. The best fitting forward models correspond to CO_2 mainly being stored in the central and lower portions of the reef. The forward modeling method allows precise mapping of the areas of the

reservoir that received most of the injected CO_2 and which zones are likely to have received less CO_2.

- For the production period, the time-lapse gravity anomaly corresponds clearly to the withdrawal of roughly 136,000 tons of CO_2. It is, however, not completely explained by the forward models presented and this could be due to the migrations of fluids in the reservoir not considered in this approach.

Overall, the field data collected in this study shows a strong correlation between the reservoir CO_2 injection and production operations. The changes in gravity and density, generally correspond with the injection zone and the most pronounced changes are in the reservoir, rather than in the overlying 5,000+ feet. This indicates that borehole gravity can be a useful tool in monitoring CO_2 injection in depleted oil fields, including under CO_2-EOR conditions. This technique could also be used for monitoring injection in saline reservoirs, given that the basic mechanisms of increasing gravity/density with injection still hold. The relative value of the borehole gravity over the other options, such as pressure, temperature, and emerging distributed fiber-optic systems remains to be seen. Some challenges include the need for precise repetition of field procedures and measurement locations. The complexity of CO_2-EOR operations overtime in fields such as Dover 33 is difficult to fully incorporate into the analyses or modeling. Furthermore, with a single monitoring well used in this study, it is difficult to evaluate lateral changes in the CO_2 plume. Perhaps if the tool is used in multiple wells in the project area, a more detailed plume distribution could be developed.

8.0 DISTRIBUTED TEMPERATURE SENSING (DTS)

8.1 Objective and Description of the Technology

DTS is a distributed sensing technology that uses fiber optic cable as a temperature sensor whereby the glass fiber is interrogated using a laser pulse and the assemblage of returned light signals over time is analyzed. The returned light signal is the result of backscattered light waves released by atoms in the matrix of the fiber in reaction to the initial laser pulse. The timing of a given returned signal is related to the location of that measurement on the fiber and the character and magnitude of the returned signal is used to compute the temperature at that point. As part of Task 5 novel monitoring techniques, DTS was installed in the Chester 16 reef for monitoring temperatures in the Chester 6-16 injection well and Chester 8-16 monitoring well. Additionally, the Chester 8-16 monitoring well is instrumented with behind-casing sensors at five depths to monitor real-time bottomhole conditions in three separate formations.

8.2 Methodology

DTS can identify which formations received the injected CO_2 by analyzing the temperature profile of formations during and after injection stops. Formations that received bulk of the cooler CO_2 will take longer to warmback once the injection has stopped, while formations that did not receive significant quantities of CO_2 will quickly revert to their reference reservoir conditions. The detailed DTS report (Mawalkar et al., 2020) presents warmback analysis of various injection periods to determine if the CO_2 injections took place within the targeted injection formations. Also, the DTS in Chester 8-16 monitoring well is used to monitor the arrival of CO_2 front by detecting a cooling zone within the A1 Carbonate Formation. The temperature readings from behind-casing sensors are used to corroborate DTS temperatures, while the pressure measurements provide additional evidence for migration of fluids in the formations of interest.

8.2.1 Instrumentation

DTS is configured to provide temperatures at every 1 m intervals, with typical measurement frequencies set at once every hour. Chester 6-16 injection well is perforated for CO_2 injection in the A1 Carbonate Formation (5884’ – 5970’ MD) and the Brown Niagaran Formation (5970’ – 6531’ MD). The well can be configured such that CO_2 can be injected to a single formation or to the combined A1 Carbonate and Brown Niagaran formations. Similarly, the Chester 8-16 monitoring well is also instrumented with the DTS. The behind-casing sensors measure pressure and temperature at every 1-minute intervals, but the data is typically averaged to every hour basis and time-synchronized with DTS data and wellhead conditions at surface which provides injection rates on an hourly basis. Figure 8-1 shows DTS installation in two wells and the locations of behind-casing sensors in Chester 8-16 well.

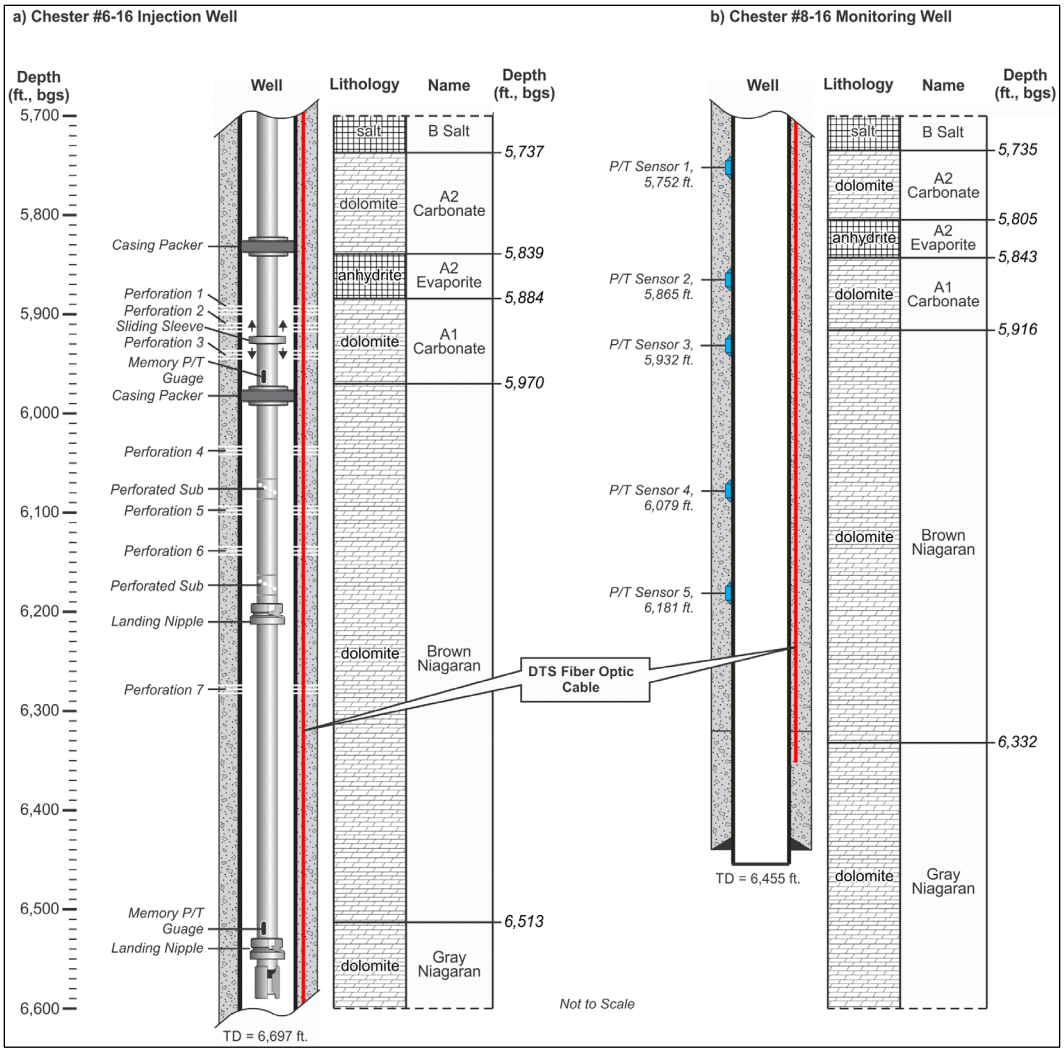

Figure 8-1. (a) DTS system and well components in Chester 6-16 injection well; (b) DTS system and behind-casing sensors in Chester 8-16 monitoring well. All depths shown are measured depths (MD).

8.2.2 Measurement Quantities

Below are the surface wellhead CO_2 injection and downhole fiber-optics and behind-casing sensor data that were monitored during the Phase III program:

- CO_2 from Chester 10 Facility – Chester 16 reef receives pure CO_2 from the Chester 10 dehydration and compression facility that delivers CO_2 at approximately 1,300 psi (supercritical phase) via a 6-inch carbon-steel pipe. Chester 16 reef does not receive any recycle gas from the Dover 36 processing facility. The injected CO_2 is metered at a Coriolis mass flow meter co-located at the Chester 6-16 injection wellhead. At surface, following parameters are measured:
  - Mass flow rate of CO_2 (MT/day) on a per minute basis, averaged to nearest hourly basis for warmback analysis.
  - Totalizer reading that provides the cumulative mass of CO_2 (MT) injected.
  - Density of CO_2 (lbs/gal).
  - Temperature of CO_2 at Coriolis flow meter (F).
  - Pressure (psi) of injected CO_2, upstream and downstream of the Coriolis flow meter.

- DTS – Temperature (F) readings at 1 m intervals, typically averaged to once every hour at Chester 6-16 injection well and Chester 8-16 monitoring well.
- Pressure (psi) and temperature (F) readings (averaged to nearest hour) in memory gauges placed at the bottom of A1 Carbonate Formation (5970' MD) and/or Brown Niagaran Formation (6352' MD) in Chester 6-16 injection well.
- Pressure (psi) and temperature (F) readings (averaged to nearest hour) at behind-casing sensors installed at five depths in Chester 8-16 monitoring well. The behind-casing sensors are installed at following depths:
  - 5752' MD in A2 Carbonate Formation
  - 5865' MD in A1 Carbonate Formation
  - 5932' MD in Brown Niagaran Formation
  - 6079' MD in Brown Niagaran Formation
  - 6181' MD in Brown Niagaran Formation

8.3 Key Results

Two types of analysis were done to discern flow distribution: an analysis of the temperature behavior during injection and analysis of the warmback behavior when injection ceased. Temperature behavior during injection shows where injectate moved within the wellbore, but it does not necessarily show where fluids entered the reservoir. This is because any given cooling or warming signal cannot distinguish between pressure changes due to flow within the wellbore and pressure changes due to CO_2 entering the reservoir. Warmback analysis (analyzing temperature warmback in depth and time in the period) after injection ceases allows inference of where fluids entered the reservoir. The depths where injection into the reservoir occurred will exhibit more cooling, and therefore will take longer to warm back to background temperatures after injection ceases. As of August 2019, ~147,000 MT of CO_2 has been injected in the Chester 16 reef. DTS data are analyzed to discern where injectate entered the reservoir for injection periods #2 through #8. Table 8-1 shows these injection periods and the target formation where CO_2 injection was monitored.

Table 8-1. CO_2 injection history of Chester 16 reef.

Injection Period	Date Range	Days Injected	Fall off Days	Target Formation	Quantity Injected (MT)
1	1/11/17 - 1/14/17	3	39	A1 Carbonate	804
2	2/22/2017 - 4/6/2017	43	16	A1 Carbonate	9,039
3	4/22/2017 - 7/24/2017	93	67	A1 Carbonate	20,585
4	9/29/2017 - 11/27/2017	59	19	Brown Niagaran	18,314
5	12/16/2017 - 1/16/2018	31	20	A1 Carbonate	9,010
6	2/5/2018 - 3/21/2018	44	67	A1 Carbonate and Brown Niagaran	10,178
7	5/26/2018 - 8/14/2018	80	66	A1 Carbonate and Brown Niagaran	18,320
8	10/20/2018 - 8/15/2019	.		A1 Carbonate and Brown Niagaran	58,226
					144,476

8.3.1 Composite Waterfall Plot of Chester 6-16 DTS

Figure 8-2 shows a composite waterfall plot of temperatures at the injection well across the entire injection period until August 15, 2019 when DTS data were processed. Here, the blue colored zone represents cooler temperatures, while red colored zones indicate warmer temperatures. It should be noted that during the injection the entire wellbore cools, but when injection is shut, the shallower formations (B Salt, A2 Carbonate and A2 Evaporite) quickly revert to reference reservoir temperatures.

Similarly, near the bottom of Brown Niagaran formation, below the bottom-most perforated zone #7 at approximately 6150' MD shows no significant cooling indicating no migration of cooler CO_2, either during injection or the falloff period when injection is shut. This waterfall plot of temperature suggests that most injected CO_2 has remained within the target zone of injections, the A1 Carbonate and the Brown Niagaran formations.

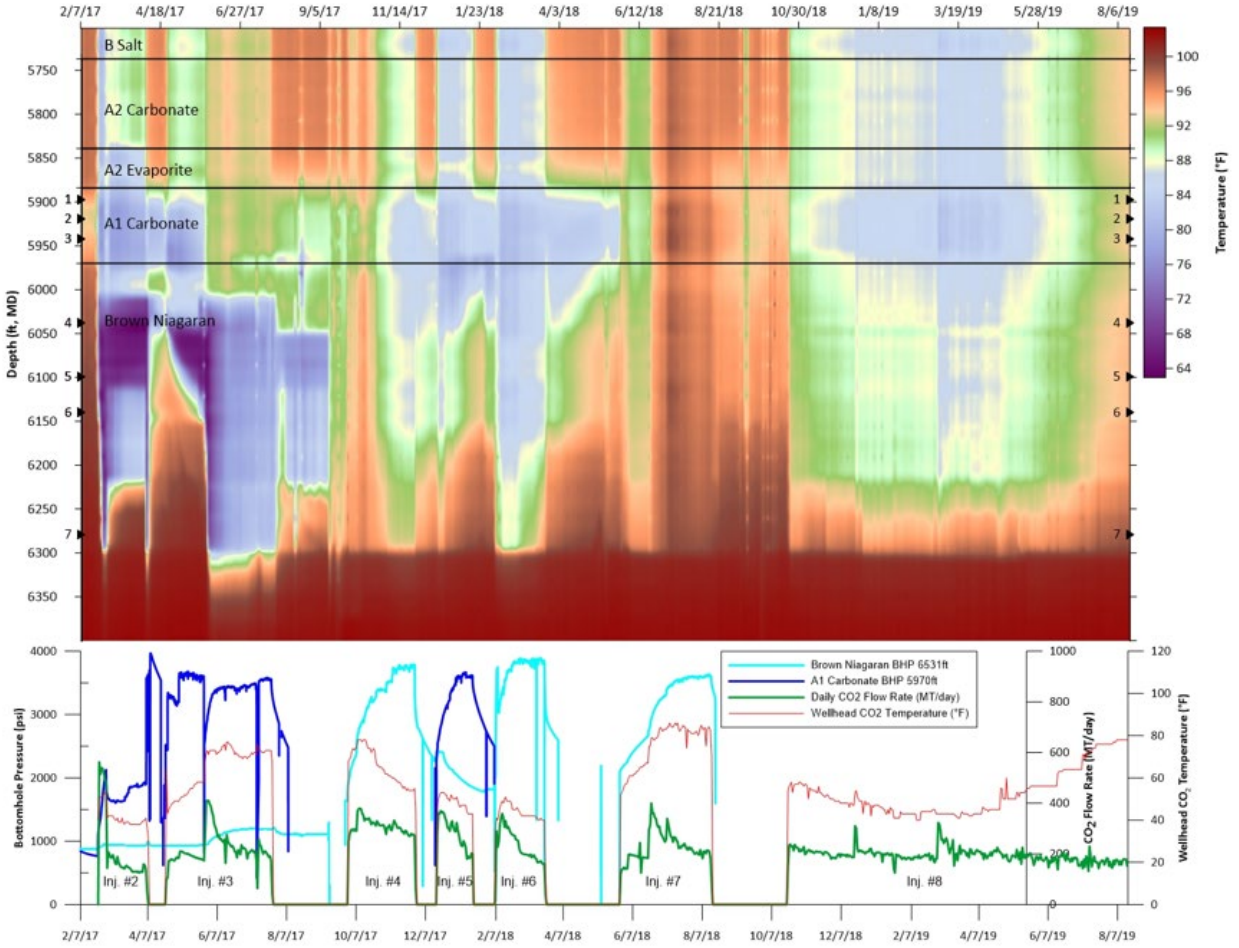

Figure 8-2. Waterfall plot of temperatures and bottomhole conditions in Chester 6-16 injection well.

8.3.2 Sample Warmback Analysis of Injection Period #5 – A1 Carbonate

During injection period #5, Core Energy targeted the A1 Carbonate Formation for injection. During this injection period of 31 days between December 16, 2017 and January 16, 2018, 9,010 MT of CO_2 were injected. This was followed by a falloff period lasting 20 days. Figure 9-3 shows a waterfall plot of this injection period until February 5, 2018, when injection period #6 resumed. During this injection period, the bulk of the CO_2 at surface was injecting relatively cool at approximately 50°F, resulting in wellbore cooling in the annular space within the A1 Carbonate Formation. Some lesser cooling also occurred in the Brown Niagaran annulus and appeared to reduce during the first half of the injection period. Warmback showed persistent cooling at perfs #1 - #3, implying those perforated zones took most of the injection and that there was negligible injection into the Brown Niagaran Formation.

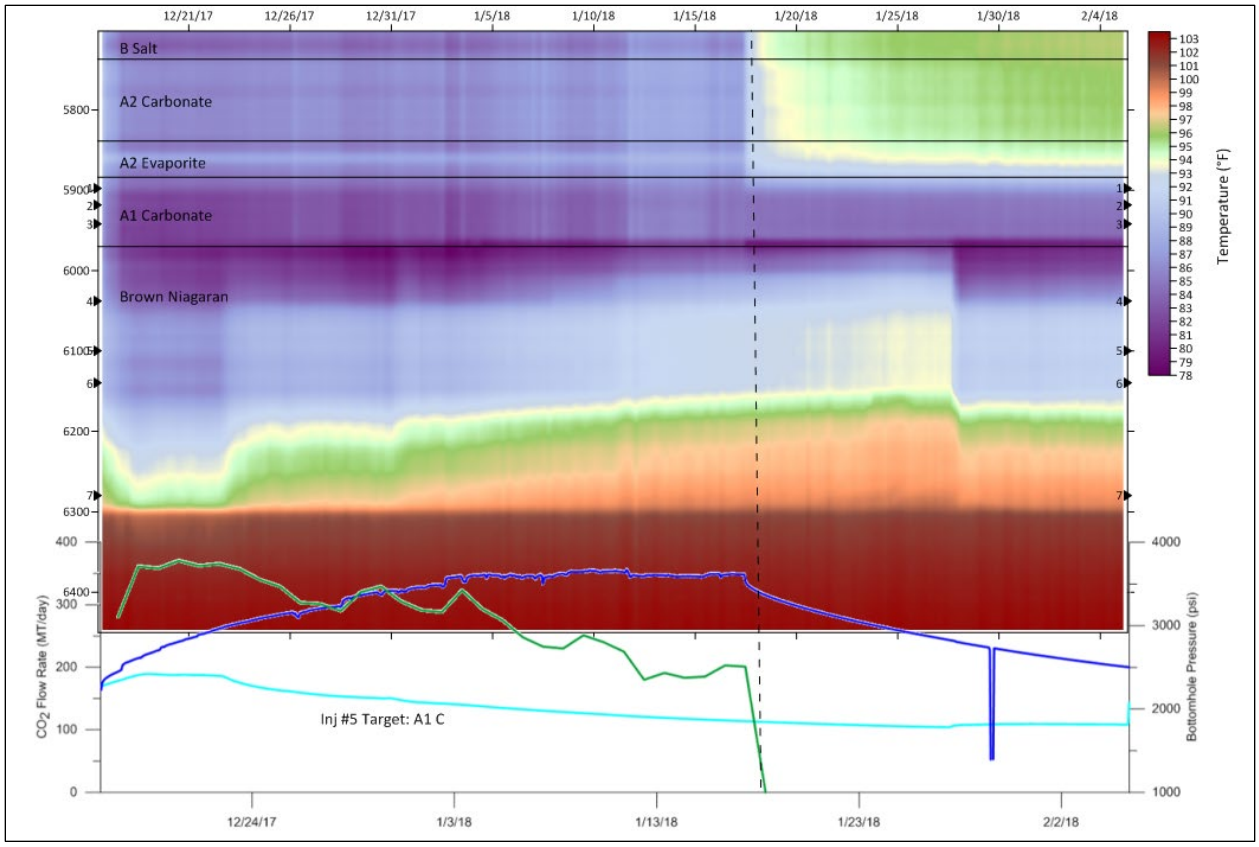

Figure 8-3. Waterfall plot of temperature for injection period #5.

Figure 8-4 shows the differential temperature waterfall for the injection period #5's warmback. The overlaying layers have relatively fast and uniform warmback, indicating no fluid injection into formation as would be expected (this is the zone above perforated zone in A1 Carbonate). The persistent cooling zone and lack of warmback in the A1 Carbonate (perf #1 to #3) indicates most of the CO_2 entered this zone. The differential temperatures within the Brown Niagaran Formation is difficult to interpret as there is no apparent warmback suggested here. However, the waterfall plot above only suggests a cooling zone above perf #5, while near perf #6 and #7, the temperatures are relatively warm, indicating lack of presence of CO_2. Finally, below perf #7 there is no warmback as this zone did not cool appreciably during injection.

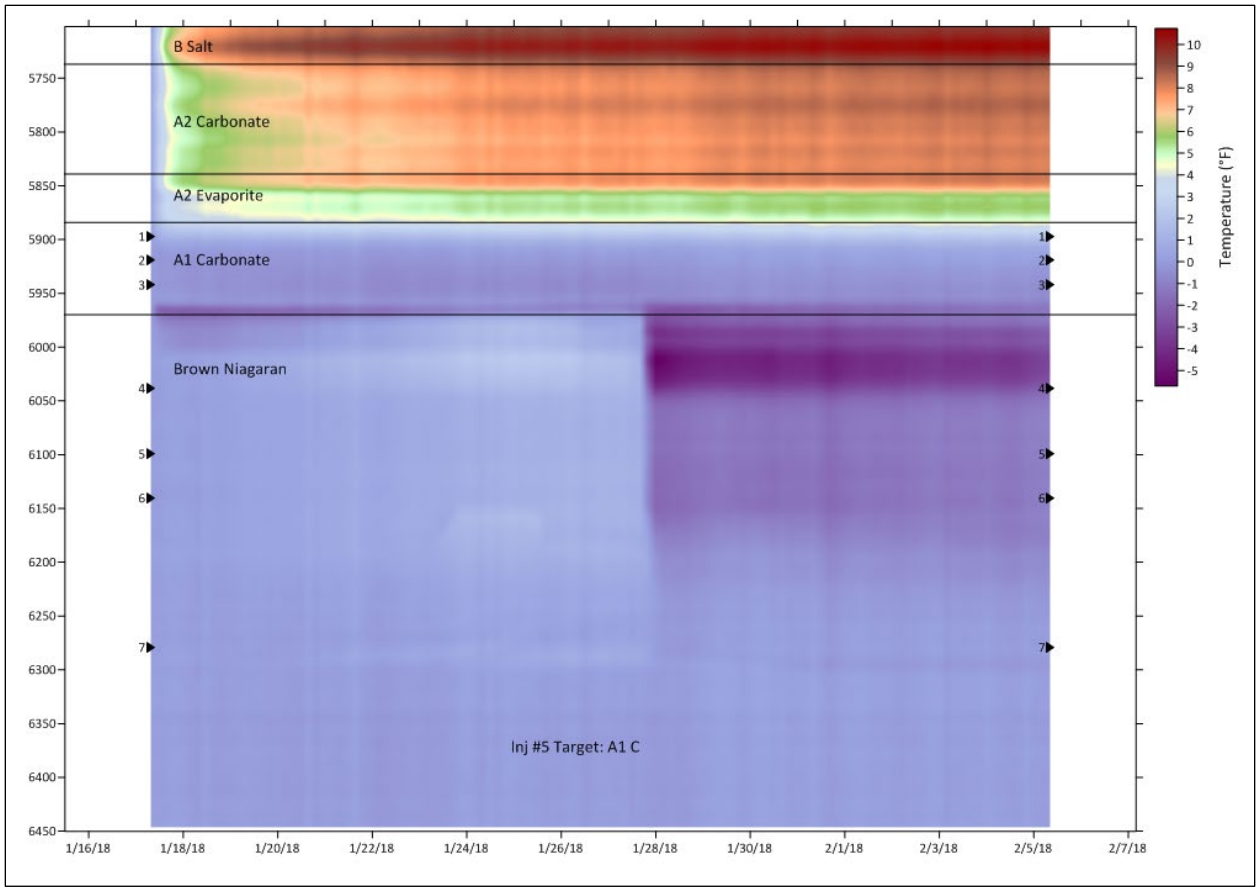

Figure 8-4. Differential temperature plot of injection period #5.

8.3.3 Detecting Arrival of the CO_2 Plume at the Chester 8-16 Monitoring Well

As cold CO_2 is injected into the reservoir and mixes with warmer reservoir fluids, slight cooling is expected to occur further out within the reservoir as the CO_2 plume migrates towards the monitoring well. Figure 8-5 shows a waterfall plot of temperatures at the monitoring well. A small cooling signature (approximately 0.5 °F) was first observed in early March 2018, which further cooled by approximately 9 °F (compared to reference reservoir temperature of ~ 104 °F) at the end of December 2018. The cooling signature is centered around 5,885 ft. in the A1 Carbonate Formation. This suggests that the cold CO_2 front first arrived at the A1 Carbonate formation at monitoring well in March 2018, continued to cool with peak cooling occurring in December 2018.

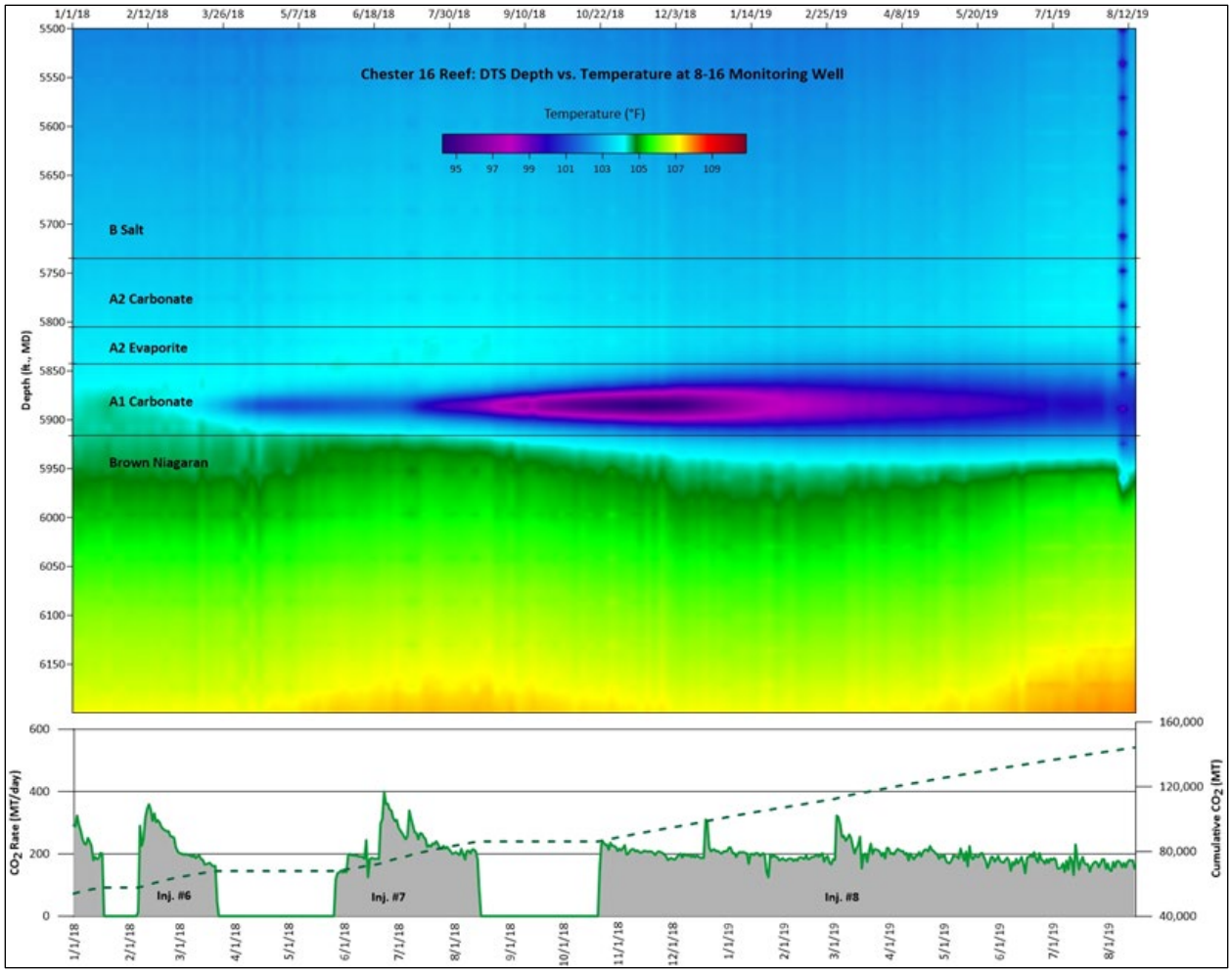

Figure 8-5. Waterfall plot of temperatures in the Chester #8-16 monitoring well.

8.4 Discussion

Results show that warmback analysis is a useful tool for determining where the CO_2 is entering the reservoir from the injection well. This analysis is limited as the warmback provides circumstantial evidence but is not a lone indicator of reservoir injectivity zones. The nature of CO_2 migration vertically along the injection wellbore can be ascertained based on the analysis of warmback periods. Relatively quick warmback above and below the perforated intervals indicates that there was no unintended CO_2 migration outside of target formations. Finally, it was shown that DTS detected the arrival of the CO_2 front at the monitoring well.

9.0 GEOCHEMISTRY MONITORING

9.1 Objective and Description of the Technology

The overall purpose of the geochemical monitoring program under Midwestern Regional Carbon Sequestration Partnership (MRCSP) is to use stable and radiogenic isotope geochemistry in concert with analysis of general geochemical parameters of fluids and gases and analysis of core samples to determine geochemical processes occurring in the reef structure because of CO_2 injection. Specifically, brine and gas samples were collected and analyzed to determine changes occurring between reefs prior to and following CO_2 injection. The analytical results for general geochemical parameters were modeled with chemical equilibrium models to determine if the injection of CO_2 resulted in the mineral dissolution or precipitation. Finally, core samples were collected and analyzed to determine if there was evidence of dissolution features or mineral precipitation. Due to the unique isotopic signature of the injected CO_2, isotopic analyses of the CO_2 in the gas and the dissolved inorganic carbon in the brine were used as tracers to monitor changes in the geochemistry and as an indicator of mineral precipitation resulting from the injection of CO_2.

9.2 Methodology

Brine, gas, and core samples were collected from the three reefs included in the geochemical study: Dover 33, Charlton 19, and Bagley Field. Table 9-1 shows the samples that were collected from each reef. Brine and gas samples were collected from each of the wells in the Dover 33 and Charlton 19 reefs, and two wells in the Bagley Field were used to collect brine and gas samples. A single core sample was collected from the Lawnichak 9-33 well in the Dover 33 reef.

Table 9-1. Sample locations for the brine, gas, and core samples.

Reef/ Well ID	Brine Sample	Gas Sample	Core Sample
Dover 33			
L-M 1-33	X	X	
L-M 2-33	X	X	
L-M 5-33	X	X	
Lawnichak 9-33	X	X	
Fieldstone 2-33	X		X
Charlton 19			
EMH 1-18	X	X	
EMH 2-18	X	X	

BRINE SAMPLING

A total of 9 brine samples were collected from the five wells in the Dover 33 reef with either a swabbing method or using the pumping system on the well (L-M 5-33). Baseline brine samples were collected from the wells in 2012, prior to restarting CO_2 injection into the reef, and repeat sampling was performed over the next six years (until 2018) to capture water samples the had interacted with the injected CO_2. Approximately 244,000 tonnes of CO_2 were injected into this reef throughout the geochemistry monitoring task. Baseline and repeat brine samples were collected from the three wells in 2015 and 2018, respectively, while CO_2 injection into the reef began shortly after collecting the baseline samples in 2015. During the injection period, approximately 285,000 tonnes of CO_2 were injected into the reef between the baseline and repeat sampling events. The Bagley Field reef complex also was used to collect true baseline (no CO_2 injection) geochemical samples in October 2015, but post- CO_2-injection samples were

not able to be collected from this reef due to the well conditions/configurations. Therefore, the samples collected from the Bagley Field only provide baseline conditions prior to CO_2 injection.

GAS SAMPLING

A total of 32 gas samples were collected from 11 wells and from the Dover 36 Gas Processing Facility (GPF) during the geochemical study—three samples from the L-M 1-33, six samples from the L-M 2-33 ,six samples (not including duplicates) from the L-M 5-33, three samples from the EMH 1-18(A), two samples from the EMH 1-19D, and one sample each from the Lawnichak 9-33, EMH 2-18, Wrubel 1-14A, J-S 3-11, J-M 1-11, and Glasser 1-14 wells. n addition, five gas samples were collected from the Dover 36 GPF from the pure, recycled, and comingled (mixture of pure and recycled gas) gas streams. These represent 'pure' CO_2 recovered from the Antrim Shale, gas that has passed through the reefs and subsequently been produced, and gas to be injected into the reefs, respectively.

CORE SAMPLING

A total of 118.15 feet of whole core, divided into seven coring runs, was recovered from the Lawnichak 9-33 well. The cored interval spans a discontinuous section of the Brown Niagaran Formation between 5,525 and 5,763 feet MD (Figure 9-1). Approximately 30 feet and 80 feet of drilling occurred between Core Runs #2 and #3 and between Core Runs #4 and #5, respectively. Plugs were selected from the whole core by inspecting the core for fracture features or vugs that may contain evidence of precipitation or dissolution. Plugs were collected from the whole core at the core laboratory with a plugging bit and nitrogen coolant, and three plugs were selected for further analysis as part of the geochemistry study. The plugs were collected from the following depths: 5,606.1, 5,690.25, and 5,700.25 feet, and represent portions of the reservoir above, at, and below the oil/water contact surface.

ANALYTICAL METHODS

Brine samples were analyzed for major and trace element composition of the brine, chemical/physical properties (e.g., pH, density), isotopic composition of water, $^{87}Sr/^{86}Sr$ ratios of dissolved Sr, and isotopic composition of DIC. Gas samples were analyzed for isotopic composition ($\delta^{13}C_{CO2}$, $\delta^{13}C_{CH4}$, δD_{CH4}, and $\delta^{18}O_{CO2}$) and major gas constituents (He, H_2, Ar, O_2, CO_2, N_2, CO, CH_4, C_2, C_2H_4, C_3, C_3H_6, iC_4, nC_4, iC_5, nC_5, and C_6+). Isotech Laboratory conducted analysis of concentrations and isotopic composition of major constituents in gas samples.

Core samples from the Lawnichak 9-33 well (Dover 33 reef) collected during the installation of the well were analyzed to investigate the presence of minerals that may have precipitated as the result of CO_2 injection in the reef, as suggested by the equilibrium model results. In addition, $\delta^{13}C$ analyses were performed on select subsamples of the core to determine the isotopic values of the matrix carbonates and secondary mineral precipitates found in the rock. The core samples were analyzed using a Scanning Electron Microscope (SEM) to examine the fine details of the core samples and to determine the chemical composition of the bulk rock and precipitates that filled pores, veins and vugs that had been identified. Also, samples were viewed under a polarizing light microscope to determine mineral phases and textures of the rock. X-Ray Diffraction (XRD) analyses were performed on the rock samples to determine the mineralogy/crystallography of the samples. Both micro- and macro- X-Ray Computed Tomography (XCT) analyses were performed on the core samples to identify zones of the rock that may exhibit indications of dissolution or precipitation. Finally, samples of the rock matrix and vug-filling precipitates were analyzed with mass spectrometry to determine the isotopic compositions of these materials.

9.3 Results

A stepwise approach was used to investigate the geochemistry in the reefs, beginning with the general geochemistry of the brines and gas from the reservoir and ending with the isotopic analysis of the matrix rock and mineral precipitates in the core samples with a goal of evaluating the overall geochemical conditions of the reservoir and the possibility of dissolution or precipitation of minerals resulting from the injection of the CO_2.

BRINE

Brine samples collected from the three reefs displayed comparable results for general geochemical properties. Overall, the brines have extremely high total dissolved solids (TDS) concentrations and are dominated by Ca, Mg, Na, and K for cations and Cl for anions, as may be expected from a brine in carbonate reef. The general geochemistry also displayed limited variation between the three reefs investigated, indicating there is not significant a variation in the brine geochemistry over the areal distribution of the reefs sampled. Also, the injection of CO_2 does not appear to change the general geochemistry.

Geochemical equilibrium modeling of the chemical parameters was performed to determine if specific mineral species were supersaturated in the brine and prone to precipitation due to CO_2 injection (Table 9-2). The data indicate that brines are supersaturated with respect to many carbonate minerals (calcite, aragonite, dolomite, huntite, and magnesite) prior to CO_2 injection and the injection of CO_2 appears to drive the brine to greater saturation levels. It should be noted that while the Pitzer equations are used for slightly higher activity brines compared to the Debye-Huckel equations, the activity levels of the brines from the Niagaran reefs are beyond the applicable conditions of the Pitzer calculations. Therefore, the results provided by the equilibrium model have some degree of uncertainty.

Table 9-2. Saturation Indices for the minerals of interest in the brine samples. Saturation Indices greater that 1.0 indicate saturation and the potential for mineral precipitation.

Sample ID	Carbonate Saturation Indices (SIs)				
	Calcite	**Aragonite**	**Dolomite**	**Huntite**	**Magnesite**
L-M 1-33 (10/11/2012)	3.2	2.9	6.0	9.1	1.9
L-M 1-33 (10/23/2012)	3.5	3.2	6.6	10.2	2.2
L-M 2-33 (11/07/2012)	3.4	3.1	6.4	9.8	2.1
L-M 2-33 (8/21/2013)	0.9	0.6	1.4	-0.3	-0.4
L-M 2-33 (12/16/2013)	3.1	2.8	5.8	8.6	1.8
L-M 5-33 (11/14/2012)	3.7	3.4	6.8	10.5	2.2
EMH 1-18 (01/28/2015)	3.0	2.7	5.6	8.2	1.7
EMH 1-19D (02/06/2015)	3.3	3.0	6.2	9.4	2.0
J-M 1-11 (10/14/2015)	3.2	2.9	5.9	8.8	1.8
J-S 3-11 (10/12/2015)	3.1	2.8	5.8	8.7	1.8
EMH 1-18A (06/21/2018)	2.5	2.2	4.5	6.0	1.2
EMH 1-19D (06/21/2018)	2.3	2.0	4.2	5.3	1.0
Fieldstone #1 (05/02/2016)	3.3	3.0	6.2	9.3	2.0
Fieldstone #2 (05/02/2016)	3.3	3.0	6.2	9.3	2.0

Carbon isotope values were also measured in the brine samples to evaluate the mixing/dissolution of the injected CO_2 with the brine waters. he injected CO_2 displays a unique $\delta^{13}C$ signature (approximately 20‰), which becomes increasingly heavier due to partitioning when the injected CO_2 is dissolved in water to form carbonic acid, bicarbonate and/or carbonate ions (approximately 30‰). Brine samples collected prior to significant interaction with the injected CO_2 displayed $\delta^{13}C$ values ranging from approximately -7‰ to 10‰, but samples of the brine that had significant interaction with the injected CO_2 displayed $\delta^{13}C$

values between approximately 20‰ and 30‰ (Figure 9-1). These data indicate that there was dissolution of the injected CO_2 and the brines within the reef.

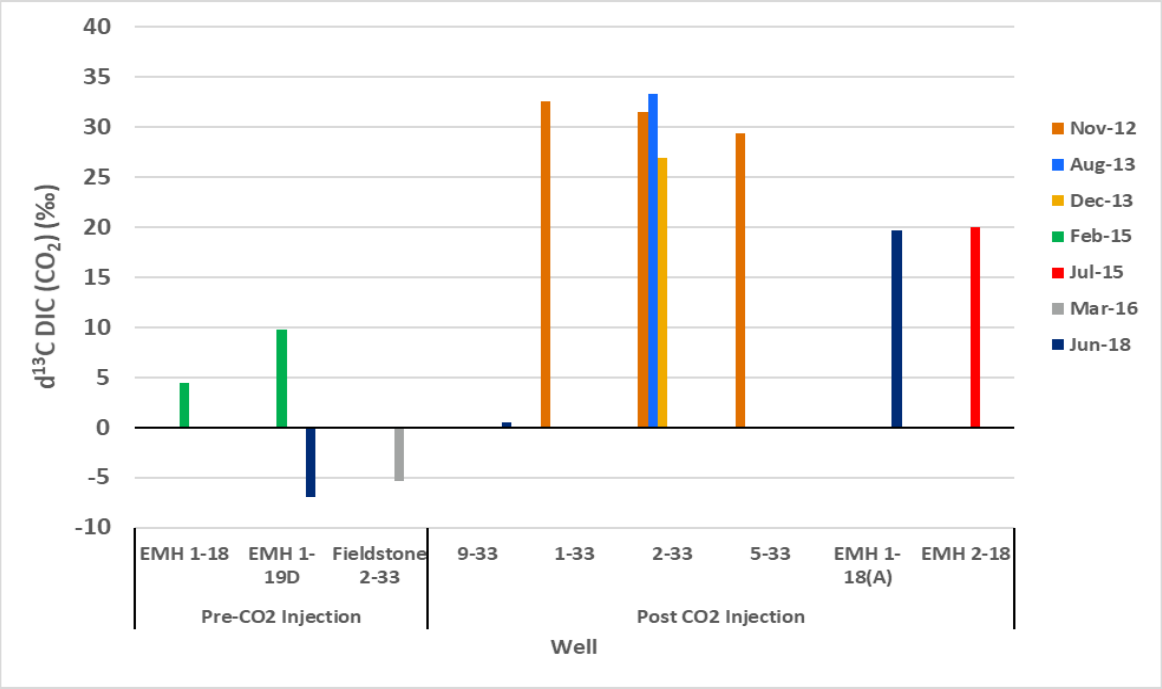

Figure 9-1. Presentation of the $\delta^{13}C$ of DIC in brine samples. Wells without CO_2 interaction on the left and wells with CO_2 interaction on the right.

Gas

Likewise, the concentration of CO_2 in the gas samples from the reefs significantly increased by the injection of the CO_2 (as expected). While the geochemical equilibrium models suggest the precipitation of carbonate minerals and secondary mineralization of carbonates are observed in the fractures and vugs of the core samples collected from the Dover 33 reef, it was not possible to correlate the timing of precipitation with the injection of the CO_2 in the core samples.

Rock Core

With the indication of dissolution of the injected CO_2 and the favorability of carbonate mineral precipitation, rock core samples were analyzed with LM, SEM, XRD, and XCT to determine if carbonate minerals are precipitating in the vugs or fractures of the rock. In addition, subsamples of the core were analyzed for $\delta^{13}C$ values to determine if the injected CO_2 had been incorporated in carbonate minerals precipitated in the pore spaces.

Analyses with LM and SEM indicated that there are no significant changes in porosity from above the oil-water contact to below the oil-water contact. The LM and SEM inspections indicated the presence of secondary mineralization of carbonates and sulfates in the vugs and fractures of the core samples. Fractures in every sample also contained fragments of its matrix. The SEM analyses (using energy-dispersive detector [EDS]) also indicated the presence of high-Mg carbonates and low-Mg calcite in the vugs and on the outer surfaces of the dolomite matrix. The timing of the secondary mineralization, however, could not be established from the SEM or LM analyses.

Portions of the core samples were analyzed with XRD to determine the mineralogy of the matrix of the core and the mineral precipitates found in the vugs. The sample collected from a depth of 5,630 feet (at the oil-water contact) displays dolomite and low-Mg calcite as the major phases of the mineralogy with minor amounts quartz, anhydrite, and halite. Core samples above and below the oil-water contact, however, only show the presence of dolomite in the bulk samples. The more complex mineralogy near the oil-water contact suggests that the combined presence of CO_2, brine, and gas may create a more geochemically active zone.

One core sample from a depth of 5,690 feet (from below the oil-water contact) was disaggregated for XRD analysis due to the presence of a relatively large vug inclusion identified through XCT. The matrix of this core sample consisted predominantly of dolomite with minor amounts of quartz and alkali feldspar. The precipitated, fine-grained material in the vug inclusion displayed a more complex mineralogy than the matrix rock with the majority of the vug inclusion composed of dolomite and anhydrite; however, the presence of beta cristobalite, quartz, fluorite, and albite also were detected.

XCT images of the core indicated that there was no strong evidence of CO_2-induced dissolution in the samples. Any evidence of CO_2-induced dissolution was subtle, comprising localized areas of elevated porosity, or slight fracture widening in some cases. Evidence for mineral precipitation lining the large pores (Figure 10-2) and even the fractures in the core was more commonly observed than dissolution. It is difficult to identify the secondary mineral from the XCT images because gray/color scale variation is small. The XCT images provide further evidence of mineralization caused by the injection of CO_2.

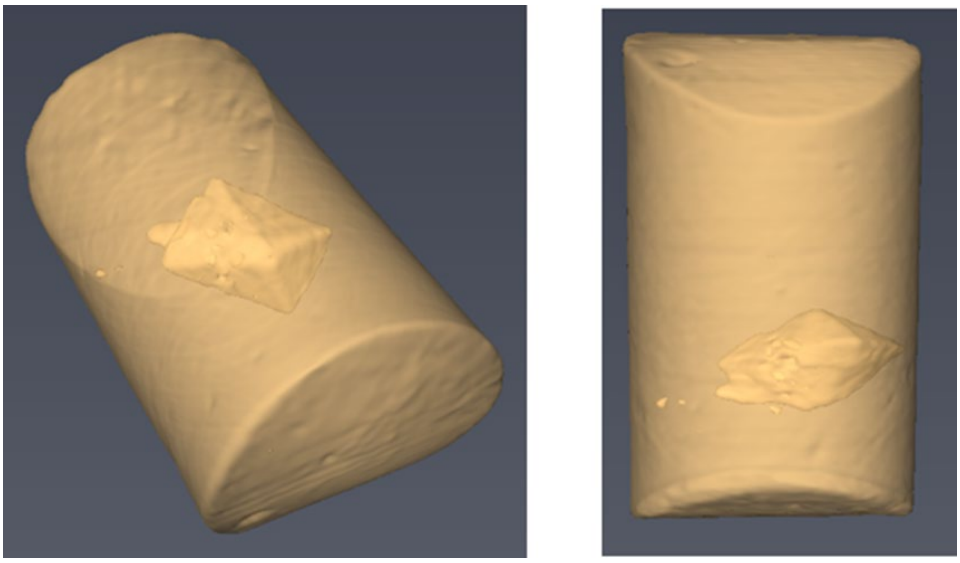

Figure 9-2. XCT scans of the core (5690.25'), including a partly infilled vug.

Carbon-13 analyses were performed on the core samples to establish the timing (pre- vs. post-CO_2 injection) of carbonate precipitation indicated by the brine and core analyses. Samples of the core matrix and the mineral precipitates within the vugs were analyzed for $\delta^{13}C$ to determine whether the vug minerals are isotopically distinct from typical matrix carbonates— isotopic analyses of the dissolved carbonate suggest that minerals formed from the injected CO_2 would be isotopically heavy (30‰) compared with the matrix carbonate minerals (3-4‰). Both the matrix material and vug precipitates displayed similar isotopic signatures of approximately 3‰ to 4‰, suggesting that post-CO_2-injection mineralization has not occurred. However, the minimal mass of carbonate precipitates in the vugs may bias the $\delta^{13}C$ values of these samples.

9.4 Discussion

In summary, the geochemistry of the brines from the Niagaran reefs included in this study show extremely high concentrations of calcium, magnesium, sodium, potassium and chloride, which is consistent with geochemical conditions of other Niagaran reefs in the State of Michigan. The general chemical analyses and modeling indicate that the reef brines are supersaturated with respect to carbonate minerals (dolomite, calcite, huntite, and magnesite), and the likelihood of precipitation increases with the injection of CO_2. The δ13C values of the dissolved carbonate in the brines appear to move in a positive direction (heavier) with the injection of the Antrim CO_2. The core sampled displayed evidence of carbonate, sulfate, and halide precipitation in the pores and fractures during the LS, SEM, XRD, and XCT analyses; however, the precipitates could not be directly tied to the injection of CO_2 through the isotopic analyses. If addition mass of the vug precipitates can be obtained, future analyses may provide a definitive δ13C value and clarity to the timing of the precipitation.

10.0 MICRO SEISMIC MONITORING

Two microseismic monitoring events were conducted 39 months apart during re-pressurization of the Dover 33 reef to evaluate the potential for CO_2-injection induced seismicity in Silurian-age carbonate reef depleted oil reservoirs. The baseline monitoring occurred in March 2013 during the start of CO_2 injection under the MRCSP III project when the reservoir pressure was low (approximately 800 pounds per square inch [psi]). Repeat monitoring took place after more than 285,000 tonnes of CO_2 had been injected and the reservoir pressure had increased to approximately 3,700 psi, which is near discovery pressure.

10.1 Objective and Description of the Technology

The objective of the microseismic monitoring study was to gain an understanding of microseismic activity during CO_2 injection into depleted Carbonate pinnacle reef oil reservoirs. Microseisms primarily occur when the injection pressures exceed the fracture pressure. In this case, however, the production of oil from the reef reduced the formation pressure, which resulted in a corresponding decrease in the fracture pressure. CO_2 injection into the reef should increase the pore pressure in the reef to near original (discovery) pressure and cause a corresponding increase in the fracture pressure (fracture pressure is dynamic and should increase as pressure is restored to original conditions).

10.2 Methodology

The baseline microseismic monitoring event was conducted over a 13-day period in March 2013 when reservoir pressure was depleted (approx. 800 psi). Monitoring was performed by Seismic Reservoir 2020 (SR2020) with 80 three-component (3C) geophones with a 50-ft spacing connected to 1.66-inch diameter tubing positioned in the 5-33 well. The repeat microseismic monitoring survey was conducted over a 28-day period in June/July 2016 when reservoir pressure was near original discovery pressure. Monitoring was performed by Paulsson Inc. using 16 OpticSeis™ 3C fiber optic seismic sensors (accelerometers connected through a fiber optic cable that extended to ground surface) with 25-ft spacing on 1.66-inch diameter drill pipe.

10.3 Key Results

10.3.1 Baseline Event

During the 13-day baseline microseismic monitoring period, a total of 76 events were detected in the field. These 76 events were classified as 34 subsurface events (Preliminary *Real*) and 42 near-borehole (false) events (events caused by electrical noises or tube waves). The 76 events included 29 post-injection events detected during the “quiet period” following injection (March 29 – April 1), seven of which were classified as subsurface (Preliminary *Real*) events. Figure 6-1 shows the timing of the 34 subsurface microseismic events relative to the CO_2 injection rate and the reservoir pressure. Note, that the close timing of events may make multiple events appear as a single event.

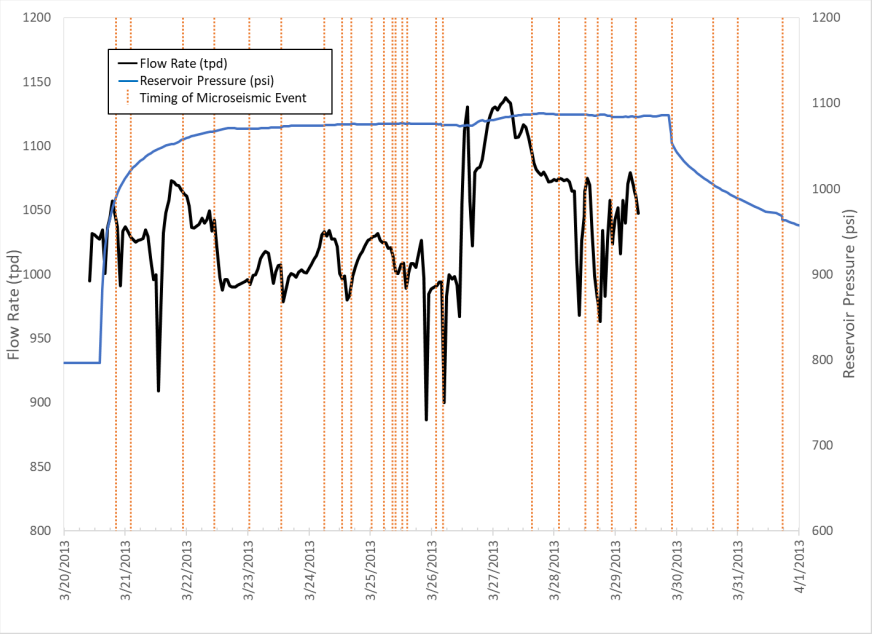

Figure 10-1. Timing of the 34 "subsurface" (Preliminary Real) microseismic events detected during the baseline monitoring event.

Figure 10-2 shows the locations of the microseismic events detected; events recorded on the last day of monitoring are shown with their own color. The figure reveals that all the events were located above the reef and many were very close to the 5-33 monitoring well. No events were detected in the reef or near the 1-33 injection well. Assessment of the field data suggested that the near-well events were likely caused by either electrically-generated noise or tube waves. A tube wave is an interference wave that occurs in cased wellbores when a Rayleigh wave encounters a wellbore and perturbs the fluid in the wellbore. the field assessment concluded that only the events classified as "subsurface" were potential *real* microseismic activity. Final processing of the field data was performed by applying noise-reduction and signal-enhancement filters. Following the filtering and data processing, only 12 of the 34 subsurface events were deemed true microseismic events. These 12 (Final Real) subsurface events were found to cluster immediately along the 5-33 monitoring well above the injection zone (Figure 11-2).

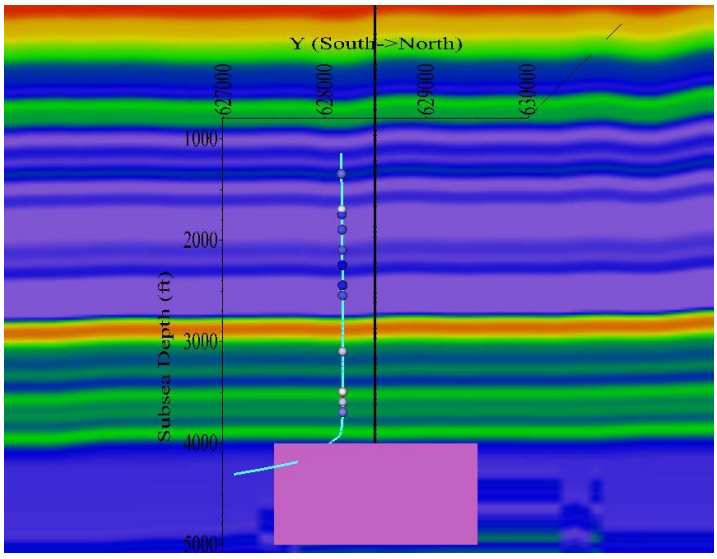

Figure 10-2. Locations of the 12 (Final Real) subsurface microseismic events following final data processing - Baseline monitoring event.

10.3.2 Repeat Event

An initial analysis of the microseismic data from the repeat monitoring event was performed by Paulsson Inc. NORSAR performed additional analyses of the data aided by proprietary microseismic data analysis tools.

PAULSSON ANALYSIS

Microseismic events were initially identified using the Itasca InSite software. Starting with the recorded data (TDI file), SEGY data files spanning 4-seconds were created (21,150 files per 24-hour period) outside of InSite and input into the program. Within the InSite software, a band-pass (100-1500 Hz) filter was applied, then an auto-search was conducted using pre-specified criteria. The triggering method that was used is the Picking Algorithm which is triggered when the picking function exceeds some thresholds. If an event was identified, the software output a 1-second SEGY data file with the beginning of the event at the center. Figure 11-3 shows the cumulative number of events detected, using the InSite software, from June 12 through July 8. Approximately 11,000 events were detected during the repeat monitoring event, including more than 4,000 events during the installation of the array from June 12 through June 18 (i.e., while the array was positioned at 15 temporary setting positions) but while CO_2 was not being injected. Figure 11-4 shows the cumulative number of events detected from June 18 through July 8, which excludes the events detected during installation of the array. A noticeable abrupt increase in event frequency occurs within a day of starting the booster pump (used to increase the CO_2 injection pressure as the reservoir pressures increased).

Paulsson performed a second analysis of the data that involved manually reviewing the data and selecting events. Four-second SEGY data files for the 21-day monitoring period were read into MATLAB, where they could be displayed and visually inspected. Before doing so, the data were filtered with an Ormsby filter (80-100-2000-3000 Hz). The events were examined and then sorted into three categories based on their magnitude and move out characteristics:

- Type 1 (79 events) – Very small (M< -2) likely further away from the monitoring well (5-33).

- Type 2 (Hundreds of events) – Near the monitoring well and very small (M< -2). Appear to be coming from above the array.
- Type 3 (Thousands of events) – Long-Duration Events. Very low magnitude (M< -3).

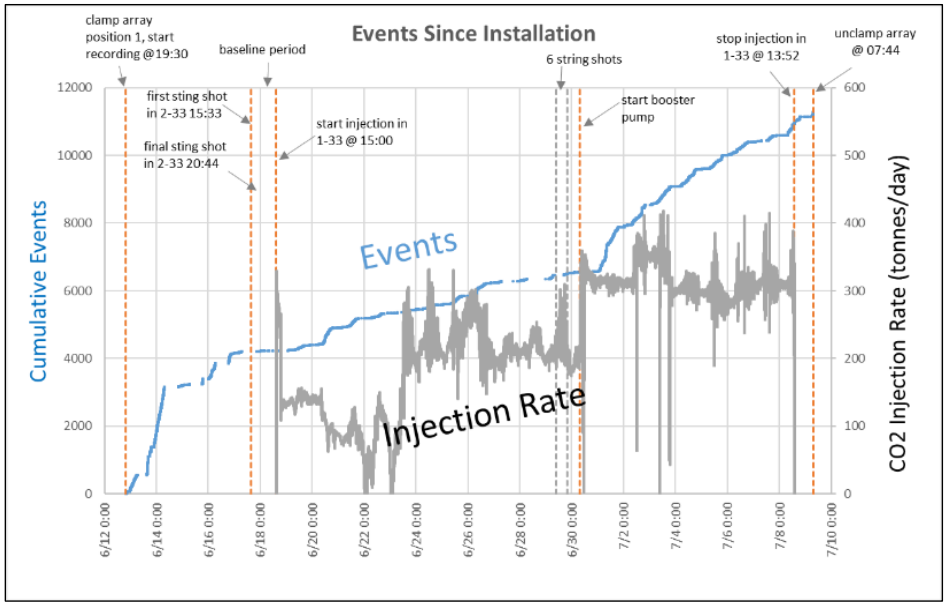

Figure 10-3. Cumulative events identified with the InSite software June 12 through July 8 (includes over 4,000 events during installation of array when CO_2 was not being injected).

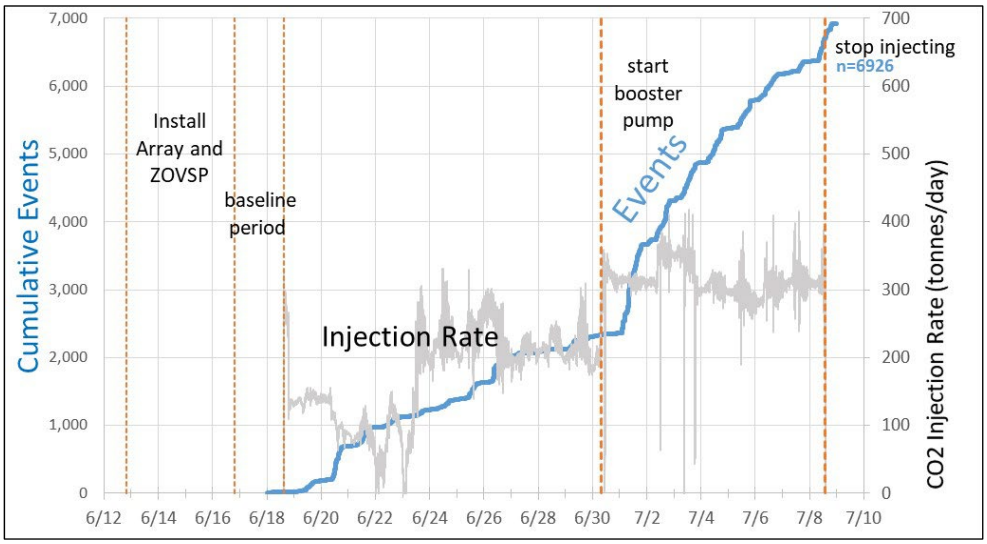

Figure 10-4. Cumulative events identified with the InSite software June 18 through July 8 (excludes events during installation of array).

NORSAR ANALYSIS

NORSAR applied machine learning/cluster analysis to process all 22 days of data. Key features were extracted from the more than 186,000 event triggers initially detected to classify the different types of events via unsupervised learning/clustering. Three classes of event triggers could be identified and were sorted into the following groups/classes.

- Class 1 – low peak frequency and wide frequency spectrum (143,951 events – 77%). The peak frequency of these events is below 500 Hz. NORSAR suggests that some of these triggers might be related to surface activities/noise.
- Class 2 – high peak frequency and wide frequency spectrum (18,363 events – 10%). The peak frequency of these events is generally between 500 and 1,500 Hz. The occurrence of these events is primarily during injection. However, the high frequency content, and a lack of low frequencies, point towards very small sources that are very close to the sensor string. However, signal moveouts are generally not observed and duration of the signals is surprisingly long (for such small signals). NORSAR did not identify a physical explanation for these event triggers and assigned them to a class of noise, likely resonance issues of the sensors.
- Class 3 – low peak frequency and narrow frequency spectrum (23,902 events – 13%). The frequency content of these events is mainly in the range from 20 to 200 Hz and rather band-limited, which is consistent with microseismic events. However, the events also had the following characteristics which are not consistent with true microseismic events:
  - Only one phase can be identified (likely P-wave, but polarization of the wave is not constant throughout the sensor array)
  - First arrival along the array is almost simultaneous for all sensors (almost no moveout)
  - The amplitudes vary from sensor to sensor in a non-systematic pattern
  - The recorded frequency content may differ from sensor to sensor

NORSAR concluded that the sensor itself (or electronics/digitizer) is responsible for the distortion of the signals, but the recorded triggers are related to some real, physical movement. Due to the distortion of the signal, it is not possible to interpret the type of signals and the origin of them (neither their location nor size).

10.4 Discussion

The main goal of this project was to decide if there is evidence of induced seismicity related to the injection of CO_2. While there is some information that could suggest CO_2 injection is the cause of some of the detected events, there is significantly more information indicating that noise, particularly instrumentation related noise, is a major source of the detected events. Below is a summary of key points.

EVIDENCE FOR INJECTION-INDUCED SEISMICITY

- Figure 10-5 (from NORSAR) shows the number of short-duration (<10 ms) and longer-duration (100 to 200 ms) events on June 17 (day before injection began) and June 18 (day that injection began). Longer-duration-trigger activity coincided with start of CO_2 injection. Some short duration (<10 ms) events are more or less correlated with well work in the 2-33 well.

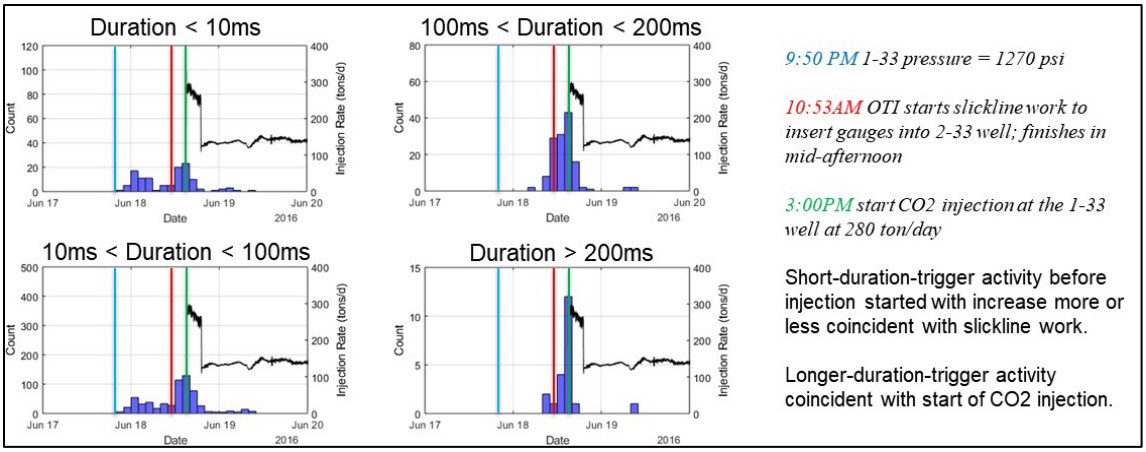

Figure 10-5. Detections on June 17 and 18 sorted by duration.

- Figure 10-6 (from NORSAR) uses vertical green bars to highlight periods of high variability in the injection rate. Times of high variance in injection rate very often coincide with higher activity of triggers in all classes.

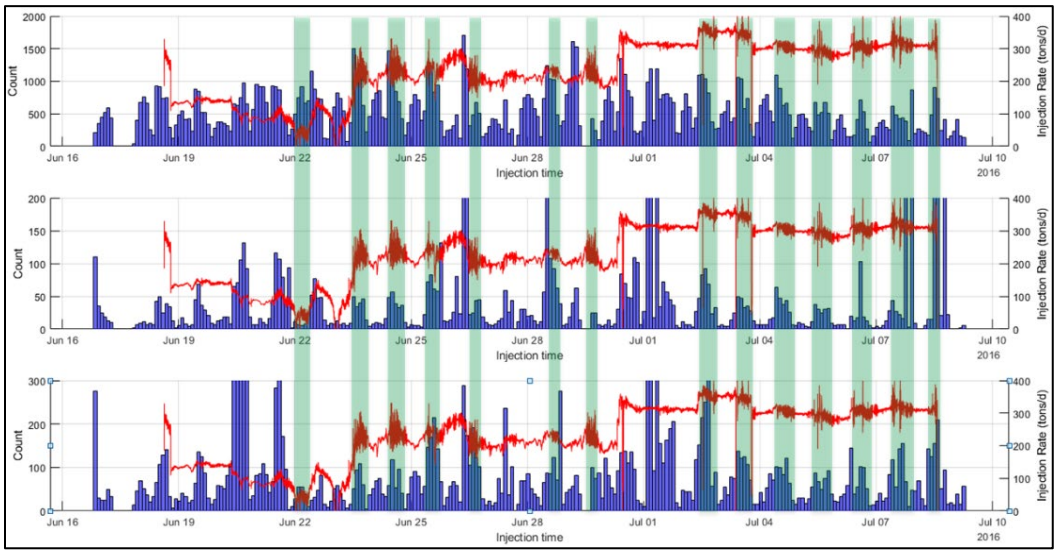

Figure 10-6. Occurrence (in two-hour increments) of the three types of triggers derived from raw features (distributions) and CO_2 injection rate. Green bars correspond to large variability in injection rate.

- Figure 10-7 (from Paulsson) shows the cumulative number of events detected from June 18 through July 8 vs injection (surface) pressure in the 1-33 well. There is a very high degree of correlation between injection pressure and the cumulative number of events. Furthermore, Figure 10-7 shows there was an abrupt increase in the occurrence rate of events when the booster pump was started, which increased pressure in the injection well. This suggest injection pressure (or booster pump) somehow effects the occurrence of some microseismic events. Figure 10-8 (from Paulsson) shows there is also a correlation between reservoir pressure and cumulative events.

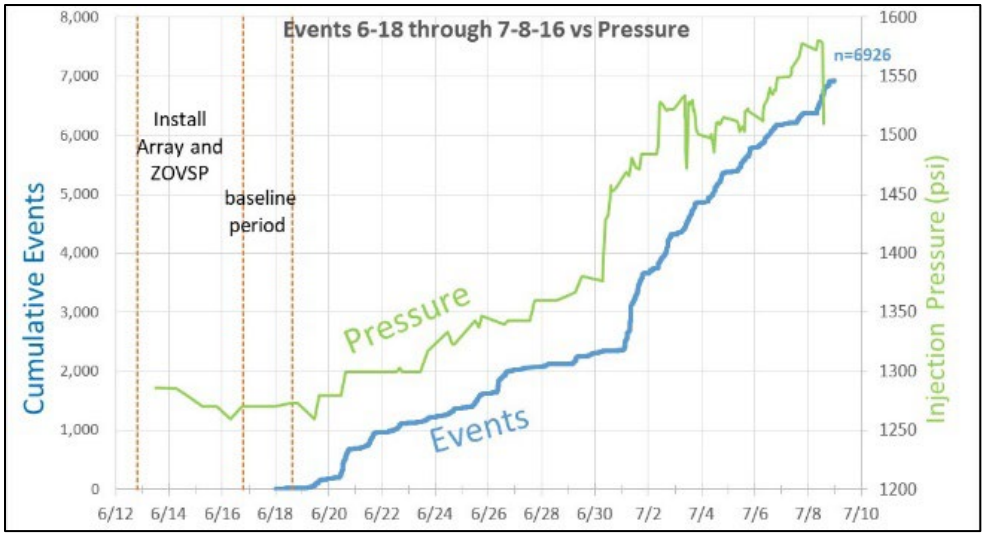

Figure 10-7. Cumulative events vs surface injection pressure.

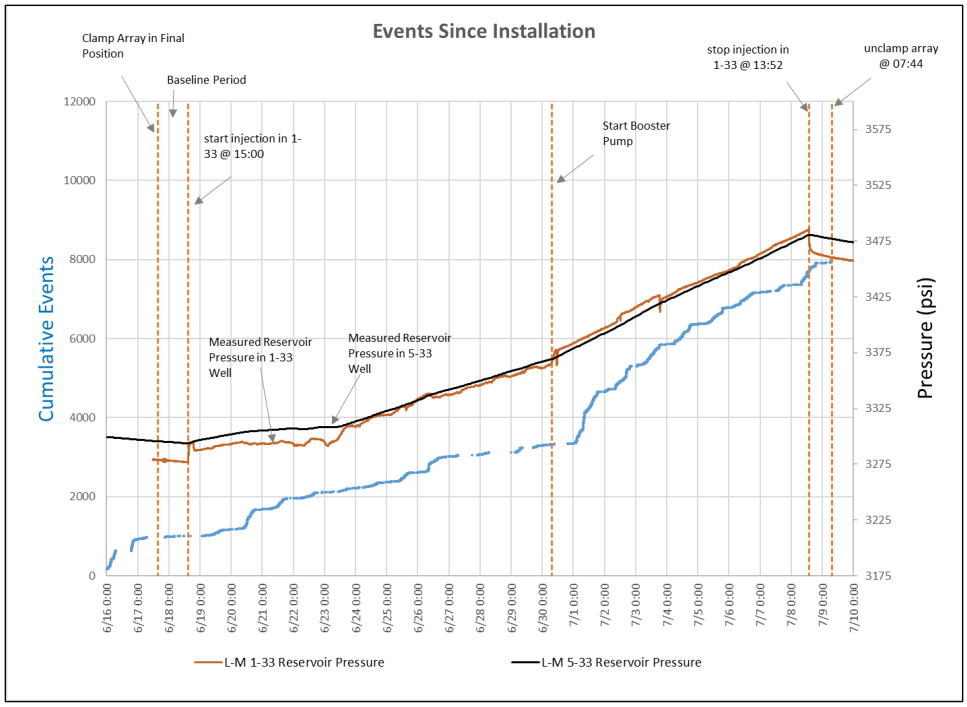

Figure 10-8. Cumulative events vs measured and estimated reservoir pressure at the 1-33 and 5-33 wells.

EVIDENCE AGAINST INJECTION-INDUCED SEISMICITY

- Figure 10-9 (from NORSAR) shows the occurrence and distribution over time of all 186,218 events in three classes derived from the cluster analysis. These data indicate that each of NORSAR's event classes are detected over the entire duration of the injection phase and including before CO_2 injection started and after CO_2 injection stopped. This suggests a non-injection source.

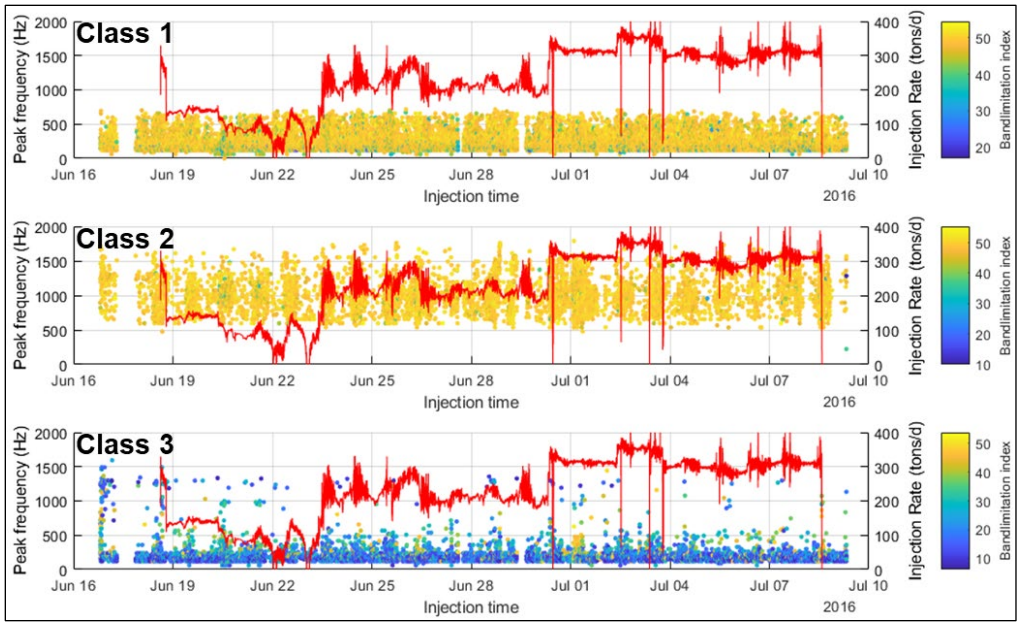

Figure 10-9. Three classes of events derived from the raw features: peak frequency and frequency. spectrum.

- Figure 10-3 (see above) shows the cumulative number of events detected using the InSite software, from June 12 through July 8. Approximately 11,000 events were detected during this period, but this includes more than 4,000 events detected during the installation of the array from June 12 through June 18 (i.e., while the array was positioned at 15 temporary setting positions) – during this time, CO_2 was not being injected.
- Figure 10-10 (from Paulsson) shows the 79 high-quality events with clear P- and S-wave (Paulsson Type 1 events) are clustered into three days - June 18, June 28, and June 30 – that coincide with well work done in well 2-33 located on the same well pad as the 5-33 well with the microseismic monitoring array (removal and re-installation of a downhole pressure gauge carrier, a steel tube-like device that houses the pressure gauges, which involved upward/downward hammering on the slickline/gauge carrier). To substantiate this hypothesis, the location of the Type 1 events was estimated. *This suggests well work may be cause at least for Type 1 events.*

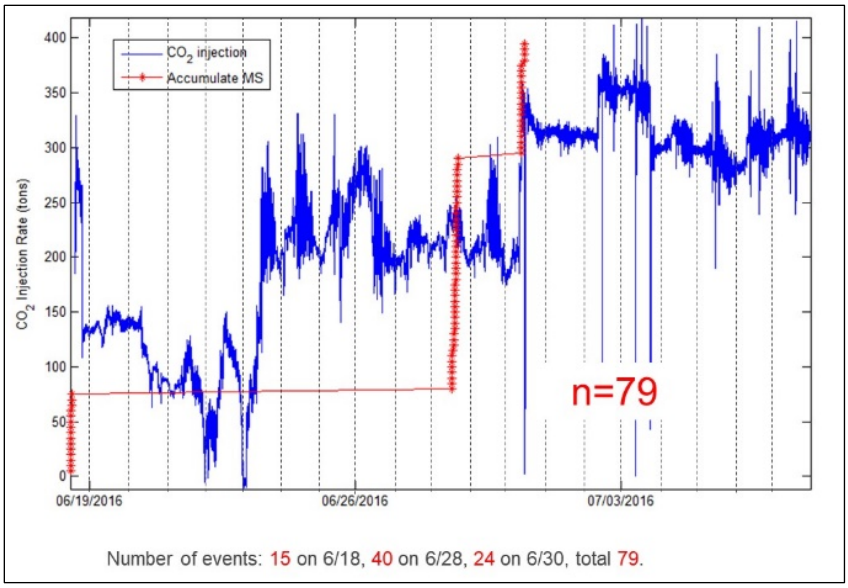

Figure 10-10. Frequency of occurrence of Paulsson Type 1 events (red) coincides with days when well work was performed in nearby well 2-33.

- NORSAR identified significant noise contamination in the data. The relative amplitudes and the frequency content at the different sensors in the well showed problems that are likely due to instrumentation/cementation and/or electronics/digitizers. The frequency analyses indicated that for both controlled and natural events the dominant frequency detected were near 1,500 Hz. The consistency of the dominant frequency could be related to the similar magnitude of the different events, or it could also be caused by the sensor response. Further evidence for sensor response or coupling issues with the microseismic array are the long codas that follow the first arrivals and the apparent damage to the lower-end frequencies that are attenuated before the higher frequency signals. There is no obvious explanation for the signal attenuation through wave-propagation effects, rather these anomalies could be explained by coupling issues and/or sensor response. See the following three figures.

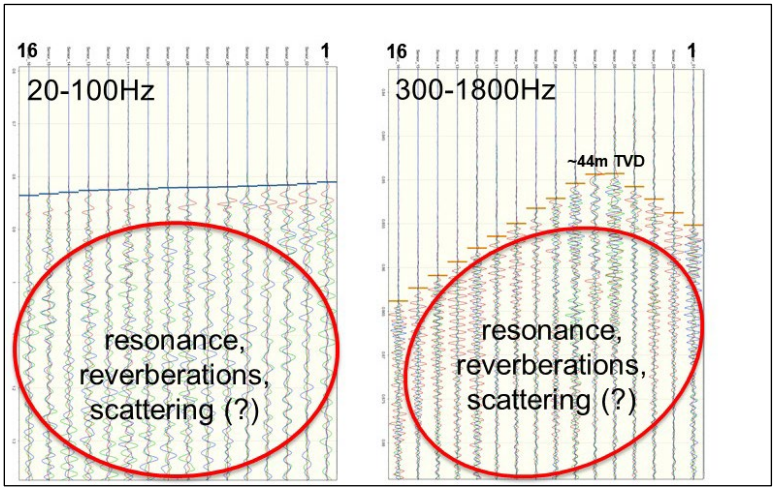

Figure 10-11. Waveforms from Orientation Shot #1 during with the microsesmic array positioned at Stage 16. First arrivals are followed by long codas. Dominant frequency is near 1.5kHz; contributions to coda could come from scattering in unconsolidated formations near the surface, coupling issues and/or bad cement.

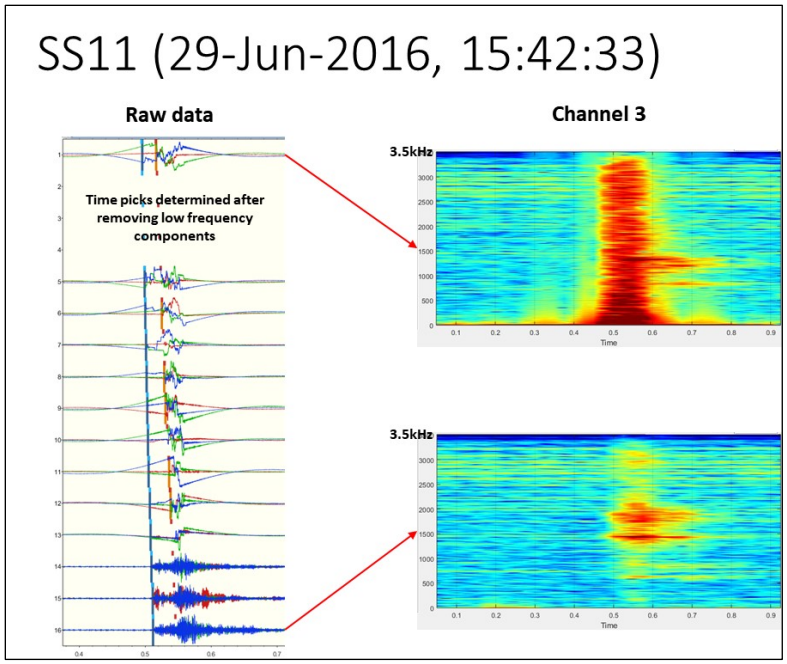

Figure 10-12. Freqency content of String Shot 11 recorded by top and bottom sensors. Low frequencies are present but the time-domain representation suggest they are damaged. Band just under 1.5kHz is dominant and appears resonant; Low frequencies are attenuated before higher frequencies within the length of the array (~115m). This is atypical and possibly related to acquisition rather than wave propagation.

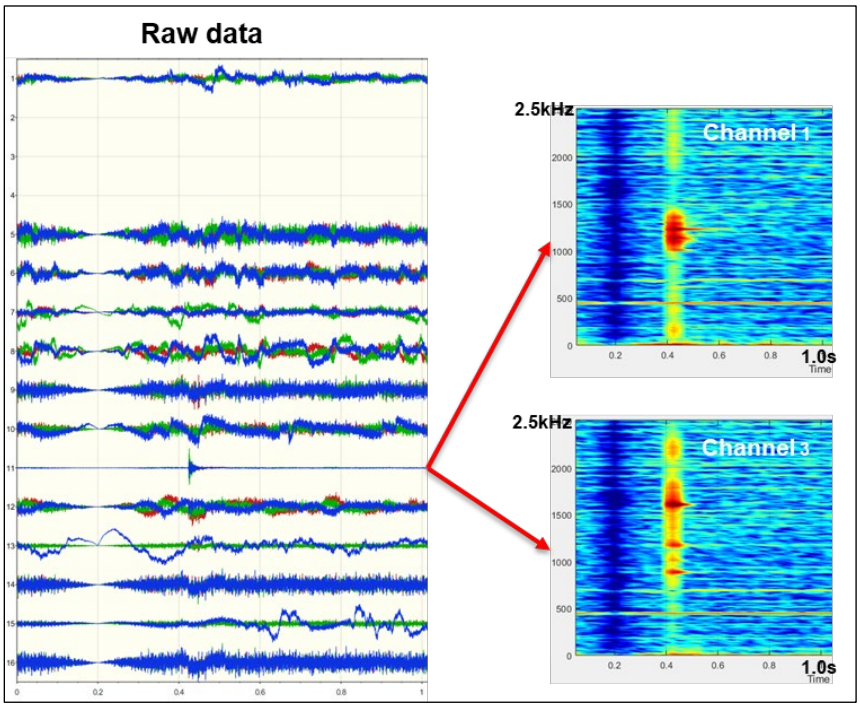

Figure 10-13. Microseismic data showing a different dominant frequency for different components of the same sensor. Arrival spectrum varies from one component to the other. Dominant frequency shifts from under 1.5kHz in channel 1 to over 1.5kHz in channel 3 in this detection. This produces inconsistency in the arrivals observed in different components.

11.0 PRESSURE MONITORING

11.1 Objective and Description of the Technology

Pressure and rate data are commonly recorded as part of a basic monitoring program in CCS projects. This section discusses the application of multiple analytical techniques to interpret pressure and rate transient data from MRCSP operations CO_2 injection and storage operations. Pressure data are recorded continuously using bottom-hole pressure gauges at the injection well and one or more monitoring wells. Rate data are collected using surface flow meters. The data interpretation techniques of interest are injection-falloff analysis, injectivity/productivity index analysis and pressure pulse arrival time analysis. Injection-falloff analysis involves log-log pressure derivative plotting for the falloff data and history-matching of the entire injection-falloff sequence to determine permeability. In the injectivity/productivity index analysis, rate-normalized pressure buildup is plotted against material balance time or ratio of cumulative injection to injection rate to determine the injectivity index (ratio of injection rate to stabilized pressure buildup) which can be related to permeability-thickness. The arrival time analysis identifies the arrival of a pressure disturbance (~0.1 psi change from ambient) to determine the hydraulic diffusivity from which permeability can be estimated.

11.2 Methodology

11.2.1 Injection-falloff analysis

Injection falloff tests record the pressure decline in an injection well following cessation of injection, and the pressure and injection for the injection period preceding the falloff. Engineering analysis of the falloff test data are performed to determine reservoir properties such as transmissibility (product of permeability and thickness), permeability, mobility (permeability divided by viscosity), distance to boundaries, and well damage if any (skin). Two primary methods of data analysis are generally carried out: Pressure Transient Analysis (PTA) and history matching.

For pressure falloff data, the common diagnostic workflow involves making a log-log plot of the pressure change, and the derivative of the pressure change against an appropriate time function. For radial flow (single well injecting into a large volume), this would result in a constant value, whereas for linear (channel flow in a bounded system) this would result in a line of ½ slope. The entire injection-falloff sequence can also be “history-matched” if a model for the well-aquifer geometry can be identified. The basic approach used in our analyses can be described as follows:

- Start with a diagnostic plot analysis of the falloff response to identify the presence of a linear segment indicating radial flow. From the stabilized value of the derivative, calculate the corresponding permeability. This is an “equivalent” single-phase permeability.
- Using an appropriate conceptual model of the system (e.g., a vertical well injecting into a 2x1 rectangular region or a multi-zone radial composite model), adjust parameters such as permeability, compressibility, radius of each zone, to match the entire injection-falloff history.

An illustrative example is presented from the 1-33 well in the Dover-33 reef. The test of interest was a 9-day injection followed by a 3-week falloff period. For the 1-33 injection well, a match to the entire injection and fall-off pressure sequence and the fall-off pressure derivative was obtained with a three-zone radial composite gas model (Figure 11-1). The gas model is deemed more appropriate because CO_2 appears to have transitioned from a gas to a liquid or supercritical fluid during injection and then back to gas phase during fall-off (based on density values). The gas model yields permeability values of 27, 4, and 14 mD for the inner, middle, and outer zones, respectively with radii of these zones being 250, 515 and 1200 ft, respectively. There is some uncertainty associated with the outer zone estimates (i.e., reversal of

derivative at late times in Figure 11-1) – hence the mobility of the middle zone is taken to be the most representative value.

Although not shown here, the history-match for the 5-33 and 2-33 monitoring wells yielded permeability values of 4.4 mD and 5.3 mD, using a gas model. As before, the gas model is considered more applicable for this test than the liquid model because reservoir pressure in the inter-well region was most likely below the critical pressure of CO_2 during most of the test. Overall, the estimated mobility values from the three wells (4, 4.4 and 5.3 mD) are reasonably consistent, with an average of 4.7 mD.

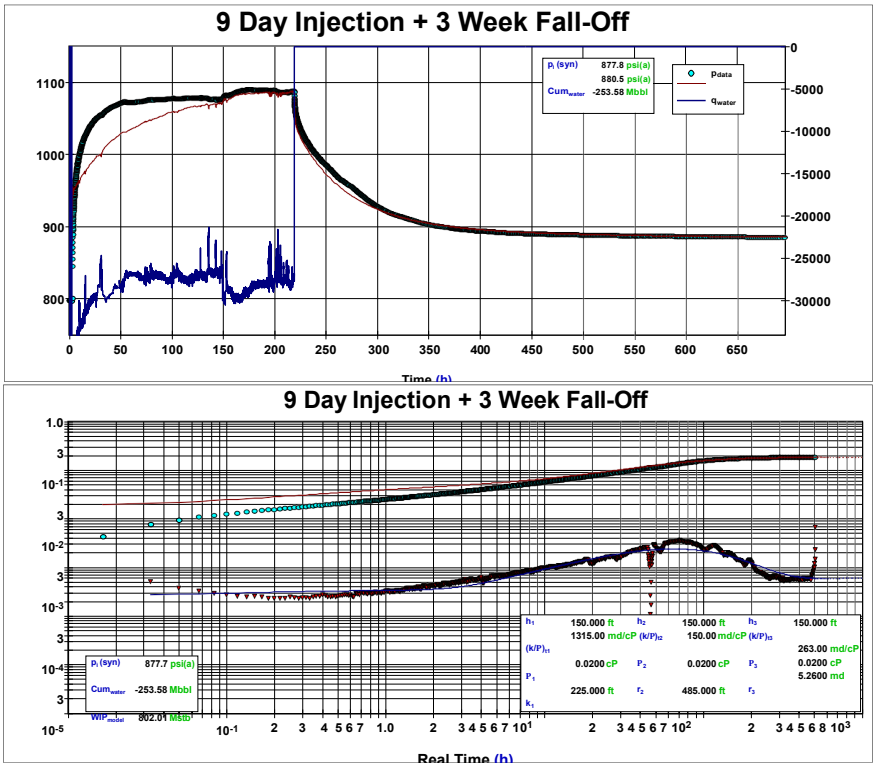

Figure 11-1. History-match for the 9-day test, pressure data, (top) cartesian plot of injection-falloff sequence, (bottom) log-log plot of falloff data, Dover 1-33 well.

11.2.2 Injectivity index analysis

Injectivity index is a commonly used concept in petroleum reservoir engineering to evaluate the capability of a well to inject fluids into a porous and permeable formation. It is defined as the ratio of the injection rate divided by the pressure difference between formation pressure and bottom-hole pressure. For closed reservoirs under boundary-dominated (pseudo-steady-state) conditions, it can be shown that the injection well pressure build-up divided by the injection rate, when plotted against the ratio of cumulative injection to injection rate, should yield a straight line with slope inversely proportional to the pore volume times compressibility, and intercept equal to the reciprocal of the stable injectivity index. This is sometimes referred to as a flowing material balance plot. For variable rate conditions, as is often the case in field projects, the dependent variable becomes a rate-normalized pressure change, i.e., $(P_i-P_{wf})/q_{sc}(t)$, and the independent variable becomes the material balance time, i.e., $Q(t)/q_{sc}(t)$. Furthermore, the injectivity index can also be correlated to the permeability-thickness product using a simple correlation based on field data and numerical simulation (Mishra et al., 2017).

An illustrative example is presented from the 8-16 well in the Chester-16 reef. The 8-16 well started injecting CO_2 in early September 2019 and provides approximately 4 months of data for analysis. Of

particular interest is the pressure response at 5865', which lies within the perforated interval from 5850' to 5900' in the A1 Carbonate formation. The flowing material balance plot corresponding to pressures at 5865' depth (which lies within the perforated interval from 5850' to 5900' in the A1 Carbonate formation) are shown in Figure 11-1

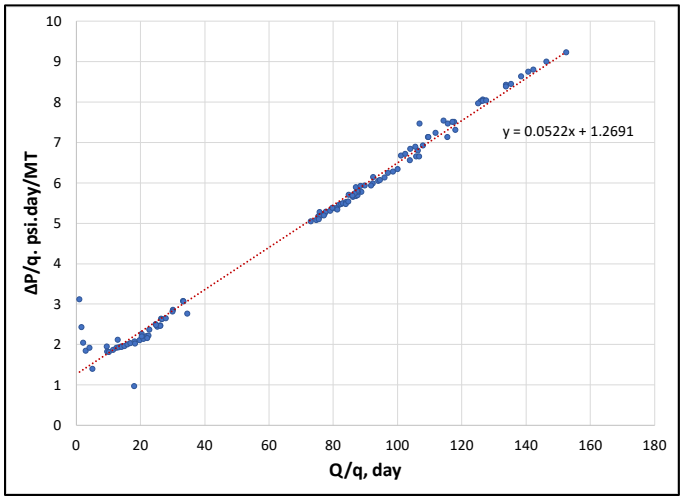

Figure 11-2. Flowing material balance plot corresponding to pressure gauge at 5865', Chester 8-16 well.

Here, the rate-normalized pressure drop is plotted against material balance time, resulting in a strong linear trend (excepting for the first few data points – which may be indicative of transient flow conditions prior to the onset of boundary effects). The strong linear trend is a clear indication of the pseudo-steady-state conditions caused by the bounded nature of the reservoir. The injectivity index is readily calculated from the reciprocal of the intercept as 288 MT/yr-psi, and can be converted to an equivalent-permeability thickness product using the relationship presented in Mishra et al. However, that correlation was based on CO_2 injection into oil/brine filled formations, whereas in this instance the fluid in the vicinity of this well is likely a mixture of CO_2 and oil at some residual saturation injection, because CO_2 has broken through in the 8-16 well. Thus, an adjustment for different viscosities needs to be made in this conversion. Assuming a CO_2 saturation of 0.7, and oil saturation of 0.3, a CO_2 viscosity of 0.067 cp and oil viscosity of 0.57 cp, and applying the Bingham-Reid mixing law for effective two-phase viscosity, we obtain an effective fluid viscosity of 0.13 cp. The formation thickness is taken to be 50 feet. Applying a similar viscosity correction where $\mu_{2\text{-phase}}$ = 0.13 cp, μ_{brine} = 0.66 cp), permeability can be estimated as: k = 281/0.07*0.13/0.66/50 = 15.8 mD.

11.2.3 Arrival time analysis

In the case of a constant rate or impulse perturbation at the injection rate, the arrival time can be obtained as the first derivative of the pressure response at the monitoring well. However, for a variable rate situation, a practical alternative is to identify this as the time at which the observed pressure deviates from the background level by some threshold value (e.g., 0.1 psi). Assuming single phase conditions, it can be shown that the arrival time is proportional to the ratio of the square of the distance between the injection and observation wells, and the hydraulic diffusivity (i.e., ratio of permeability to the product of porosity, viscosity and total compressibility).

An illustrative example is shown for the Northern lobe of the Bagley reef, where the arrival time for various injection well – monitoring well pairs was determined as the time at which the pressure change deviated from background pressure level by 0.1 psi. This required first calculating a differential plot (by subtracting

the ambient pressure from the measured values) as shown in Figure 11-3. Here, the injection well was 2-11, and the monitoring wells were 3-11 and 1-11.

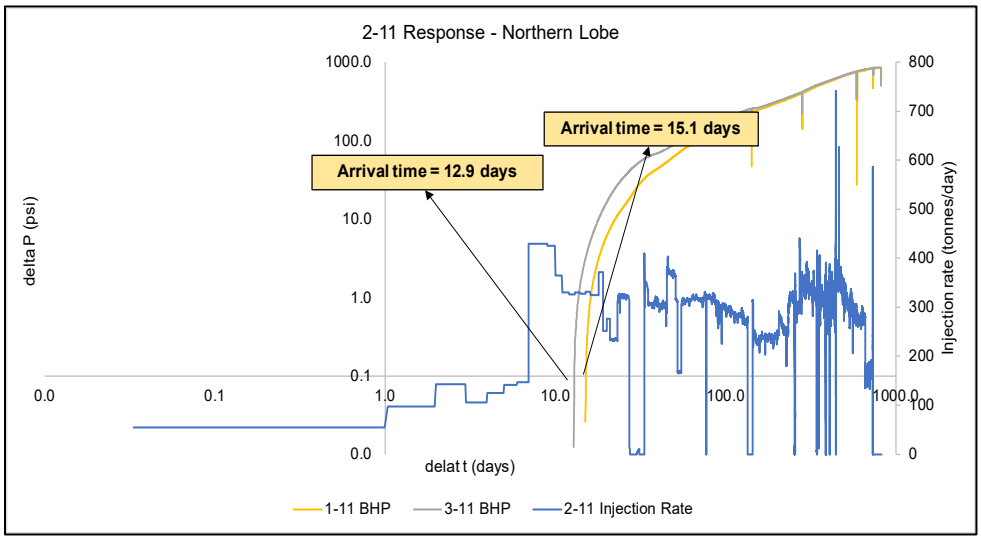

Figure 11-3. Arrival times, 2-11 injection response in the Bagley Northern Lobe monitoring wells (1-11 and 3-11).

Knowing the arrival time and the inter-well distance, the diffusivity is calculated to be 6.8E6 md-psi/cp for the 2-11 and 3-11 well pair, and 3.8E6 md-psi/cp for the 2-11 and 1-11 well pair. These can be converted into an effective permeability using μ = 0.05 cp, ϕ = 0. 08, and c_t = 4E-4 1/psi (based on independently derived information using core/log data and/or correlations). This yields the following range for permeability: k = 6.1 to 10.9 mD.

11.3 Synthesis of key results

We have only presented a few illustrative examples corresponding to each of the analytical methods utilized in the detailed. As documented in (Mishra et al., 2020), the total number of tests interpreted was considerably higher, viz: (a) Dover-33 – 8 injection-falloff tests, 18 injectivity and productivity tests, and 2 arrival times; (b) Bagley – 3 injection-falloff tests, 3 injectivity tests, and 7 arrival times; (c) Charlton-19 – 4 injection-falloff tests, 3 injectivity tests, and 1 arrival times; and (d) Chester-16 – 4 injection-falloff tests, 6 injectivity and productivity tests, and 1 arrival times. The results from these tests have been converted into equivalent permeability values (as needed), and synthesized in Table 11-1 below.For each test type and each reef, we report a permeability range and a corresponding best estimate (i.e., geometric mean value). For each reef, a best estimate permeability range is developed by considering the geometric mean values from multiple test types. Finally, a single-point estimate is provided for each reef which is based on the weight of evidence (i.e., biased towards the geometric mean, or high/low end member values, as appropriate).

Table 11-1. Permeability ranges and best estimates (in mD) from different methods across reefs.

	Dover-33	Bagley (Northern)	Charlton-19
Injection-falloff analysis	1 – 42 (6)	0.36 (outlier)	2.4 – 29.8 (15.6)
Injectivity analysis	5.7 – 20 (10.7)	10.5 – 36.9 (19.7)	4.9 – 21.3 (10.2)
Productivity analysis	3.8 – 13.4 (7.2)	N/A	N/A
Arrival time analysis	3.3 – 13.4 (6.7)	6.1 – 10.9 (8.1)	72 (outlier)
Best estimate (this report)	6 – 10.7 (7.5)	8.1 – 19.7 (13)	10.2 – 15.6 (13)
	Dover-33	**Bagley (Northern)**	**Charlton-19**
Injection-falloff analysis	1 – 42 (6)	0.36 (outlier)	2.4 – 29.8 (15.6)
Injectivity analysis	5.7 – 20 (10.7)	10.5 – 36.9 (19.7)	4.9 – 21.3 (10.2)
Productivity analysis	3.8 – 13.4 (7.2)	N/A	N/A

11.4 Discussion

In summary, valuable transient pressure and rate data collected from injection operations in four Niagaran reefs in Michigan were used in conjunction with analytical techniques used in oil and gas operations to assess reservoir properties and response to injection. As a result, the applicability of these techniques in CCS/CCUS projects has been demonstrated by using illustrative examples of CO_2 injection for each analytical technique. Application of these techniques was found to provide an enhanced understanding of reservoir response to CO_2 injection in addition to providing information on reservoir properties such as permeability, reservoir heterogeneity, and hydraulic communication between reservoir regions. These techniques thus provide a crucial strategy for analyzing monitoring data that could be used to obtain a process understanding of CO_2 injection and optimize CO_2 utilization.

12.0 EFFECTIVENESS FOR CO_2 STORAGE

The previous sections of this report provide a summary of each of the 11 monitoring technologies that were evaluated during the Phase III program, highlighting key results and lessons learned for each monitoring method. As a result of the extensive body of monitoring data developed, new information was acquired about the effectiveness of the carbonate pinnacle reefs for long-term CO_2 storage. These are summarized below.

- The carbonate reef reservoirs act as closed reservoirs because they are surrounded/overlain by low permeability carbonates and evaporites which prevent CO_2 leakage out of the reservoir, making them ideal geologic features for permanent CO_2storage. This conclusion is based on the following monitoring data:
  - DTS monitoring study (Chester 16 reef);
  - PNC logging study (multiple reefs);
  - Cross-well seismic monitoring study (Chester 16 reef).

- It is possible to recover almost all CO_2 injected into a reef during CO_2-EOR. In other words, the reefs do not irreversibly sequester significant amounts of CO_2 during the EOR process. This conclusion is based on the following monitoring data:
  - Mass balance accounting study (multiple reefs).

- CO_2 injection into the pinnacle reef reservoirs does not appear to cause ***significant*** land displacement (uplift, subsidence) in the area overlying the reefs. This conclusion is supported by the following monitoring data:
  - INSAR monitoring study (Dover 33 reef).

- CO_2 injection into the pinnacle reef reservoirs does not appear to cause ***significant*** seismic activity that could activate fractures and/or faults that could lead to CO_2 leakage out of the reservoir, even when reservoir pressure is near discovery pressure. There are indicators that suggest CO_2-injection could be the source of some of the recorded micro-seismic events. This conclusion is supported by the following monitoring data:
  - Microseismic monitoring study (Dover 33 reef).

- The carbonate reef reservoirs may contain intervals/zones of salt plugging which reduces porosity and limits CO_2 storage capacity. This conclusion is supported by the following monitoring data:
  - PNC logging study (multiple reefs).

- Lateral migration of CO_2 within the carbonate pinnacle reef reservoirs away from the injection well may occur preferentially in thin intervals (e.g., A-1 Carbonate) even though the injection well may be perforated across a much longer interval that includes the entire reservoir zone (i.e., A-1 Carbonate and upper to middle Brown Niagaran). (Note: in this case, DTS proved to be effective for detecting lateral migration and breakthrough of CO_2 at a monitoring well located in the same pod as the injection well. This outcome was facilitated by the close spacing of the monitoring and injection wells and the preferential migration of CO_2 within a thin vertical interval. The technology may not be as successful for detecting CO_2 migration under different conditions (i.e., greater well spacing and/or CO_2migration occurs within a thicker interval)). This conclusion is based on the following monitoring data:
  - DTS monitoring study (Chester 16 reef);
  - PNC logging study (Chester 16 reef).

- The carbonate pinnacle reef reservoirs may occur as single isolated “pods” (e.g., Dove 33) or in groups of two or more closely-spaced/overlapping pods (e.g., Charlton 19, Chester 16, Bagley). Within individual pods, there is a high degree of hydraulic connectivity (i.e., rapid pressure response to injection observed in monitoring wells in same pod). Interpod connectivity appears more variable (delayed and diminished pressure response to injection observed in monitoring wells in neighboring pod). This conclusion is based on the following monitoring data:
  - analysis of pressure monitoring data (multiple reefs).

- The overall low porosity of the carbonate pinnacle-reef reservoirs presents a significant challenge for using borehole seismic monitoring methods to detect and delineate the injected CO_2. Low porosity limits the amount of CO_2 per unit volume of rock which in turn limits the change in acoustic velocity caused by fluid substitution (i.e., CO_2 replacing brine or oil). If the change in velocity is too small, it will not be detectable with seismic methods. (Thick glacial till deposits in the area are likely to further limit the use of surface seismic surveys for CO_2 monitoring.) This conclusion is supported by the following monitoring data:
  - Dover 33 VSP study;
  - Chester 16 DAS VSP study;
  - Chester 16 Cross-well seismic study.

- Fracture pressures (the pressure at which the formation will fracture) in depleted formations/intervals can be extremely low owing to the lowering of pore pressure below hydrostatic. In compartmentalized reservoirs with poor water recharge drive such as the Niagaran carbonate pinnacle reefs, pore pressure may stay low for long periods of time. Reservoir depletion usually brings along lower total horizontal stresses which lower the fracture gradient and make drilling problematic because of decreased difficulty to create open-mode fractures. This has important implications for geomechanical characterization of depleted formations. Characterization must look at the role of changing internal pressures in the reef on fracture pressure to determine safe injection rates at different stages of injection. This conclusion is supported by the following data:
  - Mini-frac testing in the Chester 16 reef.

- Injection of CO_2 into the carbonate reef reservoirs increases the likelihood of precipitation of carbonate minerals (dolomite, calcite, huntite, and magnesite), owing to the extremely high concentrations of calcium, magnesium, sodium, potassium and chloride in the reef brines which causes them to be supersaturated with respect to these minerals. In this study, core samples from the injection zone displayed evidence of carbonate, sulfate, and halide mineral precipitation in the pores and fractures; however, the precipitates could not be directly tied to the injection of CO_2 through the isotopic analyses. This conclusion is supported by the following monitoring data:
  - Geochemistry monitoring study (multiple reefs).

RECOMMENDED MONITORING TO SATISFY REGULATORY REQUIREMENTS

Monitoring may be required at CO_2 storage sites for a variety of reasons, including to meet UIC Class II (EOR sites) or Class VI (storage only sites) permit requirements or EPA greenhouse gas reporting rule requirements or to qualify for tax credits under the 45Q tax credit rule. The results of this monitoring study should prove useful to operators considering using carbonate pinnacle reefs of Northern Michigan for CO_2 storage. To further aid the operators who wish to use the Niagaran carbonate pinnacle reef reservoirs for CO_2 storage, key regulatory monitoring requirements were reviewed and a monitoring program was developed/recommended that satisfies the requirements taking into account the lessons learned from the MRCSP phase III monitoring study. Table 12-1 and Table 12-2 summarize key regulatory monitoring requirements and recommended monitoring methods to satisfy the requirements.

Table 12-1. UIC Class VI Monitoring Requirements and Recommended Monitoring Methods for Niagaran carbonate pinnacle reef reservoirs.

Requirement	Recommended Monitoring
• A testing and monitoring program to verify that the project is operating as permitted and is not endangering USDWs.	Modeling and monitoring
• Monitoring of the CO_2 stream, the CO_2 plume, and pressure front both during injection and for a period following injection.	• CO_2 Mass balance accounting • Monitoring CO_2 stream chemical composition • Reservoir pressure monitoring • DTS to look for vertical leakage via injection wellbores Methods for mapping CO_2 plume (e.g., seismic, borehole gravity logging, PNC logging, geochemistry) should not be necessary because reefs are closed reservoirs with easily identifiable boundaries via pressure monitoring.
• Monitor groundwater quality throughout the lifetime of the project.	✓ Identify and monitor USDW aquifer(s) for geochemistry and pressure
• The UIC director may require air and/or soil gas monitoring	✓ Only if required
• Annual testing to determine the absence of significant fluid movement/demonstrate mechanical integrity.	✓ DTS to monitor for vertical leakage
• Other	✓ microseismic monitoring to ensure absence of induced seismicity (optional)
• Greenhouse Gas Reporting Program (GHGRP) Subpart RR.	• monitoring, reporting, and verification plan. • CO_2 Mass Balance Accounting to measure mass of CO_2 that is received, injected into the subsurface, produced, emitted by surface leakage, emitted by leaks in equipment, and emitted by venting, and the mass of CO_2 sequestered in subsurface geologic formations Monitoring CO_2 stream chemical composition

Table 12-2. UIC Class II Monitoring Requirements and Recommended Monitoring Methods for Niagaran carbonate pinnacle reef reservoirs.

Requirement	Recommended Monitoring
• Mechanical Integrity	✓ Internal—pressure test at least once every five years. ✓ External—adequate cement records may be used in lieu of logs.
• Annual fluid chemistry and other tests as needed/required by permit.	✓ Monitoring CO_2 stream chemical composition
• Injection pressure, flow rate, and cumulative volume observed weekly for disposal and monthly for enhanced recovery	✓ CO_2 Mass balance accounting
• Greenhouse Gas Reporting Program (GHGRP) Subpart UU	• CO_2 Mass balance accounting ✓ Monitoring CO_2 stream chemical composition

13.0 REFERENCES

Mawalkar, S., Burchwell, A., Keister, L., Pasumarti, A., and Gupta, N. 2020a. Mass Balance Accounting or CO_2 Storage with Enhanced Oil Recovery in Northern Michigan. MRCSP topical report prepared for DOE-NETL project DE-FC26-05NT42589, Battelle Memorial Institute, Columbus, OH

Mawalkar, S., Burchwell, A., and Gupta, N. 2020b. Distributed Temperature Sensing (DTS) to Monitor CO_2 Migration in an Enhanced Oil Recovery Field in Northern Michigan. MRCSP topical report prepared for DOE-NETL project DE-FC26-05NT42589, Battelle Memorial Institute, Columbus, OH

Mishra, S., Kelley, M., Raziperchikolaee, S., Ravi Ganesh, P., Valluri, M., Keister, L., Burchwell, A., Mawalkar, S., Place, M., and Gupta, N. 2020. Analysis of Transient Pressure and Rate Data in a Complex of Enhanced Oil Recovery Fields in Northern Michigan. MRCSP topical report prepared for DOE-NETL project DE-FC26-05NT42589, Battelle Memorial Institute, Columbus, OH